Title
Microtubule assembly and transport during axonal elongation

Author
Reinsch, Sigrid Sophie

Publication Date
1992

Peer reviewed|Thesis/dissertation

MICROTUBULE ASSEMBLY AND TRANSPORT DURING AXONAL ELONGATION

by

Sigrid Reinsch

DISSERTATION

Submitted in partial satisfaction of the requirements for the degree of

DOCTOR OF PHILOSOPHY

in

Cell Biology

in the

GRADUATE DIVISION

of the

UNIVERSITY OF CALIFORNIA

San Francisco

Date **University Librarian**

Degree Conferred: 3/23/92

for my family

ACKNOWLEDGEMENTS

I wish to first thank the other members of the Growth Cone Collective, Elly Tanaka and James Sabry. My interactions with you and our sharing of ideas, results, reagents, frustrations and elations made this thesis possible. The fruitfulness of my collaboration with Elly and James will be the gold standard for all my future scientific interactions.

To Marc Kirschner, my mentor and tormentor - I give you big hugs for all your humanity, and lashes for your knowledge of just how to push all my buttons. I applaud your incisive approach to scientific questions and for demanding me to do the same. Thank you for teaching me the power of designing my own experimental equipment rather than depend on someone else's innovations. If I gained nothing else in your lab, this one gift of knowledge from you to me made it all worthwhile. I thank you for liking me as a person (even if you don't like the way I do science) and for letting me tease you endlessly about how you laugh at your own jokes. Somehow, I think we will both miss each other a great deal.

Big thanks to Tim Mitchison for endless help with setting up the microscope, photoactivation and video apparatus, and for making me feel like all my requests for reagents were actually doing you a favor. Thanks especially for encouraging me to do the photoactivation experiments in *Xenopus* neurons. I will always appreciate the tact you demonstrated in pointing out to me obvious experiments or interpretations of results while serving as my thesis committee member.

Thanks also to my other faculty supporters - to Lou Reichart as my strong supporter on both my orals and thesis committee; and to Judy White, Bruce Alberts, Zach Hall, Christine Guthrie and Reg Kelly for help along the way.

To the guys in the shop - this thesis could never have been done with out your help. Special thanks to Doug McVay, who never said no to my urgent pleas for immediate modifications to microscope equipment; to Bob Shadel who taught me how to use a drill press; and to Mike O'Grady who helped me through the horrible hell of electrical noise. Thanks to all the

Kirschnerites who provided me with other help and reagents. Special thanks go to David Drechsel in this regard who patiently listened to my endless questions about protocols, and whose gospel singing made stripping meninges almost a pleasure. To my two wonderful baymates, Gary Ward and Tim "Goldenfingers" Stearns - thanks for enduring my endless whining and babbling with chuckles and smiles. "Mega"-thanks again, to Tim Stearns who gave me every reagent I could wish for in my last few frantic months, I'll love you forever. Thanks also to Fady Malik for providing me with the fruits of his trips to the slaughter house - purified kinesin - for some of these experiments. To the folks of MTGM, I bid you adieu - thanks for making every Tuesday evening a special experience.

Thanks to the breakfast club cum graduate women's support group - Evi, Debbie, Stephanie, Caroline, Dana and Jill. Howard's at 8:30? To my coffee mates - James, Bill and Jordon, I'll miss those early morning conversations which help to start the day out right. To Chris Field and Cammie Lesser - thanks for being my allies in the game of life and in the fun and games of life, respectively. To Tina Lee, Karen Butner, and Enrique Amaya - thanks for providing all the hugs I needed to get through each day in the Kirschner lab and to Louise Evans for all the laughs.

To Terri Burgess, my dearest friend, thanks for showing me that friendship can be more wonderful than I ever dreamed. And to Carl, Gisela, Pablo, Larry, Helen, Gerard, Pascal, and Heike - thanks for brightening my life here at UCSF. To the other graduate student parents - Janet, Sandra and Jay, Audie, Debbie, and Byron - Good Luck and thanks for all the support!

Finally, the biggest thanks go to my family. If I tried to thank them all individually, it wouldn't all fit in this thesis. To all my parents, Mom and Dad and Sallie and Jack - thanks for being so proud of me. I really appreciate it. To Selene and Nika - I thank you for making me feel like I was able to be a good Mom in spite of my time away from you. And to David, who really deserves the most credit for getting me from the start to the finish, we've traveled a hell of a road together - "Will you marry me?"

MICROTUBULE ASSEMBLY AND TRANSPORT

DURING AXONAL ELONGATION

by

Sigrid Reinsch

Marc W. Kirschner
Chair, thesis committee

ABSTRACT

Cellular morphogenesis is the dynamic process by which the internal components of a cell are organized to cause a change in cell shape or function. This thesis describes experiments which investigate microtubule dynamics during cellular morphogenesis; how a particular microtubule arrangement is generated and maintained within the cell. In these experiments the assembly and transport of the microtubule cytoskeleton during axonal elongation was studied using the technique of photoactivation of fluorescence. To understand where assembly of microtubule polymer occurs which contributes to net axonal elongation, we have followed the fate of microtubule polymer in elongating embryonic *Xenopus* axons using a photoactivatable fluorescent tubulin derivative. We have followed photoactivated fluorescent regions of labeled polymer during axonal elongation and correlated the fluorescent signal with phase images from the same elongating neurons. Our data indicate that microtubule polymer is continually translocated as a coherent phase from the cell body distally during axonal elongation. This vectorial polymer movement was observed at all levels of the axon and even in the absence of axonal

elongation. We followed polymer movement as close as 15mm from the cell body; therefore significant microtubule assembly must occur proximal to this level of the axon. Microtubule assembly also occurs distally in the axon since, in general, microtubule polymer moved slower than the growth cone, even when marks were made very close (3mm) to the growth cone. Finally, polymer movement near the growth cone appeared to respond in a characteristic manner to growth cone behavior, while polymer more proximally in the axon moved more consistently.

Preliminary results are also presented which examine role of ATP in the stability of microtubules in cultured fibroblast cells and how this stability might be regulated by microtubule-associated proteins. Evidence is provided that ATP hydrolysis is required for the depolymerization of microtubules assembled with MAPs.

TABLE OF CONTENTS

CHAPTER 1

Introduction

INTRODUCTION

Throughout my graduate work I have sought to understand how microtubules are involved in cellular morphogenesis. As opposed to tissue morphogenesis which involves the organization of groups of cells into organs and tissues, cellular morphogenesis is used here to describe the internal arrangements of the components of a cell which effect a change in cell shape intricately related to cell function. The term "cellular morphogenesis" can be used to describe changes or processes which occur in dividing cells such as the generation of a mitotic spindle, or the directed movement of a fibroblast. It can also be used to describe processes which occur in differentiated post-mitotic cells, such as neurite elongation, or the fusion of myoblasts during muscle development. The dissection of the role of particular cytoskeletal elements in various processes of cellular morphogenesis is generally not simple. This ambiguity is largely due to the fact that nature has engineered a redundancy of function and form in cellular components. Genetic manipulations or drug disruption which are useful for dissecting the components of many cellular processes often yield negative or ambiguous results with redundant systems. For example, during polarized pseudopod extension in response to a chemotactic signal in *Dictyostelium*, actin bundling proteins are thought to be responsible for cross-linking of actin filaments to form a hydrated actin gel (Condeelis et al., 1990). However, mutant strains lacking α-actinin or gelation factor, two different abundant actin cross-linking proteins, are phenotypically normal (Brink et al., 1990; Gerisch et al., 1989; Schleicher et al., 1988). Only if both proteins are lost, are effects seen on the development of *Dictyostelium,* though several major functions such as growth, chemotaxis, phagocytosis and pinocytosis, were unaltered (Witke et al., 1992). While such redundancy

provides ultimate benefits for cell and organismal survival, it makes a dissection of function and mechanism that much more difficult for the lowly researcher.

A role for microtubules has been shown in myriad cell types undergoing cellular morphogenesis and differentiation. Microtubules are directly implicated in such varied processes as the rapid visual adaptation to darkness in teleost retina (Burnside, 1976), and the dorsal-ventral axis specification of the early frog embryo (Houliston and Elinson, 1991). Several aspects of microtubules make them versatile elements for achievement of a permanent differentiated state, or conversely for transient changes in cell shape and function. We can gain much information by studying the properties of purified cellular components such as microtubules *in vitro*, however, the activities of purified components *in vitro* may not fully reveal their cellular functions. Some general features of microtubules and their associated proteins are reviewed below.

First, purified tubulin shows interesting polymer kinetics, termed "dynamic instability" (Mitchison and Kirschner, 1984). Within a population, some individual polymers are growing while others are shrinking. These dynamic properties of microtubules can be described by four parameters for each end of the microtubule: 1) the growth rate (the plus end of the microtubule is defined as the faster growing end, and the minus end is the slower growing end); 2) the shrinkage rate (the plus end shrinks faster relative to minus end); 3) the catastrophe frequency (the transition from growing to shrinking) and 4) the rescue frequency (the transition from shrinking to growing). The ability of microtubules to display these dynamic characteristics imparts flexibility to the microtubule network within the cell.

Second, these kinetic states of growth, shrinkage and the transition from one state to the other can be modified *in vivo*. One mechanism which is believed to affect these parameters *in vivo* is by the binding of microtubule

associated proteins. The binding of microtubule associated protein, tau, has been shown to effect these kinetic parameters during the assembly of purified bovine brain tubulin (Cleveland, 1977) Drechsel, in preparation). The binding of different microtubule associated proteins to microtubules within the cell is regulated both temporally and spatially. The ability of the cell to regulate microtubule dynamics allows for changes in the spatial distribution of polymers, or conversely for the generation of a persistent, organized structure containing microtubules. Until recent years, our definition of microtubule associated proteins was limited to those proteins which copurified with tubulin through cycles of assembly and disassembly. More recently, technical improvements such as the purification of microtubule associated proteins by microtubule polymer affinity chromatography, has afforded a broader definition of the term "microtubule associated protein" (Kellogg et al., 1989). Microtubule associated proteins linked to organizing structures such as centrosomes are involved in the nucleation of microtubule polymer assembly within the cell. These nucleating centers control the amount, and the polarity of microtubule polymer assembly - both spatially and temporally. The binding of microtubule associated proteins may also provide a link between the microtubules and the other components of the cytoskeleton such as microfilaments and intermediate filaments. This link may allow the different cytoskeletal components to act coordinately during morphogenetic events such as during pathfinding by neuronal growth cones. In other instances, this linkage may allow one cytoskeletal component to act as a framework for the later assembly of a second cytoskeletal component. An example of such a linkage is during myogenesis where microtubules may provide the first longitudinal framework for a myotube, and only later is the actin-myosin network laid down (Antin et al., 1981; Toyama et al., 1982).

Third, microtubules are able to perform or support physical work. One form of work may result from polymerization of microtubules such as during the active extension of a cellular process (Hotani and Miyamoto, 1990; Madreperla and Adler, 1989; Tilney et al., 1966; Tilney and Porter, 1965; Tilney and Porter, 1967) or the depolymerization of microtubules as during anaphase movement of chromosomes (Koshland et al., 1988). Often the work is accomplished via binding of mechanochemical motors as in the metaphase movement of chromosomes in the mitotic spindle (Hyman and Mitchison, 1991; Pfarr et al., 1990; Steuer et al., 1990), or the beating of cilia or flagella to propel a cell, microbe or sperm (Dustin, 1984).

Fourth, again via the binding of mechanochemical motors, microtubules function as transport routes for organelles from one part of the cell to another and have a key role in the spatial arrangement of cytoplasmic organelles including the nucleus (Huffaker et al., 1988; Pringle et al., 1986), endoplasmic reticulum (Terasaki et al., 1986), golgi apparatus (Rogalski and Singer, 1984; Tassin et al., 1985), lysosomes and endosomes (Matteoni and Kreis, 1987). An asymmetric distribution of microtubules within the cell results in asymmetric or polarized distribution and transport of organelles within the cell, such as, the transport of synaptic vesicles within the axon (Hollenbeck and Bray, 1987; Ochs, 1972), or the polarized delivery of cytolytic vesicles during killing by cytotoxic T-cells (Kupfer et al., 1983). The polarized delivery of vesicles to the plasma membrane may be involved in local control of membrane expansion such as occurs in migrating fibroblasts or elongating neurites (Vallee and Bloom, 1991).

Finally, microtubules help provide a structural framework for the cell. As relatively rigid polymers, their form and placement are often crucial determinants of cell shape. For example, bundled microtubules are common in

stable structures such as the erythrocyte marginal band or the axons and dendrites of neuronal cells. However, the interrelationship between the different cytoskeletal elements is apparent in these structures as combinations of different cytoskeletal elements usually comprise stable structures. In many instances, however, the role of microtubules in determining cell shape is negligible. For example, the treatment of many cells such as fibroblasts with microtubule depolymerizing drugs results in no rapid change in cell morphology. In these cases, arguably, the other components of the cytoskeleton are more important for maintaining the cell morphology.

These varied roles for microtubules within a single cell during the process of morphogenesis makes it inherently difficult to dissect how microtubules are involved in the process of morphogenesis *in vivo*. Numerous models for morphogenesis have been proposed for different cell types. I began my graduate career by studying what I naively viewed as a simple example of cell morphogenesis - the polarization of the microtubule cytoskeleton of cytotoxic T-lymphocytes during the killing of a specific target cell (Kupfer et al., 1983). This, I reasoned, was a simple example of morphogenesis since it involved only an internal restructuring on a very rapid time scale (minutes) with no requirement for protein synthesis or cell growth, and no visible external change in cell shape. In terms of the microtubules, they were definitely required for the killing process, did not change in terms of numbers, polarity, length, or nucleation site; only their positioning was altered. Therefore, this project addressed a possible first step in morphogenesis - how microtubule placement occurs within the cell to generate an asymmetric array of microtubules. My hypothesis was simple; the binding of a target cell via specific receptors generated a localized signal on the the outside of the cytotoxic T-lymphocyte. This extracellular signal was translated into an intracellular signal via signal

transduction pathways (my understanding of which at that time was only embryonic at best) resulting in a change in orientation of the microtubule organizing center and concomitant rearrangement of microtubules. As a first year graduate student who had never really known failure, I was naively confident in my ability to master cell biology, immunology and biochemistry all in one fell swoop. However, this project was not designed for the uninitiated graduate student, working singly, armed only with her wits and pitiful practical knowledge in the above-mentioned fields. The biology of the system was too difficult. I succeeded only in reproducing the results already presented in the literature. It's still an intriguing problem - ideally tackled by a well-trained cell biologist with expertise in biochemistry, signalling pathways and the cytoskeleton, working closely with immunologists who can nurture and continuously assay the proper functioning of the cells used in this project.

My next project, with much humbler goals, was to try to understand a second aspect of microtubules and morphogenesis, that is, the conversion of a random array of microtubules into an asymmetric array. There are several possibilities for how an asymmetric or polarized array can be generated from a random array of microtubules. As suggested by Kirschner and Mitchison (Kirschner and Mitchison, 1986), selective stabilization of some of the microtubules in the cell could occur by plus-end dependent "capture" of microtubules. A plus-end capture mechanism may stabilize microtubules in kinetochore fibers in the mitotic spindle (Huitorel and Kirschner, 1988; Mitchison and Kirschner, 1985) or at the cell surface as in *Drosophila* wing epidermal cells (Mogensen et al., 1989). Alternatively microtubules may be stabilized along their length by the binding of microtubule associated proteins. The local regulation of microtubule associated proteins for binding to and stabilizing microtubules could occur via a post-translational mechanism such as local

phosphorylation/dephosphorylation. The specific question that I addressed, the results of which are presented in the first chapter of this thesis, was "how are stable microtubules generated?" or conversely "how are microtubules destabilized?" Several phenomena reported in the literature indicated a role for ATP in the active destabilization of microtubules. In one case, normal ATP levels in cells are required for the action of microtubule depolymerizing agents; that is, depletion of intracellular ATP levels causes the microtubules in the cell to become stable to drugs such as nocodazole or colchicine (Bershadsky and Gelfand, 1981; De Brabander et al., 1981). A second finding which supported a role for ATP in destabilizing microtubules was that when cultured cells are permeabilized in the absence of ATP, the microtubules are stable, however, when ATP is added to the permeabilization buffer, the microtubules fall apart rapidly (Bershadsky and Gelfand, 1981; Bershadsky and Gelfand, 1983). We reasoned that the stabilization of the microtubules during ATP depletion and during permeabilization in the absence of ATP might be due to a microtubule associated protein whose binding was increased in the absence of ATP, thereby stabilizing the microtubules. This project actually progressed rather well during the several months that I spent working on it. I succeeded in reproducing the results in the literature very quickly and generated the novel result that the non-hydrolyzable analog AMP-PNP would stabilize the microtubules in permeabilized cells to depolymerization by ATP. Since at that time it was known that kinesin bound to microtubules in a rigor state in the presence of AMP-PNP and released from microtubules in the presence of ATP, we believed that kinesin or a molecule with similar microtubule binding characteristics was acting to stabilize the microtubules in these permeabilized cells. While the results of these studies are still rather preliminary, they point to some interesting candidate mechanisms for the stabilization/destabilization of

microtubules. My work on this project was (fortunately) interrupted by the arm-twisting Marc Kirschner who wanted me to take over a project which he had spent several months in the lab developing. By that time of my graduate career, I had realized the advantages of working on a project in which Marc was interested; that is, there would be a greater likelihood of interaction with him. I did return to this project in my final few months at UCSF, to try to determine whether purified kinesin will stabilize microtubules assembled *in vitro.* This question is still unresolved.

My third and final project involved a much more challenging question of morphogenesis - the generation of the axonal cytoskeleton. During development, nerve cells make connections by extending neuritic processes which accurately find targets that are located far from the nerve cell bodies. Neurons require microtubules to establish and maintain neurites, and to respond to targeting cues. They are also essential for transporting important vesicular components to the growth cone, which contribute to net membrane transport.

At the time I began examining how the microtubule cytoskeleton of neurites is laid down, the current dogma of the field held that growth of the axonal microtubule cytoskeleton occurred at the distal end of the process, in the structure termed the growth cone (as reviewed in (Mitchison and Kirschner, 1988). While advances had been made in studying microtubule dynamics in live fibroblasts by injecting fluorescently labeled tubulin into live cells in culture (Gorbsky and Borisy, 1989; Sammak and Borisy, 1988; Sammak and Borisy, 1987; Schulze and Kirschner, 1988), no direct measurements of microtubule dynamics had yet been made in neuronal cells.

Neuronal cells present several problems for examining microtubule dynamics using injected fluorescent label. First, they are very difficult to

microinject. Second, the presence of stable microtubules within the axon precludes uniform incorporation of the microinjected label by simple microtubule turnover as in the fibroblast cells. To achieve uniform incorporation of the microinjected tubulin, the stable microtubules must be first depolymerized by incubation in the cold or in microtubule depolymerizing drugs and then allow the microtubules to repolymerize. Marc's several months in the lab were spent developing a bulk-labeling protocol for embryonic *Xenopus* neurons by injecting labeled tubulin into the fertilized egg. The advantages of a bulk labeling protocol are that direct microinjection is avoided, and if the bulk labeling is done before neurite outgrowth (and the generation of stable microtubules), then the tubulin pool will be uniformly labeled.

The approach that Marc took was to try to label the embryonic neurons by cytoplasmic inheritance of labeled tubulin injected into the early blastomeres of the *Xenopus* embryo. Microinjection of horse radish peroxidase (HRP) into early blastomeres had been used to determine cell lineages within the *Xenopus* embryo; the injected HRP does not affect normal development and is retained in the injected cell and all its descendants (Hirose and Jacobson, 1979). Since the *Xenopus* embryo does not change in size until hatching and feeding stages (individual cells within the embryo become smaller), the injected marker is passed undiluted into the daughter cells. Marc was able to show that like HRP, rhodamine labeled tubulin was inherited by the daughter cells of injected blastomeres without perturbing development, and that the injected label persisted until the neurula stage. Marc also worked out preliminary conditions for growing the *Xenopus* neural tube cultures. While Marc did some initial imaging on these cultures, both Tim Mitchison and Eric Schulze were instrumental in helping to set up the imaging apparatus for these experiments and teaching me the ins and outs of video microscopy. Eric had done a lot of

fluorescence imaging of microtubules in fibroblasts and made the initial purchase and set-up of the inverted microscope, and the IMAGE1 image processing system. Tim was also helpful with the microscope set-up, the purchase and later modification of the ISIT camera, and teaching me how to purify and label tubulin.

I initially attempted to study microtubule dynamics within the growth cone - the only location within the neuron where the dynamics of single microtubules could possibly be visualized and characterized. Within the axon, the microtubules are bundled and individual microtubules cannot be resolved. The flattened growth cone has often been likened to a "fibroblast on a leash," and immunofluorescence of neurons in culture indicated that the ends of microtubules splayed from the axon into the growth cone (Bamburg et al., 1986; Letourneau, 1982). It was interesting and important to determine whether microtubules within the growth cone had dynamics which paralleled those observed within fibroblast cells. In particular it was interesting to determine whether microtubules within the growth cone had behavior characteristic of "dynamic instability."

The imaging of the microtubules in these neurons using the ISIT camera was not ideal, however, and it was not possible to clearly visualize individual microtubule dynamics within the growth cone though we could sometimes see what we believed were individual microtubules. We felt that a significant part of the problem was due to the level of the signal within the *Xenopus* neurons, and I spent eight months trying to boost the stoichiometry of the rhodamine label on the tubulin or use imaging techniques which were more sensitive. Another problem was the uneven labeling of the neurons. Although we were injecting into the two-cell stage of the embryo, and would expect labeling in 50% of the neurons, we found that the label was bright in some neurons but fairly dim in

others and present in less than half the neurons. Marc thought it would be useful to look at the distribution of the label in fixed embryos at different times after injection to see if we could understand the uneven labeling. Marc enjoyed teaching me the rudiments of paraffin embedding, sectioning and histology and we were able to conclude that the microinjected tubulin was not diffusing throughout the embryo as we had expected, but stayed localized fairly close to the site of injection within the embryo. Such localization was possibly due to rapid incorporation into cytoplasmic microtubules near the site of injection. I next attempted to target the injections to the presumptive dorsal region of the embryo, so that the tubulin would be inherited by the future neuroblasts in the neural tube of the embryo.

Two developments interrupted my work on imaging microtubules within the growth cone: First, was the development of caged-fluorescein by Tim Mitchison. Tim had spent a lot of time trying to develop a reagent to allow the marking of microtubules in the mitotic spindle where the bundling of microtubules within the kinetochore fibers makes the study of individual microtubule dynamics impossible. His rapid success with this reagent in the study of poleward flux in the spindle (Mitchison, 1989) made promising the study the bulk dynamics of the axonal microtubules where the bundling of microtubules also occurs. The second development was the arrival of Elly Tanaka in the lab, who under the tutelage of Eric Schulze had developed a great love for the study of microtubule dynamics in living cells. I handed off the "microtubule dynamics in growth cones" project to Elly, happy to have another student with whom to share in the battle on the idiosyncrasies of growing primary *Xenopus* neurons in culture and set about to tackle the question of how the axonal cytoskeleton was actually generated.

The axonal cytoplasm contains longitudinally bundled microtubules which are present, likely as discontinuous segments, from the cell body to the distal growth cone. This distance may be hundreds of microns to meters in length in some neurons. However, although individual microtubules within the axon vary in length, as well as nucleation and termination sites (Bray and Bunge, 1981; Chalfie and Thompson, 1979; Tsukita and Ishikawa, 1981), they share a common polarity; the plus ends are oriented distally towards the growth cone and the minus ends are oriented towards the cell body (Baas et al., 1989; Baas et al., 1988; Baas et al., 1987; Burton and Paige, 1981; Heidemann et al., 1984; Heidemann et al., 1981; Heidemann and McIntosh, 1980).

This plus end distal polarity is similar to that observed in non-neuronal cells where it has been demonstrated that microtubules are nucleated with the minus end at the centrosome and the plus end distal in the cell. Furthermore, it has been shown that microtubule assembly occurs from the centrosome toward the periphery with subunits added at the distal plus ends of microtubules. With this analogy in mind, one might predict that in neurons tubulin subunits are similarly added to the distal plus ends of the microtubules. However, the long distances from the site of monomer synthesis in the cell body to the distal plus ends of microtubules in the growth cone might require a specific transport form of tubulin monomer in the axon. In such a model, the microtubules of the axon would be stationary relative to the cell body and might serve as a framework upon which the tubulin would be transported.

As I was beginning my experiments with photoactivation of fluorescence in the axon, several labs reported the results of photobleaching studies in isolated neurons. These results supported the notion that microtubule polymer is stationary and, by implication, supported a model of net microtubule assembly at or near the growth cone (Lim et al., 1990; Lim et al., 1989; Okabe

and Hirokawa, 1990). Such an explanation of microtubule growth is incomplete since these experiments do not address how tubulin reaches the growth cone. Presumably, tubulin is transported as soluble dimer or in some nonpolymeric form at the rate of slow axonal transport. Paradoxically, these photobleaching experiments also indicated that while microtubules do not translocate in the axon, they are dynamic and exchange subunits. Although these experiments show no movement of the axonal microtubules and tend to support a model of distal growth and monomer (or oligomer) transport, they suffer from a general concern that photobleaching experiments generate photodamage that may sever microtubules and inactivate motor or other enzymatic processes.

An earlier model proposed to account for growth of the cytoskeleton was that microtubules and their components were assembled in the cell body and transported down the axon as polymer. This model derives from metabolic labeling studies on axons both *in situ* and *in vitro* . Results from these experiments indicate that microtubule protein is transported in an insoluble form away from the cell body in the "slow component" of axonal transport along with neurofilament protein, spectrin, and numerous other proteins. This form could be the microtubules themselves. However, while these experiments show that tubulin enters the axon and is transported in an insoluble form, it is not clear that the insoluble form is microtubule polymer rather than some non-polymeric transport form of tubulin. Axonal transport of microtubule protein is also supported by the photobleaching experiments of Keith (1988) who showed that photobleached zones of neurons labeled with fluorescent tubulin translocate distally at rates comparable to those determined by metabolic labeling.

Finally, subunits could be assembled at sites along the axonal cytoskeleton. Such a model has all the weaknesses of both proximal and distal addition. Some form of tubulin transport would be needed to support local

growth along the axon. If these tubulin subunits were derived from the microtubules themselves, then there would need to be some mechanism of microtubule extrusion. Alternatively, the tubulin could be transported in some other form. Although many axonal microtubules are stable, there is good evidence for intercalary growth in the axon (Baas and Black, 1990; Okabe and Hirokawa, 1988).

These experiments taken together may indicate that neurons have multiple microtubule assembly sites and it is possible, therefore, that the models are not mutually exclusive. However, a disturbing feature of all the experiments is that each leads to contradictory conclusions and there is no way to evaluate quantitatively which means of microtubule assembly contributes significantly to axonal growth.

With the knowledge of these conflicting models for axonal growth, we felt that the technique of photoactivation of fluorescence would quickly clarify our picture of neuronal growth. We strongly favored the model of microtubule assembly at the growth cone, and predicted that we would be able to detect a moving transport phase of monomer or oligomer. However, the answer to our question was not immediate. The success of caged-fluorescein tubulin in the study of axonal microtubule dynamics was not as rapid as in the study of the mitotic spindle. The caged-fluorescein tubulin is used to follow a fluorescent "mark" on the axonal microtubule bundle. However, since the axons are moving and elongating along the substrata, it was important to be able to correlate the position of the photoactivated mark in the epifluorescence channel and the movement of the axon in phase. These different images require not only the ability to control shutters on two different light paths on the microscope (which our image processing system was already equipped to handle), but the images also have very different light levels and hence different camera gains.

In mitctic cells Tim was able to skirt this problem by controlling the camera manually during the experiment. The process was as follows: He would take a phase image at the outset of the experiment to record the position of the spindle within the cell at a low gain setting, manually change the camera gain to the setting for epifluorescence, record a series of epifluorescence images to monitor the poleward flux, then again manually switch the camera gain back to the phase setting and take another phase image of the cell to determine whether the position of the spindle had changed within the cell. Any cell in which the position of the spindle had changed could not be used to measure poleward flux. This same process was not feasible for studying axonal microtubules since the axons are elongating in culture and constantly moving. Tim Mitchison once again helped out by designing a way to have the cameras set at two different gain controls and the switching between these two controls could be electronically controlled by the image processor. We sent the ISIT camera off to the company with his design specifications and a short time later the camera was returned with the requisite modifications.

The second major problem with the photoactivation experiment was again the labeling of the tubulin. The caged-fluorescein is very insoluble and therefore yields tubulin with a low stoichiometry of labeling. While the initial batches of labeled tubulin gave results which were promising but certainly not publishable, it took a while and some luck to label the tubulin to a level which gave a good signal in these neurons.

The results we obtained were very surprising. I have very distinct memories of showing Marc my first movie. The neuron had a beautiful growth cone, pulling a long segment of axon with a clear photoactivation mark moving at about the same rate as the axon. Marc jumped up and down and bellowed **"It's moving! The spot's moving, I don't believe it!!!"** in his

characteristic enthusiastic manner. The implications of the moving spot were clear: that microtubule polymer itself is transported distally in the axon, and as such serves as **the** transport form for tubulin within the axon. Within several weeks I took enough movies of moving spots to convince myself and Marc that the result was reproducible and consistent in these neurons. Then everything stopped working. I couldn't get the neurons to grow well, or the photoactivations to work. I assumed that I was doing something horribly wrong with my cultures and/or injections. Amusingly, Elly had also had a successful result with imaging microtubules in *Xenopus* neurons at the same time that I was enjoying my first real success; and then was experiencing problems similar to mine with her *Xenopus* cultures. She made the same assumptions about her technical skills. It took us almost a month to get together and realize that we both had the same problems and that it was probably not due to our individual techniques. Neither of us had much experience with primary *Xenopus* cultures, which we now know are prone to horrible infections and seasonal troubles. Together with Elly Tanaka, I spent weeks and weeks identifying the problem with our culture and then developing a more suitable media for growing these neurons. However it took another eleven months to generate a more definitive picture how the axonal microtubule cytoskeleton was generated. These results are presented in chapter 2 and have recently been published in The Journal of Cell Biology.

I would like to take the time here to mention that the picture that I present here of axonal growth, was not created in a vacuum. I can only take some small credit for the work that I have done. Of critical importance in designing these experiments and working out the problems were the ideas of many people. Most significantly, the ideas and results from the work of Elly Tanaka and James Sabry in the lab were instrumental in creating a picture of axonal growth.

Together we spent a lot of time analyzing each others results in the context of our individual results and those presented in the literature. Marc and Tim, of course, worked hard to keep our ideas on track and suggest further experiments. While these experiments certainly do not completely resolve the controversies in the field, and generate more questions than they answer, they go a long way to provide an understanding for how axonogenesis occurs. In regards to my goals as a graduate student to try to understand the role of microtubules in cellular morphogenesis, I feel that I have learned a great deal, but there is still a lot of open territory for experimentation. In the conclusions to this thesis, I suggest a number of experiments which would help create a clearer picture of how the axonal cytoskeleton is generated.

Antin, P. B., S. Forry-Schaudies, T. M. Friedman, S. J. Tapscott, and H. Holtzer. 1981. Taxol induces postmitotic myoblasts to assemble interdigitating microtubule-myosin arrays that exclude actin filaments. *J. Cell Biol.* 90: 300-308.

Baas, P. W., and M. M. Black. 1990. Individual microtubules in the axon consist of domains that differ in both composition and stability. *J. Cell Biol.* 111: 495-509.

Baas, P. W., M. M. Black, and G. A. Banker. 1989. Changes in microtubule polarity orientation during the development of hippocampal neurons in culture. *J. Cell Biol.* 109: 3085-3094.

Baas, P. W., J. S. Deitch, M. M. Black, and G. A. Banker. 1988. Polarity orientation of microtubules in hippocampal neurons: uniformity in the axon and nonuniformity in the dendrite . *Proc Natl Acad Sci U S A.* 85: 8335-9.

Baas, P. W., L. A. White, and S. R. Heidemann. 1987. Microtubule polarity reversal accompanies regrowth of amputated neurites. *Proc. Natl. Acad. Sci. USA.* 84: 5272-5276.

Bamburg, J. R., D. Bray, and K. Chapman. 1986. Assembly of microtubules at the tip of growing axons. *Nature.* 321: 778-790.

Bershadsky, A. D., and V. I. Gelfand. 1981. ATP-dependent regulation of cytoplasmic microtubule assembly. *Proc. Natl. Acad. Sci. USA.* 78: 3610-3613.

Bershadsky, A. D., and V. I. Gelfand. 1983. Role of ATP in the regulation of stability of cytoskeletal structures. *Cell Biol. Int. Reports.* 3: 173-187.

Bray, D., and M. B. Bunge. 1981. Serial analysis of microtubules of cultured rat sensory neurons. *J. Neurocytol.* 10: 589-605.

Brink, M., G. Gerisch, G. Isenberg, A. A. Noegel, J. E. Segall, E. Wallraff, and M. Schleicher. 1990. A Dictyostelium mutant lacking an F-actin cross-linking protein, the 120-kD gelation factor. . *J Cell Biol.* 111: 1477-89.

Burnside, B. 1976. Microtubules and actin filaments in teleost visual cone elongation and contraction. *J Supramol Struct.* 5: 257-275.

Burton, P. R., and J. L. Paige. 1981. Polarity of axoplasmic microtubules in the olfactory nerve of the frog. *Proc. Natl. Acad. Sci. USA.* 78: 3269-3273.

Chalfie, M., and J. N. Thompson. 1979. Organization of neuronal microtubules in the nematode *Caenorhabditis elegans. JCB.* 82: 278-289.

Cleveland, D. W., Hwo, S.-Y. and Kirschner, M.W. 1977. Purification of tau, a microtubule-associated protein that induces assembly of microtubules from purified tubulin. 116: 207-225.

Condeelis, J., A. Bresnick, M. Demma, S. Dharmawardhane, R. Eddy, A. L. Hall, R. Sauterer, and V. Warren. 1990. Mechanisms of amoeboid chemotaxis: An evaluation of the cortical expansion model. *Dev. Gen.* 11: 333-340.

De Brabander, M., G. Geuens, R. Nuydens, R. Willebrords, and J. De May. 1981. Microtubule assembly in living cells after release from nocodazole block: the effects of metabolic inhibitors, taxol and pH. *Cell Biol. Int. Reports.* 5: 913-920.

Dustin, P. (1984). Microtubules . New York: Springer-Verlag.

Gerisch, G., J. E. Segall, and E. Wallraff. 1989. Isolation and behavioral analysis of mutants defective in cytoskeletal proteins. . *Cell Motil Cytoskeleton.* 14: 75-9.

Gorbsky, G. J., and G. G. Borisy. 1989. Microtubules of the kinetochore fiber turn over in metaphase but not in anaphase. *J. Cell Biol.* 109: 653-662.

Heidemann, S. R., M. A. Hamborg, S. J. Thomas, B. Song, S. Lindley, and D. Chu. 1984. Spatial organization of axonal microtubules. *J. Cell Biol.* 99: 1289-1295.

Heidemann, S. R., J. M. Landers, and M. A. Hamborg. 1981. Polarity orientation of axonal microtubules. *J. Cell Biol.* 91: 661-665.

Heidemann, S. R., and J. R. McIntosh. 1980. Visualization of the structural polarity of microtubules. *Nature.* 286: 517-519.

Hirose, G., and M. Jacobson. 1979. Clonal organization of the central nervous system of the frog. I. Clones stemming from individual blastomeres of the 16-cell and earlier stages. *Dev. Biol.* 71: 191-202.

Hollenbeck, P. J., and D. Bray. 1987. Rapidly transported organelles containing membrane and cytoskeletal components: their relation to axonal growth. . *J Cell Biol.*

Hotani, H., and H. Miyamoto. 1990. Dynamic features of microtubules as visualized by dark-field microscopy. . *Adv Biophys.* 26: 135-56.

Houliston, E., and R. P. Elinson. 1991. Evidence for the involvement of microtubules, ER, and kinesin in the cortical rotation of fertilized frog eggs. *J Cell Biol.* 114: 1017-1028.

Huffaker, T. C., J. H. Thomas, and D. Botstein. 1988. Diverse effects of β-tubulin mutations on microtubule formation and function. *J. Cell Biol.* 106: 1997-2010.

Huitorel, P., and M. W. Kirschner. 1988. The polarity and stability of microtubule capture by the kinetochore. *J Cell Biol.* 106: 151-159.

Hyman, A. A., and T. J. Mitchison. 1991. Two different microtubule-based motor activities with opposite polarities in kinetochores [see comments] . *Nature.* 351: 206-11.

Kellogg, D. R., C. M. Field, and B. M. Alberts. 1989. Identification of microtubule-associated proteins in the centrosome, spindle, and kinetochore of the early Drosophila embryo. *J. Cell Biol.* 109: 2977-2991.

Kirschner, M. W., and T. Mitchison. 1986. Beyond self-assembly: from microtubules to morphogenesis. *Cell.* 45: 329-342.

Koshland, D. E., T. J. Mitchison, and M. W. Kirschner. 1988. Polewards chromosome movement driven by microtubule depolymerization *in vitro.* *Nature.* 331: 499-504.

Kupfer, A., G. Dennert, and S. J. Singer. 1983. Polarization of the golgi apparatus and the microtubule-organizing center within cloned natural killer cells bound to their targets. *Proc. Natl. Acad. Sci. USA.* 80: 7224-7228.

Letourneau, P. C. 1982. Analysis of microtubule number and length in cytoskeletons of cultured chick sensory neurons. *J Neurosci.* 2: 806-814.

Lim, S. S., K. J. Edson, P. C. Letourneau, and G. G. Borisy. 1990. A test of microtubule translocation during neurite elongation. *J Cell Biol.* 111: 123-130.

Lim, S. S., P. J. Sammak, and G. G. Borisy. 1989. Progressive and spatially differentiated stability of microtubules in developing neuronal cells. *J Cell Biol.* 109: 253-263.

Madreperla, S. A., and R. Adler. 1989. Opposing microtubule- and actin-dependent forces in the development and maintenance of structural polarity in retinal photoreceptors . *Dev Biol.* 131: 149-60.

Matteoni, R., and T. E. Kreis. 1987. Translocation and clustering of endosomes and lysosomes depends on microtubules. . *J Cell Biol.* 105: 1253-65.

Mitchison, T., and M. Kirschner. 1988. Cytoskeletal dynamics and nerve growth. *Neuron.* 1: 761-772.

Mitchison, T., and M. W. Kirschner. 1984. Dynamic instability of microtubule growth. *Nature.* 312: 237-242.

Mitchison, T. J. 1989. Polewards microtubule flux in the mitotic spindle: evidence from photoactivation of fluorescence. *J. Cell Biol.* 109: 637-652.

Mitchison, T. J., and M. W. Kirschner. 1985. Properties of the kinetochore in vitro. II Microtubule capture and ATP-dependent translocation. *J. Cell Biol.* 101: 766-777.

Mogensen, M. M., J. B. Tucker, and H. Stebbings. 1989. Microtubule polarities indicate that nucleation and capture of microtubules occurs at cell surfaces in Drosophila. . *J Cell Biol.* 108: 1445-52.

Ochs, S. 1972. Fast transport of materials in mammalian nerve fibers. *Science.* 176: 252-260.

Okabe, S., and N. Hirokawa. 1988. Microtubule dynamics in nerve cells: analysis using microinjection of biotinylated tubulin into PC12 cells. *J. Cell Biol.* 107: 651-664.

Okabe, S., and N. Hirokawa. 1990. Turnover of fluorescently labeled tubulin and actin in the axon. *Nature.* 343: 479-482.

Pfarr, C. M., M. Coue, P. M. Grissom, T. S. Hays, M. E. Porter, and J. R. McIntosh. 1990. Cytoplasmic dynein is localized to kinetochores during mitosis [see comments] . *Nature.* 345: 263-5.

Pringle, J. R., S. H. Lillie, A. E. M. Adams, C. W. Jacobs, B. K. Haarer, K. G. Coleman, J. S. Robinson, L. Bloom, and R. A. Preston. (1986). Cellular morphogenesis in the yeast cell cycle. In Yeast Cell Biology, J. Hicks, ed., (New York: Alan R. Liss), pp. 47-80.

Rogalski, A. A., and S. J. Singer. 1984. Associations of elements of the golgi apparatus with microtubules. *J. Cell Biol.* 99: 1092-1100.

Sammak, P., and G. Borisy. 1988. Detection of single fluorescent microtubules and methods for determining their dynamics in living cells. *Cell Motility Cytoskel.* 10: 237-245.

Sammak, P. J., and G. G. Borisy. 1987. Microtubule dynamics: direct observation of fluorescent microtubules in living cells. *J. Cell Biol.* 105: 90a.

Schleicher, M., A. Noegel, T. Schwarz, E. Wallraff, M. Brink, J. Faix, G. Gerisch, and G. Isenberg. 1988. A Dictyostelium mutant with severe defects in alpha-actinin: its characterization using cDNA probes and monoclonal antibodies. . *J Cell Sci.*

Schulze, E., and M. Kirschner. 1988. New features of microtubule behaviour observed in vivo. 334: 356-359.

Steuer, E. R., L. Wordeman, T. A. Schroer, and M. P. Sheetz. 1990. Localization of cytoplasmic dynein to mitotic spindles and kinetochores [see comments] . *Nature.* 345: 266-8.

Tassin, A.-M., M. Paintrand, E. G. Berger, and M. Bornens. 1985. The golgi apparatus remains associated with microtubule organizing centers during myogenesis. *J. Cell Biol.* 101: 630-638.

Terasaki, M., L. B. Chen, and K. Fujiwara. 1986. Microtubules and the endoplasmic reticulum are highly interdependent structures. *J. Cell Biol.* 103: 1557-1568.

Tilney, L. G., Y. Hiramoto, and D. Marsland. 1966. Studies on the microtubules in Heliozoa. III. A pressure analysis of the role of these structures on the formation and maintenance of the axopodia of *Actinosphaerium nucleofilum* (Barrett). *J. Cell Biol.* 29: 77-95.

Tilney, L. G., and K. R. Porter. 1965. Studies on the microtubules of Heliozoa. I. The fine structure of *Actinosphaerium nucleofilum* (Barrett) with particular reference to the axial rod structure. *Protoplasma.* 60: 317-344.

Tilney, L. G., and K. R. Porter. 1967. Studies on the microtubules in Heliozoa. II. The effect of low temperature on the formation and maintenance of the axopodia. *J. Cell Biol.* 34: 327-343.

Toyama, Y., S. Forry-Schaudies, B. Hoffman, and H. Holtzer. 1982. Effects of taxol and colcemid on myofibrillogenesis. *Proc. Natl. Acad. Sci. USA.* 76: 5719-5723.

Tsukita, S., and H. Ishikawa. 1981. The cytoskeleton in myelinated axons: serial section study. *Biomed. Res.* 2: 424-437.

Vallee, R. B., and G. S. Bloom. 1991. Mechanisms of fast and slow axonal transport. *Annu Rev Neurosci.* 14: 53-92.

Witke, W., M. Schleicher, and A. A. Neogel. 1992. Redundancy in the microfilament system - abnormal development of *Dictyostelium* cells lacking 2 f-actin cross-linking proteins. *Cell.* 68: 53-62.

CHAPTER 2

The stability to dilution of microtubules assembled in the presence of MAPs *in vivo* and *in vitro* : effects of nucleotides and ionic strength

ABSTRACT

Previous experiments have indicated a role for ATP in the depolymerization of microtubules in cultured fibroblasts. Fibroblasts which have been depleted of ceilular ATP with the metabolic inhibitor, azide, have microtubules which are stable to the effect of the microtubule depolymerizing drug nocodole (Bershadsky and Gelfand, 1981). Fibroblasts which have been permeabilized in the absence of ATP have microtubules which are stable to dilution for long periods in the absence of soluble tubulin. When ATP is added to these permeabilized cells, the microtubules depolymerize rapidly (Bershadsky and Gelfand, 1981). In this chapter, I have repeated the findings on the effects of ATP depletion in cultured fibroblasts. I have also repeated the findings on the effect of ATP in permeabilized cells in both fibroblasts and with microtubules assembled in extracts of *Xenopus* eggs. These findings have been extended to show that high ionic strength buffers also induce the depolymerization of microtubules in permeabilized cells and that the non-hydrolyzable analog of ATP, 5'adenylylimido diphosphate (AMP-PNP), but not other ATP analogs, stabilizes the microtubules to the effects of ATP on microtubules disassembly in permeabilized cells. These results are discussed in light of the finding that several known MAPs such as kinesin and eg-5 bind to microtubules in the presence of AMP-PNP and release from microtubules in the presence of ATP and may have a role in the microtubule stability observed in these two situations.

INTRODUCTION

A great deal of our understanding about microtubule behavior has come from the study of microtubule assembled *in vitro*. The differences between the activities of purified components *in vitro* and the observed behavior of these components *in vivo* reveal how cellular factors modify these behaviors. This study was undertaken to examine several interesting phenomena in cultured cells where microtubules are more stable than purified tubulin. Presumably, an understanding of these particular phenomena will shed some light on the normal regulation of microtubule dynamics in cultured cells. The first phenomenon is that when cultured cells are treated with agents that deplete cellular ATP levels, the microtubules become resistant to drugs (nocodozole or colchicine) which normally depolymerize the microtubules. The second phenomenon is that when cultured cells are permeabilized under certain buffer conditions ("microtubule stabilizing conditions" including millimolar magnesium, low ionic strength, no calcium), the soluble proteins are removed from the cells and the cytoskeleton composed of microfilaments, microtubules and intermediate filaments and their associated proteins is left behind. Under these conditions the monomeric tubulin concentration is virtually zero, however, the microtubules will remain stable for very long periods (up to several hours) and depolymerize only slowly. If, however, ATP is added to the permeabilization buffer, the depolymerization of microtubules is greatly accelerated (Bershadsky and Gelfand, 1981).

Under both of these conditions microtubules display unusual stability which is contrary to what "normally" happens to microtubule polymer assembled from pure tubulin; that is, 1) microtubule polymer *in vivo* and *in vitro* normally depolymerizes when treated with microtubule depolymerizing drugs such as

nocodozole or colchicine, and 2) microtubule polymer *in vitro* depolymerizes when diluted into buffer in the absence of monomeric tubulin. The phenomenon of stability during ATP depletion demonstrates that ATP is required for the action of microtubule depolymerizing drugs *in vivo* and possibly for depolymerization of microtubules in untreated cells, a requirement not seen *in vitro.* This raises the question: what is the role of ATP in cytoskeletal dynamics in normal interphase cells and how does depletion of ATP *in vivo* confer stability to microtubule depolymerizing drugs? The second phenomenon of microtubule stability in permeabilized cells contrasts to the depolymerization that occurs upon dilution of microtubules assembled from pure tubulin *in vitro.* This stability could result from a factor such as a MAP that binds to microtubules *in vivo* and remains bound to and stabilizes these microtubules upon permeabilization in the absence of ATP, and whose release in the presence of ATP allows the microtubules to depolymerize.

In this preliminary and as yet incomplete study, we have repeated the results obtained by others on depletion of ATP in cultured cells *in vivo*, and extended the results on examining the acceleration of microtubule depolymerization in permeabilized cells to include the effects of ionic strength, nucleotides and nucleotide analogs and the effects of cell density. In an effort to develop an assay with more purified components which would be amenable to direct manipulation, we also examined the same phenomenon with microtubule asters assembled onto sperm centrioles in *Xenopus* egg extracts. In addition, preliminary experiments were conducted using purified tubulin and purified kinesin assembled *in vitro* in an attempt to determine if binding of kinesin was responsible for stabilizing microtubules to dilution.

MATERIALS AND METHODS

Materials: ATP, GTP, UTP, CTP, ATPγS, cAMP, ADP and GDP were purchased from Sigma. AMP-PCP, GMP-PCP, GMP-PNP were gifts from Tim Mitchison.

Cells: BSC-1 cells were grown according to Schulze and Kirschner. Briefly, cells were cultured in DME + 10% fetal calf serum. Cells were plated at varying density overnight on acid washed coverslips. For most experiments, an optimal plating density of 5 X 10^3cells/cm^2 was used. At this density a good acceleration of depolymerization in the presence of ATP over 30 minutes was seen.

Azide/nocodozole treatment of cultured cells: Cultured cells grown on 12mm glass coverslips were rinsed twice in PBS and then incubated in PBS containing 10^{-2}M sodium azide for 60 minutes at 37°C. Nocodozole (20μg/ml) was added in the continued presence of azide and the cells incubated for varying amounts of time. Cells were permeabilized in MTSB (80mM KPipes, 5mM EGTA, 1mM $MgCl_2$, pH6.8) containing 0.5%NP40 for 30 seconds, and then fixed in MTSB/0.5% NP40/0.5% glutaraldehyde for 10 minutes. After fixation, cells were placed in PBS containing 1mg/ml $NaBH_4$ for 6 minutes to quench the glutaraldehyde.

Studies in permeabilized cells: Initial permeabilization studies were performed using cells plated on 12 mm coverslips at varying initial plating density. Cells were rinsed in PBS at 37°C, permeabilized in MTSB/0.5% NP40 with or without 1mM specified nucleotide (all incubations involving added nucleotide also contained additional $MgCl_2$ equimolar to nucleotide), incubated for varying lengths of time and then fixed as above. Later studies comparing the effects of ionic strength on permeabilized cells used KAc buffer (X mM

potassium acetate, 15mM KPipes, 10mM EGTA, 2mM $MgCl_2$, 0.5% NP40, pH6.8). Ionic strength was varied by changing the concentration or potassium acetate (ie. moderate ionic strength buffer was designated 150KAc and contained 150mM potassium acetate, 15mM KPipes etc.)

Immunofluorescence and photography: Fixed cells were incubated in PBS/1%BSA/0.1% Triton X-100 and stained with mouse monoclonal DM1β anti-β tubulin and rhodamine labelled goat anti-mouse secondary. Stained coverslips were mounted in PBS/90% glycerol/1 mg/ml para-phenylenediamine. Figures 1 was photographed on a Zeiss Photomicroscope using hypersensitized Kodak Tech-Pan (2415) film. Hypersensitaization was carriout out in a Lumicon Model 1200 hypersensitization chamber (Livermore, CA). The film was developed in Kodak D-19. Figures 2 and 3 were photographed using Kodak TMax400 film on a Zeiss Axiophot microscope. The film was developed using Kodak TMax developer.

Microtubule assembly in *Xenopus* extracts: *Xenopus* extracts prepared from unfertilized eggs naturally arrested in metaphase of meiosis II (CSF-extracts) and *Xenopus* sperm nuclei were a kind gift from Tim Stearns and prepared exactly as previously described (Murray et al., 1989). To generate centrosomes for nucleation of microtubules, 4 µl demembranated sperm nuclei (10 x 10^6 nuclei/ml) (Murray and Kirschner, 1989) were added to 20µl CSF extract containing 2µg/ml nocodozole. Nuclei were incubated for 10 minutes at room temperature, diluted with 400 µl BRB80 (80mM KPipes, 4mM $MgCl_2$, 1mM EGTA) and then spun onto 12 mm coverslips through 2 ml of BRB80/33% sucrose in modified corex tubes (Mitchison et al., 1986) for 10 minutes at 5000 RPM in an HB6 rotor. Microtubule asters were assembled by adding 10µl extract and 1µl rhodamine labeled bovin brain tubulin (Hyman et al., 1990) to a final concentration of 0.2mg/ml directly to the coverslip.

either alone, with 1mM ATP, or 1mM AMP-PNP and 1mM ATP (all incubations with added nucleotide also added equimolar magnesium to compensate for chelation by nucleotide). Coverslips were incubated in dilution buffer for 20 minutes at room temperature and were then fixed by incubating in MTSB/0.5%NP40/0.5% glutaraldehyde for 10 minutes at room temperature, quenched in $NaBH_4$ in PBS (1 mg/ml) for 6 minutes, stained with Hoechst dye and mounted in PBS/90% glycerol/1 mg/ml para-phenylenediamine.

RESULTS:

Azide treatment confers stability to nocodozole:

First, we confirmed previous results which demonstrated that treating cultured cells with agents which deplete cellular ATP levels causes the microtubules to become stable to antimicrotubule drugs. Azide causes the depletion of ATP levels by blocking mitochondrial respiration. Since glycolysis is not blocked, this effect is reversible in the presence of glucose. We examined microtubule stability in three different lines of cultured cells, African Green Monkey kidney fibroblast (BSC-1), canine kidney (MDCK), and mouse fibroblast (L929) cells and found similar results in all three cell types growing at low density in exponential phase cultures. The cell types differed in their general microtubule stability in that L929 cells had the most labile microtubules, MDCK cells the most stable, and BSC-1 had microtubules of intermediate stability. We will limit the discussion to the results in BSC-1 cells which were then followed in additional studies.

BSC-1 cells treated for 60 minutes with 10mM azide had significant resistance to a subsequent challenge with nocodozole. After a 60 minute treatment with azide, the microtubules seemed quite abundant and were often

very straight (figure 1b). This contrasts with control cells, not treated with azide or nocodozole, where the microtubules were more wavy (figure 1a). When azide-treated cells were challenged with a 40 minute treatment with nocodozole in the continued presence of azide, the cells still contained a large array of microtubules (figure 1d). In contrast, cells treated with nocodozole for 40 minutes without azide pretreatment contained very few microtubules especially in smaller cells (figure 1c) while larger cells contained more microtubules (figure 1e). After two hours in nocodozole all microtubules were depolymerized in cells without azide pretreatment (not shown), while azide treated cells still contained large microtubule arrays comparable to those seen after a 40 minute treatment with azide and nocodozole (figure 1f). We found that short treatments (10 to 20 minutes) with 10 mM azide were insufficient to confer a detectable resistance to subsequent challenge with nocodozole in the continued presence of azide (not shown). In BSC-1 cells, we also found that azide treatment conferred resistance to cold depolymerization in addition to resistance to nocodozole (data not shown).

FIGURE 1: Azide treatment confers stability to nocodozole treatment. Immunofluorescence staining of microtubules in BSC-1 fibroblasts: *a.* Control - incubated 60 min in PBS. The microtubule array is dense with many wavy microtubules. *b.* treated 60 minutes with 10mM sodium azide in PBS - note the dense array of straight microtubules. *c.* and *e.* treated with 20μg/ml nocodozole for 40 min. *d.* pre-treated with 10mM azide for 60 min. and then nocodozole 20μg/ml for 40 min. - the microtubule array is very dense compared with *c* and *e.* and *f.* pre-treated with 10mM azide for 60 min. and then nocodozole 20μg/ml for 2 hours. The microtubule array is slightly less dense than control cells. Bar: 50 μm.

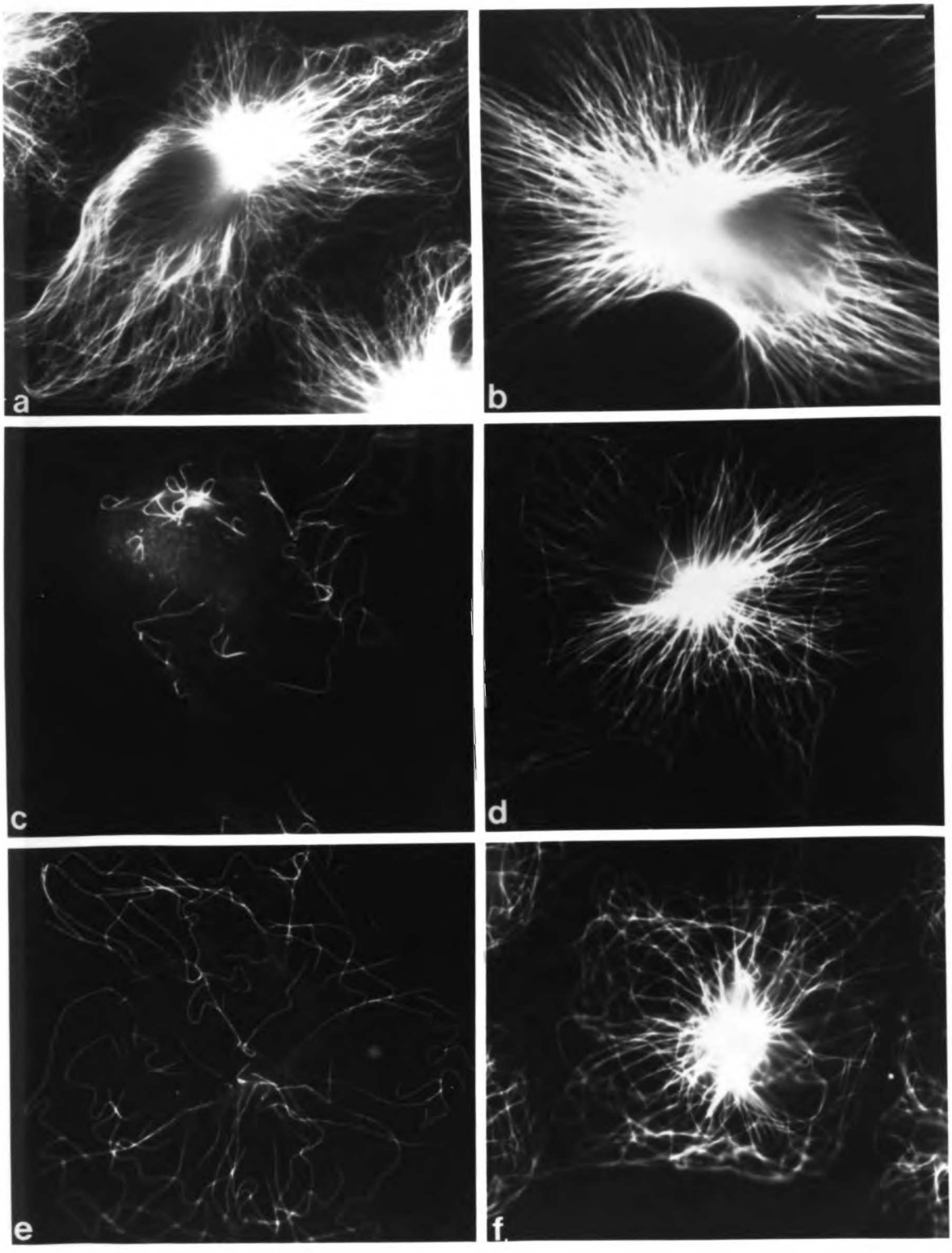
a
b
c
d
e
f

ATP causes accelerated microtubule depolymerization in permeabilized cells:

We repeated the experiment of Bershadsky and Gelfand (1981) showing that in permeabilized cells ATP accelerated microtubule depolymerization (figure 2a,b). Two cell types, BSC-1 and MDCK, were investigated for permeabilization studies. In BSC-1 cells the microtubule arrays were mostly centrosomal based, while MDCK cells contained a large number of non-centrosomal microtubules in addition to the centrosomal array. The results of the permeabilization studies varied slightly between the two cell types but the major effects were the same in these two cell types at low density in exponentially growing cultures and differed mostly at higher plating density and in older cultures. At higher plating density, MDCK cells contained microtubules which were much more stable to the effects of nucleotide and ionic strength. Since we determined that the responses of the BSC-1 were more consistent in these experiments, we did not take any photographs of the results in MDCK cells. We will restrict our discussion to the effects in BSC-1 cells at low density (subconfluent) since these cultures gave reproducible results in all experiments.

We first examined the time dependence of the ATP effect on microtubules in permeabilized cells. Cultured BSC-1 cells were incubated in permeabilization buffer for varying lengths of time in the presence and absence of 1mM ATP. Our preliminary experiments used our standard laboratory microtubule stabilizing buffer (MTSB - see materials and methods), while later experiments used a moderate strength potassium acetate buffer (150KAc - see materials and methods). In this buffer (150KAc), we found that after a 15 minute incubation in the absence of ATP, the permeabilized cells still contained a

moderate microtubule array (figure 2a). Most cells on subconfluent coverslips in the absence of ATP had about 20% depolymerization in 15 minutes compared to cells fixed 15 seconds after permeabilization (not shown). The effect of permeabilization in the presence of ATP was quite striking. After a 15 minute incubation In the presence of ATP, the microtubules in most permeabilized cells were almost completely depolymerized (figure 2b). We noted that cells on the edges of clusters were much more susceptible to the ATP depolymerization than cells that had multiple contacts with other cells. In addition, larger, often multinucleate cells seemed more resistant to ATP than smaller cells. These results supported the results on azide and nocodozole treated cells indicating that larger diameter cells and cells at higher plating density contain more stable microtubules. Therefore the following discussion pertains only to smaller size cells (50 to 70μm diameter), with few or no contacts with adjacent cells which gave consistent results in these experiments.

We reasoned that the stability of microtubules in permeabilized BSC-1 cells might be due to a factor(s) such as a MAP bound to the microtubules. The binding of a factor to microtubules both in permeabilization buffer and in buffer plus ATP might also be influenced by the ionic strength. In the next series of experiments (data not shown) we determined that low ionic strength permeabilization buffer (50KAc) and absence of nucleotide were stabilizing factors, while higher ionic strength (200KAc) permeabilization buffer was able to depolymerize microtubules even in the absence of ATP. Under low salt conditions (50KAc), the microtubules do not fall apart in the presence of nucleotide unless much higher ATP concentrations are used or after much longer time points. For example, cells permeabilized in low salt buffer without ATP (50KAc) had stable microtubules for several hours (we looked at 2 hours). These cells had little or no depolymerization in the presence of ATP after 30

minutes but showed significant depolymerization after 2 hours ("significant" roughly estimated to be 90% of microtubules present in cells fixed after permeabilization in MTSB for 15 seconds). Cells permeabilized at high ionic strength (200KAc) in the absence of ATP showed some depolymerization at 30 minutes and complete depolymerization at 2 hours. When ATP was added to the high ionic strength permeabilization buffer, the microtubules depolymerized in 10 minutes. Therefore, in order to assay for the effects of nucleotide on microtubules in permeabilized cells, in higher ionic strength buffers, shorter time points should be used, while in low ionic strength permeabilization buffer, a longer time point should be used. We found it convenient to assay cultures after 15 minutes incubation in a moderate ionic strength buffer (150mM KoAc, 15mM KPipes) since microtubule arrays were moderate in the absence of ATP and depleted in the presence of ATP. The following discussion of nucleotide effects used this assay condition.

Bershadsky and Gelfand (1981) found that this effect of nucleotide to accelerate depolymerization of microtubules in permeabilized cells was specific to ATP and that other nucleotides would not cause the accelerated depolymerization (Bershadsky and Gelfand, 1981). To test if the effect in BSC-1 cells was specific to ATP, we incubated permeabilized cells with various nucleotides and hydrolysable and nucleotide analogs. Representative results of these experiments are shown in figure 2. We found that millimolar UTP, GTP, CTP and ATPγS would also cause accelerated microtubule depolymerization to the same extent as ATP. As shown in figure 2*a* and *b* for ATP, microtubules would completely depolymerize within 30 minutes when cells were permeabilized in the presence of millimolar GTP, UTP, CTP and ATPγS. No effect was seen with ADP, cAMP, GDP, or pyrophosphate and the microtubule arrays resembled those shown in figure 2a. We also controlled for effects of

chelation of Mg^{2+} by ATP by varying the Mg^{2+}concentration in the presence of ATP, with no detectable effect. The non-hydrolysable analogs AMP-PNP, AMP-PCP, GMP-PNP, and GMP-PCP also did not accelerate the depolymerization of microtubules in permeabilized cells; (AMP-PCP is shown in figure 2*c* and AMP-PNP in figure 2*e*). The microtubules in cells permeabilized in the absence of all nucleotides, or in cells permeabilized in the presence of the non-hydrolyzable analogs AMP-PNP, AMP-PCP, GMP-PNP, and GMP-PCP looked essentially the same. However in cells permeabilized in the presence of AMP-PNP, the microtubules seemed more abundant. We determined that nucleotides besides ATP were not as effective in accelerating microtubule depolymerization as ATP, since ATP was effective at concentrations down to 50μM, while UTP and GTP were effective only in the millimolar range.

5'Adenylylimido diphosphate (AMP-PNP) stabilizes the microtubules to ATP-induced depolymerization:

Since the non-hydrolysable analogs did not accelerate the depolymerization of microtubules in permeabilized cells, we wondered whether these analogs were even interacting with the microtubules and/or MAPs, and if so, whether they might moderate the effects of the nucleotides. We incubated permeabilized cells first with non-hydrolyzable analogs for 15 minutes, and then with nucleotide plus analog for an additional 15 minutes. While we did not use all possible combinations, we found that in all cases AMP-PNP stabilized the microtubules to the depolymerizing effects of all nucleotides tested (ATP, UTP, GTP, ATPγS in the millimolar range). Figure 2*e* shows cells permeabilized in the presence of AMP-PNP. The microtubule array is very similar to control cells permeabilized in the absence of nucleotide (compare 2*e* with 2*a*). If cells

which are permeabilized in the presence of AMP-PNP are then treated with ATP in the continued presence of AMP-PNP, the microtubules do not depolymerize (figure 2*f*) and the microtubules appear similar to control cells permeabilized in the absence of all nucleotide (compare figure 2*f* with 2*a*). Therefore, the non-hydrolyzable analog AMP-PNP appears to confer a stability to the effects of ATP as well as to the other nucleotides which cause depolymerization in permeabilized cells (GTP, UTP, CTP and ATPγS - data not shown). None of the other non-hydrolysable analogs tested (AMP-PCP, GMP-PNP, GMP-PCP) significantly diminished the accelerated depolymerization caused by added nucleotide in the continued presence of the non-hydrolysable analog. Figure 2*d* shows cells treated first with AMP-PCP for 15 minutes and then with AMP-PCP in the presence of ATP. Unlike the abundant array of microtubules present in cells which were permeabilized in the presence of AMP-PNP and then treated with ATP(figure 2*e* and *f*), there are few microtubules remaining after ATP treatment (figure 2*d*) in cells permeabilized in the presence of all other non-hydrolyzable analogs besides AMP-PNP that we tested; (AMP-PCP is shown in figure 2*e* and 2*f*; GMP-PNP and GMP-PCP data not shown).

We also briefly examined whether treatment with azide would stabilize the microtubules to permeabilization in the presence of ATP. We found little difference in response to ATP- accelerated depolymerization of microtubules between cells which had been treated before fixation with azide and cells with no azide treatment (data not shown).

FIGURE 2: ATP causes microtubules in permeabilized cells to depolymerize more rapidly, and AMP-PNP stabilizes the microtubules to the effects of ATP. BSC-1 cells were permeabilized in moderate ionic strength permeabilization buffer (150KAc - see Materials and Methods) containing the following additions: *a.* buffer alone for 30 minutes; *b.* buffer alone for 15 minutes then buffer plus 1mM ATP for 15 minutes; *c.* buffer plus 1mM AMP-PCP for 30 minutes; *d.* buffer plus 1mM AMP-PCP for 15 minutes, then buffer plus 1mM AMP-PCP plus 1mM ATP for 15 minutes; *e.* buffer plus 1mM AMP-PNP for 30 minutes; *f.* buffer plus 1mM AMP-PNP for 15 minutes, then buffer plus 1mM AMP-PNP and 1mM ATP for 15 minutes. The cells were then fixed with glutaraldehyde and processed for immunofluorescence with mouse anti-tubulin antibody and rhodamine goat anti-mouse secondary. Note that in cells treated first with AMP-PNP (*e, f*), the microtubules don't depolymerize in the presence of ATP, whereas cells treated with ATP without prior treatment with AMP-PNP have significant microtubule depolymerizaion (*a, b*). Note also that microtubules in cells permeabilized in the presence of other non-hydolyzable ATP analogs still depolymerize in the presece of ATP; (*c, d*) show the effects of AMP-PCP, but the same effect was seen with GMP-PNP and GMP-PCP (not shown). Bar: 50 μm.

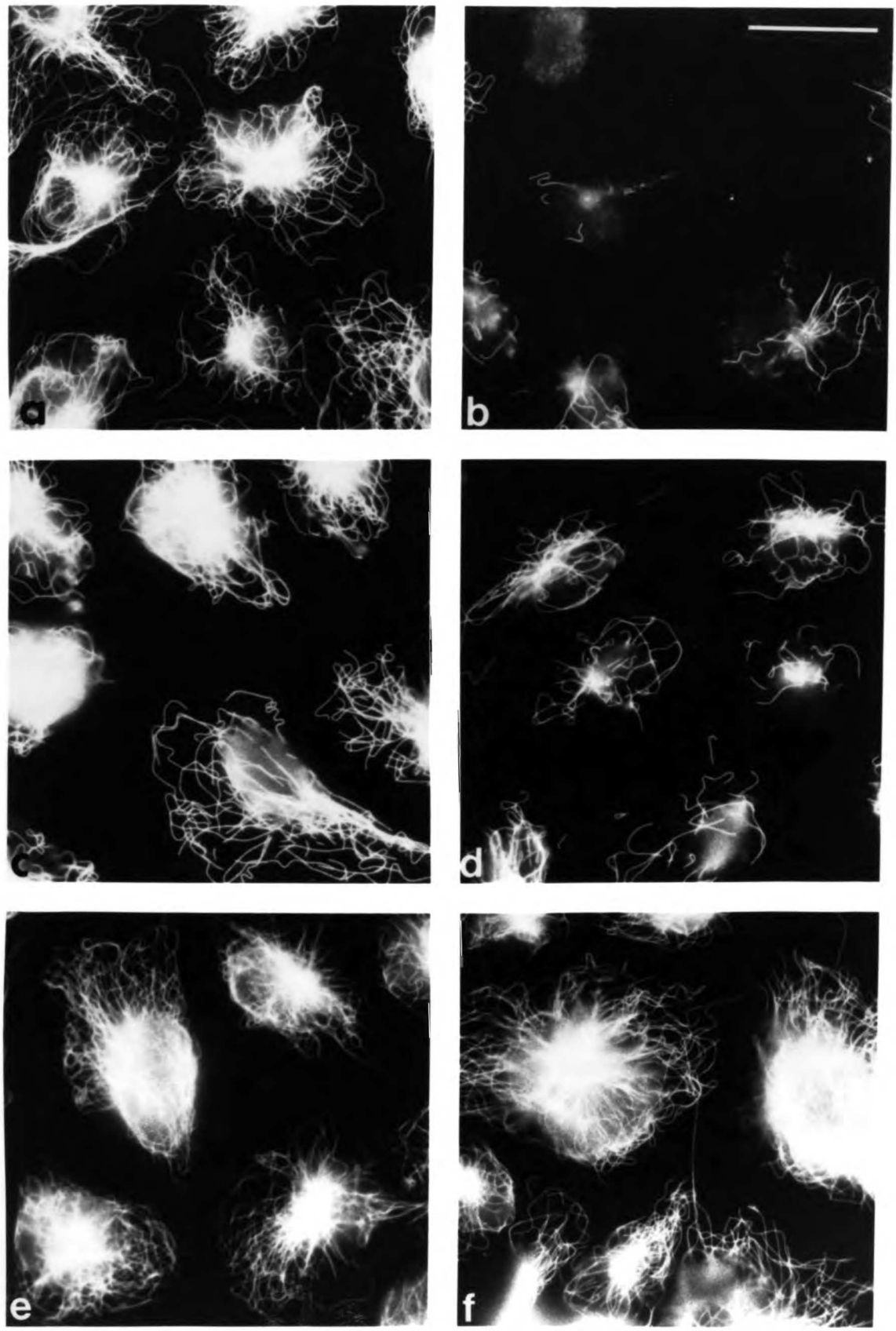
a
b
c
d
e
f

Microtubules assembled in *Xenopus* extracts show the same nucleotide specificities as cultured mammalian cells:

A preliminary attempt was made to characterize the phenomenon of AMP-PNP stabilization of microtubules in a system which might be more amenable to direct manipulation. Extracts of *Xenopus* eggs arrested in metaphase II of meiosis (CSF-*Xenopus* extracts)* contain large amounts of tubulin and centrosomal components and readily assemble microtubule asters when demembranated sperm nuclei are added (Sawin and Mitchison, 1991). These asters can be easily visualized if tubulin derivitized with rhodamine is added to the egg extract. The extracts can also be diluted, fractionated, programmed for mitosis or interphase, etc. and are ideal for examining and manipulating microtubule dynamics.

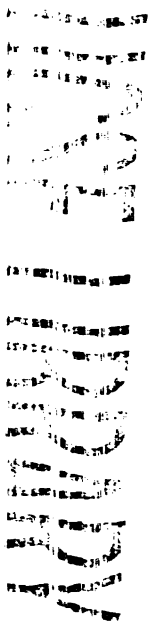

To assay whether microtubules assembled in these *Xenopus* extracts show similar dynamics when the microtubules are diluted as do cultured fibroblasts when permeabilized, we assembled rhodamine-tubulin labeled asters in CSF-*Xenopus* extract for 10 minutes, and then diluted the extract 100-fold in microtubule stabilizing buffer (MTSB - see Materials and Methods) with or without nucleotide for 20 minutes and then fixed the asters. Figure 3a shows the large asters assembled for 10 minutes, diluted for twenty minutes in MTSB/0.5%NP40, and then fixed. These asters are only slightly smaller than those fixed immediately after assembly (not shown). In addition, the figure shows that many non-centrosomal microtubules have assembled in the extract. Figure 3b shows the Hoechst staining of the sperm nuclei. There are many

* These have been termed CSF extracts by Murray et al. (1989) since they are prepared from unfertilized eggs which are naturally arrested in metaphase of meiosis II, through stabilizing effects of cytostatic factor (CSF) (Masui, 1971) on the activity of maturation promoting factor (Murray, 1989).

non-nuclear small dots that also stain with the Hoechst dye, these are presumably mitochondria and appear to be very numerous in the microtubule aster.

When ATP was added to the dilution buffer and incubated for 20 minutes, the asters contained many fewer microtubules (figure 3c) and the aster size decreased from 65μm to 30μm (compare figure 3a and 3c). There were very few non-centrosomal microtubules remaining after ATP treatment. The Hoechst staining also shows that the number of non-nuclear small dots was very much reduced (figure 3d) while the nuclear staining remained the same. Therefore, like the microtubules in permeabilized cultured mammalian cells, the microtubules assembled in *Xenopus* egg extract also depolymerize more rapidly when diluted in the presence of ATP.

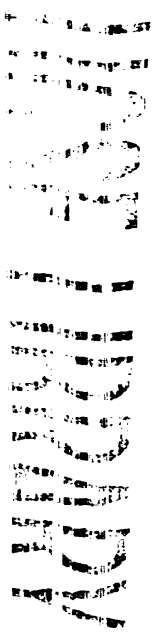

Figure 3e shows that the microtubules in assembled *Xenopus* egg CSF extract are stabilized in the presence of AMP-PNP. AMP-PNP was added both to the extract during assembly as well as to the dilution buffer which contained ATP. The asters which remained after 20 minutes are much larger than those diluted in MTSB with ATP as well as those diluted in MTSB without ATP (compare figure 3e with figures 3c and 3a). We did not examine the effects of other nucleotides or nucleotide analogs in the *Xenopus* extracts. However it is clear that like the microtubules in BSC-1 fibroblasts, AMP-PNP stabilizes the microtubules in *Xenopus* extracts to the effects of dilution in the presence of ATP.

Figure 3. Microtubules assembled in *Xenopus* extracts show the same nucleotide specificities as cultured mammalian cells. Microtubules were assembled in *Xenopus* extracts as described in Materials and Methods. After assembly for 10 minutes at room temperature, the asters were diluted in MTSB containing the following for 20 minutes: *a.* and*b.* MTSB alone; *c.* and *d.* MTSB plus 1 mM ATP; and *e.* and *f.* MTSB plus 1mM AMP-PNP and 1mM ATP. The diluted asters were then fixed with glutaraldehyde and stained with antibody against β-tubulin (panels *a, c,* and*e*) and with Hoechst dye to show the nuclei where the centrosomes are located (panels *b, d,* and *f*). Note the large microtubule arrays in the presence of AMP-PNP plus ATP (panels *e,* and *f*) and the absence of such arrays in the presence of ATP alone (panels *c* and*d*) Bar: 50 μm.

Does binding of purified kinesin stabilize microtubules assembled from pure tubulin in vitro? - preliminary experiments:

The above finding that AMP-PNP stabilizes the microtubules assembled *in vivo* and in *Xenopus* extracts to dilution in the presence of ATP indicated that binding of kinesin, or a similar molecule might be acting to stabilize the microtubules to the enhanced depolymerization in the presence of ATP. Kinesin is abundant in cultured cells and in *Xenopus* eggs. In *in vitro* assays for microtubule gliding, kinesin binds to microtubules in a rigor state in the presence of AMP-PNP and allows microtubule gliding in the presence of ATP. We therefore set about to develop an assay for stabilization of microtubules assembled *in vitro* in the presence of kinesin. Several different methods were used, all of which had limitations and gave ambiguous results. These will be discussed briefly without showing any primary data, and ideas for better assays will be presented.

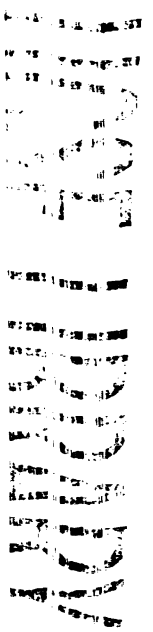

The first assay was to try to mimic the conditions in cells by assembling microtubule asters on purified centrosomes under conditions where nucleated microtubule assembly was favored over free assemlby. We used centrosomes assembled in *Xenopus* CSF extracts onto *Xenopus* sperm nuclei and then spun through a sucrose cushion onto coverslips. We attempted to assemble purifed rhodamine labeled bovine brain tubulin in the microtubule assembly buffer, BRB80, (see materials and methods) at 37°C onto centrosomes. However, no centrosomal based-assembly was seen. At concentrations favoring centrosomal assembly no assembly at all was seen, and at higher concentrations, only free microtubules were assembled. Further experiments indicated that centrosomes assembled in *Xenopus* CSF extract 1) inactivate rapidly at 37°C, 2) inactivate rapidly in BRB80 (and several lower ionic strength

purifed *Xenopus* tubulin which normally assembles at room temperature. Several attempts were made to use free microtubules assembled on coverslips (without centrosomes) as an assay system. The problems with this assay were that microtubules assembled in the presence of kinesin stick to coverslips better than microtubules assembled without kinesin, and AMP-PNP causes microtubules to bind to kinesin even stronger. Therefore, the only microtubules which bind to the coverslip are those with kinesin bound to them, and in the presence of AMP-PNP more microtubules bind to the coverslip via kinesin - not necessarily because there is more assembly nor because the microtubules are more stable.

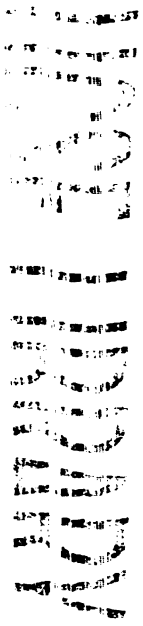

Finally, we assayed the ability of kinesin to stabilize microtubules to dilution using purfied bovine brain tubulin and kinesin assembled at 37°C onto stable seeds in solution and then fixed and spun onto coverslips. The advantage that this assay presented over the previous assays was that all microtubules were fixed and spun onto coverslips and could be measured, and not just the microtubules which stuck to the coverslips via kinesin as in the previous assay. The seeds were made with very bright rhodamine labeled tubulin assembled in the presence of GMP-CPP. Microtubules were assembled with less intense rhodamine tubulin so that polarity-marked microtubules were generated (Hyman and Mitchison, 1990; Koshland et al., 1988). We compared microtubules assembled in the presence or absence of kinesin and then diluted 10-fold in BRB80. Microtubules were assembled with or without kinesin under three conditions: with either AMP-PNP, ATP or no added nucleotide, and then diluted in BRB80 containing the same nucleotide concentration. Microtubules were fixed at various time points during assembly, after addition of kinesin and after dilution. They were then spun down onto coverslips, imaged, and photographed for quantitation. There were several problems with this assay,

however a few conclusions can be made. First microtubules assembled in the presence of kinesin with AMP-PNP or no added nucleotide become bundled. No bundling was seen in the presence of ATP except that microtubules with two seeds were prevalent in the sample. Microtubules with two seeds could arise by annealing of two microtubules end-on, or by two microtubules bound together via kinesin. No bundled microtubules or microtubules with more than one seed were seen with tubulin assembled in the absence of kinesin. All microtubules containing a single seed appeared to shrink at the same rate, whether in the presence or absence of kinesin and regardless of nucleotide. Microtubules with two seeds, in the presence of ATP shrunk back to the seeds with a microtubule length between. Microtubules with kinesin assembled and diluted in AMP-PNP or BRB80 remained bundled during dilution. It was not clear whether these bundles contained microtubules with a single seed, or microtubules with a stable seed at each end. If these bundles contained microtubules with a single seed, then kinesin could stabilize microtubules which are bundled.

DISCUSSION

The data presented here confirm previous results showing that depletion of cellular ATP in cultured cells confers stability to microtubule depolymerizing drugs. These results also confirm the results of Bershadsky and Gelfand which showed that in detergent extracted secondary cultures of mouse fibroblasts, the presence of ATP accelerates the depolymerization of microtubules. We have found that all nucleoside triphosphates and ATPγS will accelerate microtubule depolymerization in the BSC-1 fibroblasts. This contrasts to the results of Bershadsky and Gelfand which showed that the accelerated depolymerization

of microtubules was specific to ATP (Bershadsky and Gelfand, 1981). We have also shown that microtubules assembled *in vitro* in extracts of *Xenopus* eggs are stable to dilution in microtubule stabilizing buffer in the absence of soluble tubulin. Like the microtubules in cultured cells, microtubules assembled in these extracts will depolymerize when diluted in the presence of ATP.

We have extended the results on the ability of ATP to accelerate the depolymerization of microtubules to show that the non-hydrolyzable analog AMP-PNP stabilizes the microtubules to the effect of nucleotide during permeabilization in BSC-1 fibroblasts and during dilution of microtubules assembled in *Xenopus* extracts. An attractive hypothesis for how AMP-PNP is acting to stabilize microtubules assembled *in vivo* and in *Xenopus* extracts to ATP-accelerated depolymerization is that a microtubule associated protein (MAP) like kinesin remains bound to the microtubules after detergent extraction. In the presence of AMP-PNP kinesin binds microtubules in a rigor state, whereas ATP allows kinesin to move along the microtubules. This differential action of AMP-PNP and ATP on kinesin binding to microtubules is useful for purification of kinesin and has been demonstrated in microtubule gliding assays *in vitro* (Shimizu et al., 1991). A simple explanation for our results is that kinesin remains bound to and confers stability to microtubules in permeabilized cells in low salt and is released from the microtubules in the presence of ATP allowing them to fall apart, but binds even stronger in the presence of AMP-PNP so the microtubules are stable. AMP-PNP has been shown to induce a rigor state at the kinetochore in *in vitro* assays and prevents both plus-end and minus-end directed movements (Hyman and Mitchison, 1990). Interestingly, the minus-end directed movements which result in shortening of the microtubules attached to kinetochores are only inhibited if the AMP-PNP is added before microtubule-kinetochore complexes are diluted which initiates catastrophe.

An alternative but less likely explanation of our results is that a microtubule associated protein is bound to and stabilizes the microtubules in phosphorylation-dependent manner. This model would require that 1) the stabilizing factor be bound to and stabilize the microtubules in the dephosphorylated state and release from and destabilize the microtubules upon phosporylation; 2) the stabilizing factor be a kinase whose autophosphorylation causes release from the microtubules or that the stabilizing factor be tightly associated with a kinase on the cytoskeleton; and 3) that the kinase show the same pharmacology as kinesin - that is to use ATP in the micromolar range but other nucleotides in the millimolar range and to bind AMP-PNP stronger than ATP. Kinases have been shown to be associated with the cytoskeleton (Lamb et al., 1990; Palazzo et al., 1989; Serrano et al., 1989; Zhou et al., 1991). If this stabilizing activity is due to a factor whose binding is regulated by phosphorylation, then the kinase reponsible for the phosphorylation would have to be a very special kinase.

The ability of nucleotides other than ATP to cause accelerated depolymerization may occur via several mechanisms which will be discussed in turn. First, there may be contaminating ATP in our stocks of other nucleotides. This possibility was not investigated further but could be assayed. Second, a nucleoside diphosphate (NDP) kinase could be associated with the cytoskeleton could convert ADP associated with the cytoskeleton to ATP. NDP kinases are associated with cytoskeletal preparations from brain (Nickerson and Wells, 1984; Penningroth and Kirschner, 1977) and colocalize with microtubules in murine fibroblasts and *Drosophila* SD19 cells (Biggs et al., 1990). This possibility is consistent with the result that nucleotides other than ATP were required in the millimolar range to see an effect on depolymerization, however we that the substrates for these NDP kinases, that is NMP and NDP,

might not be associated with the cytoskeleton under the high dilutions used in these experiemtns. A third explanation is that nucleotides other than ATP bind with decreased affinity relative to ATP directly to the microtubule-associated factor (MAP) which then causes release of that factor. The cytoskeletal motors kinesin, dynein and heavy meromyosin have been shown to be able to use other naturally occuring NTPs and some nucleotide analogs as substrates for microtubule gliding as well as for substrates of the ATPase, usually with decreased efficiency compared to ATP (Shimizu et al., 1991).

It is tempting to speculate that the effects of depleting ATP *in vivo* and the microtubule stability seen during permeabilization of cultured cells or dilution of microtubules assembled in *Xenopus* egg extract is due to the same mechanism: the binding of a factor to microtubules in the absence of ATP which confers stability to the microtubules. In BSC -1 cells which contain normal ATP levels, the microtubules undergo continuous assembly and disassembly with an average half-life of 5 to 10 minutes (Schulze and Kirschner, 1986). Cells which contain normal levels of ATP are susceptible to treatment with nocodozole which causes the disassembly of microtubules. Microtubules in cells with depleted ATP levels do not depolymerize in the presence of nocodozole. This result would support the notion that microtubule depolymerization *in vivo* requires ATP and that the action of nocodozole is to inhibit repolymerization of microtubules rather than enhancing depolymerization. The microtubules in cultured BSC-1 cells and in *Xenopus* egg extracts are assembled in the presence of microtubule associated proteins. The ATP concentration inside the cell and in the *Xenopus* extract is in the millimolar range, and therefore within the range where a factor which releases from microtubules in the presence of ATP would be only transiently bound to the microtubules. Our results would be consistent with the model that there are MAP(s) whose binding to microtubules

is transient in the presence of the high ATP concentration *in vivo*. Larger amounts of MAPs may bind during ATP depletion (azide treatment), and cause the microtubules to become more stable than normal. The normal depolymerization of the microtubules might require the release of bound MAP from the microtubules. Therefore during azide treatment, there may be increased MAP binding to microtubules and decreased depolymerization of microtubules.

Our results do not rule absolutely rule out that the binding of the stabilizing MAP is regulated by phosphorylation of a microtubule-associated protein. However the model of phosphorylation has so many caveats that we favor the more simple model of a stabilizing factor whose binding is directly affected by added nucleotide such as kinesin. In addition to the indirect evidence presented here which may implicate a kinesin-like molecule in stabilization of microtubules, there are several other candidates proteins which may be involved in stabilizing microtubules *in vivo* and *in vitro*. Eg-5, a kinesin-like molecule present in PTK cells and *Xenopus* eggs binds very strongly to microtubules in the presence of AMP-PNP (Sawin and Mitchison, personal comm). When Eg-5 is bound to microtubules in the presence of AMP-PNP, release requires much higher ATP and salt concentrations. As a candidate for binding regulated by phosphorylation, recently a microtubule associated protein (pp170) has been purified from HeLa cells whose binding to microtubules is regulated by ATP (Kreis 1991). In the presence of ATP, pp170 becomes phosphorylated and releases from microtubules, while the unphosphorylated form is able to bind to microtubules. pp170 has not yet been shown to stabilize microtubules and our result with AMP-PNP would indicate that the ATP-induced depolymerization is not due to phosphorylation.

The experiments presented here are only indirect evidence that binding

The experiments presented here are only indirect evidence that binding of a microtubule associated protein like kinesin may stabilize microtubules *in vivo* and *in vitro.* In future experiments, it will be important to demonstrate directly whether the binding of purified kinesin or a related molecule can stabilize microtubules. How the stabilization of microtubules which is important for cellular morphogenesis occurs *in vivo* is still largely unknown. If a cytoskeletal motor such as kinesin could be demonstrated to confer stability to microtubules, this would indicate that microtubules which are used for transport within cells required for cellular processes such as morphogenesis and polarization might be preferentially stabilized.

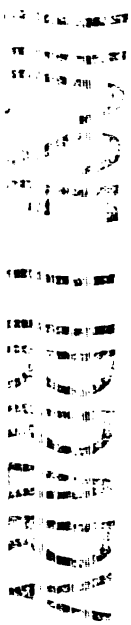

REFERENCES:

Bershadsky, A. D., and V. I. Gelfand. 1981. ATP-dependent regulation of cytoplasmic microtubule assembly. *Proc. Natl. Acad. Sci. USA.* 78: 3610-3613.

Biggs, J., E. Hersperger, P. S. Steeg, L. A. Liotta, and A. Shearn. 1990. A Drosophila gene that is homologous to a mammalian gene associated with tumor metastasis codes for a nucleoside diphosphate kinase . *Cell.* 63: 933-40.

Hyman, A., D. Drechsel, D. Kellog, S. Salser, K. Sawin, P. Steffen, L. Wordeman, and T. J. Mitchison. 1990. Preparation of modified tubulins. *Methods Enzymol.* 196: 478-485.

Hyman, A. A., and T. J. Mitchison. 1990. Modulation of microtubule stability by kinetochores *in vitro* . *J Cell Biol.* 110: 1607-16.

Koshland, D. E., T. J. Mitchison, and M. W. Kirschner. 1988. Polewards chromosome movement driven by microtubule depolymerization *in vitro*. *Nature.* 331: 499-504.

Lamb, N. J., A. Fernandez, A. Watrin, J. C. Labbe, and J. C. Cavadore. 1990. Microinjection of p34cdc2 kinase induces marked changes in cell shape, cytoskeletal organization, and chromatin structure in mammalian fibroblasts. *Cell.* 60: 151-65.

Masui, Y., C. L. Markert. 1971. Cytoplasmic control of nuclear behavior during meiotic maturation of frog oocytes. *J. Exp. Zool.* 177: 129-146.

Mitchison, T., L. Evans, E. Schulze, and M. Kirschner. 1986. Sites of microtubule assembly and disassembly in the mitotic spindle. 45: 515-527.

Murray, A. W., and M. W. Kirschner. 1989. Cyclin synthesis drives the early embryonic cell cycle. *Nature.* 339: 275-280.

Murray, A. W., M. J. Solomon, and M. W. Kirschner. 1989. The role of cyclin synthesis and degradation in the control of maturating promoting factor activity. *Nature.* 339: 280-286.

Nickerson, J., and W. Wells. 1984. The microtubule-associated nucleoside diphosphate kinase. *J. Biol. Chem.* 265: 11297-11304.

Palazzo, R. E., T. J. Lynch, J. D. Taylor, and T. T. Tchen. 1989. cAMP-independent and cAMP-dependent protein phosphorylations by isolated goldfish xanthophore cytoskeletons: evidence for the association of cytoskeleton with a carotenoid droplet protein. *Cell Motil Cytoskeleton.* 13: 21-9.

Penningroth, S. M., and M. W. Kirschner. 1977. Nucleotide binding and phosphorylation in microtubule assembly in vitro. *J. Mol. Biol.* 115: 643-673.

Sawin, K. E., and T. J. Mitchison. 1991. Mitotic spindle assembly by two different pathways in vitro. . *J Cell Biol.* 112: 925-40.

Schulze, E., and M. Kirschner. 1986. Microtubule dynamics in interphase cells. 102: 1020-1031.

Serrano, L., M. A. Hernandez, N. J. Diaz, and J. Avila. 1989. Association of casein kinase II with microtubules. *Exp Cell Res.* 181: 263-72.

Shimizu, T., K. Furusawa, S. Ohashi, Y. Y. Toyoshima, M. Okuno, F. Malik, and R. D. Vale. 1991. Nucleotide specificity of the enzymatic and motile activities of dynein, kinesin, and heavy meromyosin. *J Cell Biol.* 112: 1189-97.

Zhou, R. P., M. Oskarsson, R. S. Paules, N. Schulz, D. Cleveland, and W. G. Vande. 1991. Ability of the c-mos product to associate with and phosphorylate tubulin. *Science.* 251: 671-5.

CHAPTER 3

Microtubule polymer assembly and transport during axonal elongation

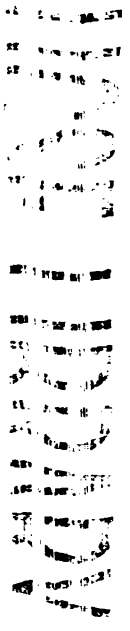

ABSTRACT

As axons elongate, tubulin, which is synthesized in the cell body, must be transported and assembled to generate the axonal microtubule bundle. The mechanism of tubulin transport and the location of assembly of microtubules are currently unknown. We report here the use of tubulin tagged with a photoactivatable fluorescent group to investigate microtubule transport and assembly. Photoactivatable tubulin was microinjected into frog embryos at the 2-cell stage, and the embryos were allowed to develop to neurula stage. The photoactivatable tubulin persisted in injected embryos and was detectable in axonal microtubules in neurons cultured from neural tubes of injected embryos. Local activation in the axon produced a fluorescent mark on the microtubules allowing direct study of transport and turnover. Microtubules in elongating axons were generated in or near the cell body and continually transported distally; marked microtubules remained coherent during axon elongation. This vectorial polymer movement was observed at all levels of the axon, even in the absence of axonal elongation. In addition to transport of polymer from the cell body, new polymer also appeared to be generated by polymerization along the axon and by assembly at the growth cone. Although polymer movement was generally continuous in the axon, near the growth cone polymer movement appeared to respond to growth cone behavior. These results suggest that microtubule translocation is the principal means of tubulin transport and that polymer translocation plays an important role in generating new axon structure at the growth cone.

INTRODUCTION

Cytoplasmic flux in axons was first demonstrated in the classic experiments of Weiss when vesicular elements were found to accumulate at the site of an artificial constriction (Weiss and Hiscoe, 1948). Direct visualization of this transport, both in the axon (Burdwood, 1965; Matsumoto, 1920; Nakai, 1964) and later in isolated axoplasm (Brady et al., 1982; Brady et al., 1985) led to an appreciation that vesicular movements occur on microtubules in both a retrograde and anterograde manner, and later led to the purification of the proteins responsible for generating these movements (for review, see Schroer and Sheetz, 1991; Vale, 1987; Vallee and Bloom, 1991). Although these were important advances in our understanding of axon growth and function, they left unanswered the question of how the structural components of the axon, such as microtubules, are transported and assembled.

Experiments which focussed on cytoskeletal transport in the axon have generated two diametrically opposed explanations of axonal growth (for review, see Bamburg, 1988; Hollenbeck, 1989). In one view, based primarily on metabolic labeling studies, microtubules are thought to be assembled in the cell body and transported down the axon (Hoffman and Lasek, 1975; Lasek et al., 1984). In the other view, based on photobleaching experiments (Lim et al., 1990; Lim et al., 1989; Okabe and Hirokawa, 1990) and local application of microtubule depolymerizing drugs (Bamburg et al., 1986), tubulin is thought to be transported down the axon as monomer and assembled into microtubules at the growth cone. In order to resolve this conflict, we have applied the recently developed technique of photoactivation of fluorescence (Krafft et al., 1986; Mitchison, 1989), and a novel method for labeling microtubules in cultured neurons (Tanaka and Kirschner, 1991) with a photoactivatable tag, to study the transport of microtubules and their sites of assembly in the growing axon.

[redacted]

[redacted]

By marking axonal microtubules using photoactivation, and following the fate of these marks, we can decide among several models for assembly and transport. For example, if tubulin monomer diffused or was transported down the axon and assembled into microtubules at the growth cone, then the mark on the axonal microtubules would be stationary relative to the cell body (the monomeric tubulin would quickly disperse) and, as a consequence, the mark to growth cone distance would increase. If microtubules were assembled at the cell body and subsequently transported down the axon, then the distance from the cell body to the mark would increase and the mark to growth cone distance would remain fixed. If a specialized, slowly diffusing transport form of tubulin were transported relative to a stationary array of microtubules (Weisenberg et al., 1988; Weisenberg et al., 1987), the photoactivated mark would split, with one part remaining stationary and the other moving down the axon. Photoactivation can also be used to determine monomer/polymer dynamics along the axon. For example, if exchange between monomer and polymer were rapid, the photoactivated marks would fade rapidly. If exchange were slow and there was an appreciable pool of monomer, there would be rapid partial fading of the labeled zone, followed by a much slower fading of the remaining signal as it exchanged out of the polymer. There are several possible kinetic behaviors predicted by different models. Though these kinetic properties cannot prove mechanisms, they can be used to rule out mechanisms.

We show here that microtubules are continuously translocated as a stable array distally during axonal elongation. By analyzing the translocation rates of microtubule polymer at different distances along the axon we can determine where microtubule assembly occurs and how much assembly occurs at each site. These results indicate that assembly occurs at both the cell body and the growth cone; microtubule assembly along the axon may also at times

contribute to axonal elongation. Tubulin is transported in the form polymer, and this mechanism of transport probably provides most of the subunits required both for microtubule assembly along the axon and at the growth cone.

MATERIALS AND METHODS

Labeling, Incubation and Plating of Xenopus Embryos

Xenopus embryos were fertilized, injected, incubated and dissected as described in the accompanying paper (Tanaka and Kirschner, 1991) with the following modifications: We used bis-caged fluorescein (C2CF) labeled bovine brain tubulin (Hyman et al., 1990; Mitchison, 1989) or C2CF-labeled dextran at a concentration of 50 μM. For plating labeled neural tubes, two protocols were used: (1) explants were cultured as described (Tanaka and Kirschner, 1991), or (2) neural tubes were dissociated by incubation for five minutes in Steinberg's dissociating medium (58 mM NaCl, 0.67 mM KCl, 4.6 mM Tris pH 7.8-8, 0.4 mM EDTA) before plating, and cultured in RTM (12 mM NaCl, 4 mM KCl, 0.05 mM CaCl, 10 mM $MgSO_4$, 56 mM Na-Isethyanate, 4 mM Na_2HPO_4, 5 mM NaHepes (pH 7.8), 20% L15 with 0.1% gentamycin) supplemented with 1% embryo extract (Harris et al., 1985). All cultures were plated on 40 mm glass coverslips which were sealed with VALAP (vaseline:lanolin:paraffin 1:1:1) over a 35 mm hole drilled in 60 X 15 mm tissue culture dishes and then coated with polylysine and complex extracellular matrix (Tanaka and Kirschner, 1991).

Dextran Labeling

All operations were performed at 25°C. Aminodextran, 10 kD, 3.1 amino groups/mole (Molecular probes, Eugene, OR) was dissolved in DMSO (Aldrich Sure/Seal grade) at 30 mg/ml. C2CF-SNHS (Mitchison, 1989) was added from a 0.1M stock in DMSO to give a final concentration of 1.6 moles/mole dextran,

followed by tri-ethylamine to the same final concentration. After 1 hour, the labeled dextran was precipitated with 5 volumes of ethylacetate, and collected by centrifugation (10 kG for 5 minutes). The dextran was resuspended in DMSO and reprecipitated with ethylacetate. The dextran was then dissolved in aqueous 0.1M $NaHCO_3$ and precipitated with 5 volumes of ethanol. This step was repeated once more. The final pellet was dissolved in water at 50 mg/ml, cleared by sedimentation at 100 kG for 5 minutes, frozen in aliquots and stored at -80^{o}C. The labeling stoichiometry was estimated to be 1.3 C2CF/dextran, and the preparation was free of detectable uncoupled dye as assayed by TLC on silica gel in benzene: acetone: acetic acid 80:20:2. In this system the free dye migrates with an rf of approximately 0.5, while the dextran remains at the origin.

Microscopy

The experiments were performed using an inverted microscope (model IM35; Carl Zeiss) with modifications for photoactivation and epifluorescence as described previously (Mitchison, 1989). Photoactivation and fluorescence observation were performed using a 100/1.3 phase/neofluor objective (Zeiss) and a Hoffman condenser (Modulation Optics, Greenvale, NY) or a Plan APO 60/1.4 oil DM objective (Nikon) and a Nikon phase-contrast 1.25 achromat condenser used as a water immersion condenser. Fluorescent and phase-contrast images were collected with an intensified silicon-intensified target (ISIT) camera (DAGE-MTI, Michigan City, IN) modified for operation with two independent manual gain controls for phase and for epifluorescence. The ISIT camera was directly mounted on the top port of the microscope. Switching between the two gain controls was controlled by the image processor via a digital input/output (DIO) board (DT2817, Data Translation, Marlboro, MA). The

video signal was processed using an IMAGE1 image processing system (Universal Imaging, West Chester, PA). Both trans- and epi-illumination used 100W halogen light sources. To minimize photodamage and photobleaching, and to allow sequential phase and epifluorescence images to be collected, both light sources were controlled by shutters interfaced to the image processor via the DIO board. The photoactivation set-up was as detailed (Mitchison, 1989). Images were stored using either an Optical Disc Recorder (Panasonic model TQ-2028F) or a MacinStor erasable optical device (Storage Dimensions, San Jose, CA).

Photoactivation and Data Collection

Before photoactivation, the labeled neuronal cell was positioned relative to the irradiation beam such that the axon lay perpendicular to the irradiation slit. Labeled cells were distinguished from unlabelled cells by a low background fluorescence. The photoactivation beam was applied for a period of 1 sec to generate a photoactivation mark approximately 5 μm long and spanning the width of the axon. A pair of fluorescence and phase images were collected within 3 seconds, and then at regular intervals (usually 30 or 60 seconds). Typically, the fluorescence image used the epifluorescence halogen source at maximum intensity, the ISIT set at about half-maximal gain (constant for a given run but optimized for each axon), with the shutter open for 1 second to collect 32 frames for a summed image. The phase image used the light source at ~25% maximal intensity, the ISIT camera at low gain, and the shutter open for 0.25 second to collect 8 frames for a summed image. For visualization of microtubules in the growth cone, cooled CCD (Charge Coupled Device) imaging of *Xenopus* growth cones was carried out as described (Tanaka and Kirschner, 1991). However, total microtubules in C2CF-labeled growth cones

were first photoactivated by exposure to a one-second exposure to the mercury lamp through a Hoechst excitation filter (λ=360 nm). The low-intensity fluorescein signal required 2-second exposure times.

Detergent extraction of Xenopus neurons

Xenopus neurons labeled with C2CF-tubulin were photoactivated and phase and epifluorescence images were recorded. Subsequently, 75% of the culture medium was slowly withdrawn and 3/2 vol of microtubule stabilizing buffer (MTSB): 80 mM K-Pipes pH 6.8, 5 mM EGTA, 1 mM $MgCl_2$, 0.5% NP40, containing 20% glycerol, and 10 µm taxol was carefully added to the culture. Phase and fluorescence images were then recorded.

Image Analysis

Line intensity measurements (Figure 4*C/D*) and distance measurements (Figure 5, Figure 6*C/D*) were made using the IMAGE-1 software. For line intensity measurements, a one-pixel-wide line (~0.2 µm wide) was positioned along the center of the axon and the intensity was measured along that line. The preactivation scan was used to determine the average background intensity along the axon which was mathematically subtracted from subsequent scans. Direct image subtraction was not possible because the neurites are constantly moving in the field. For distance measurements, the peak of intensity was used for the position of the photoactivated mark, and the position of the growth cone neck was determined as described (Tanaka and Kirschner, 1991).

Microinjection and Imaging of C2CF-tubulin in BSC-1 Fibroblasts

BSC-1 fibroblasts were cultured and microinjected as described previously (Schulze and Kirschner, 1986) using an automated pressure

injection device (Eppendorf Microinjector 5242, Eppendorf, Freemont, CA). Injected cells were incubated for various amounts of time before total labeled cytoplasmic microtubules were photoactivated by a one-second exposure of the objective field to 360nm light from the mercury lamp in the epifluorescence light path filtered through a Hoechst excitation filter (λ=360 nm). Microinjected cells were then permeabilized for 30 seconds in MTSB to remove soluble tubulin and fixed in MTSB plus 0.5% glutaraldehyde for 10 minutes at room temperature. Fixed cells were rinsed in PBS, quenched for 6 min in PBS containing 1mg/ml $NaBH_4$, rinsed in PBS and were mounted in PBS containing 90% glycerol and 1 mg/ml para-phenylenediamene (Sigma). Fixed cells were observed with the optical system described above.

RESULTS

Labeling Xenopus neural tube axons with photoactivatable tubulin

As discussed in the accompanying paper (Tanaka and Kirschner, 1991), it is possible to label the microtubules of primary neurons from the neural tube by injecting derivatized tubulin into cleaving *Xenopus* embryos. This procedure achieves complete labeling of microtubules without perturbing cellular functions as evidenced by the normal development of the embryos. In the following experiments, we have used this method to introduce photoactivatable bis-caged-fluorescein labeled tubulin into *Xenopus* neuronal cells.

To examine critically the incorporation of photoactivatable tubulin into cellular microtubules, we first injected caged-fluorescein tubulin into BSC-1 fibroblasts, a cell with very favorable morphology. No microtubules were seen without activation. After activation, typical microtubule arrays with resolution to the level of single microtubules were easily seen (Figure 1*A*). There was no accumulation of fluorescent label in any other structure. When cells were fixed

shortly after microinjection, only short fragments of microtubules were visible, most of which were assembled in the periphery of the cell onto the ends of existing microtubules (data not shown). These results were identical to those obtained after injection of biotin-labeled tubulin (Schulze and Kirschner, 1986) suggesting that caged-fluorescein tubulin behaved similarly to other forms of derivatized tubulin in interphase cultured cells. To determine whether the photoactivatable tubulin probe assembled into normal microtubule arrays in neurons, we examined the growth cone, where individual microtubules can be resolved. After photoactivation, individual microtubules can be resolved in the growth cone using a cooled CCD camera, as shown in Figure 1*B*. These images were comparable to those from embryos injected with rhodamine-labeled bovine tubulin (figure 1*C*) and (Tanaka and Kirschner, 1991). In the rest of the experiments reported in this paper, we have studied microtubules in axons, where their tight packing and overlap makes it is impossible to resolve them individually. For these experiments the lower resolution of the ISIT camera is sufficient to follow the bulk microtubule mass. The loss of resolution is compensated for by the greater effective sensitivity of the ISIT camera which requires shorter exposure times and lower light intensities than the CCD.

Figure 1. Incorporation of derivatized bovine brain tubulin in cultured fibroblasts and growth cones of labeled *Xenopus* neurons. *A.* ISIT image of fluorescein signal in BSC-1 fibroblast microinjected with photoactivatable tubulin, incubated 5 minutes, then UV photoactivated, permeablized and fixed. *B.* CCD image of fluorescein signal after UV-photoactivation of live growth cone from *Xenopus* embryo labeled with photoactivatable tubulin. *C.* CCD image of rhodamine signal of live growth cone from *Xenopus* embryo labeled with rhodamine tubulin (courtesy of Elly Tanaka). Bar: (*A*) 20 μm; (*B* and *C*) 5 μm.

Figure 1

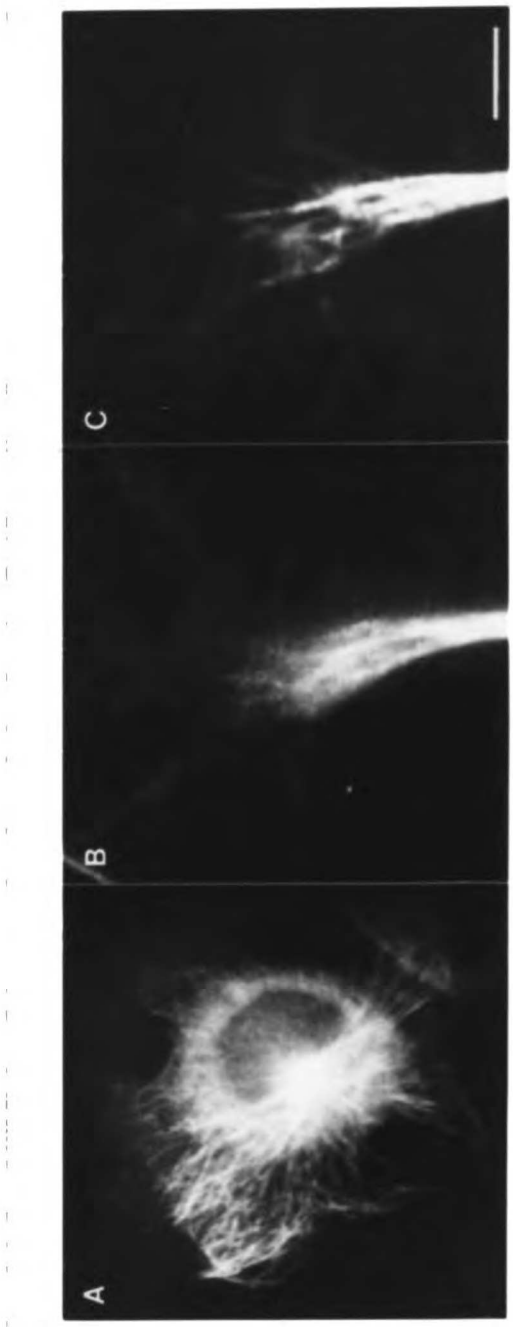

Microtubule polymer translocates distally during axonal outgrowth

To examine the sites of microtubule assembly, the transport of tubulin and the stability of microtubules in elongating axons, we followed the fate of fluorescent marks made by photoactivation in neurons labeled with photoactivatable tubulin. Figure 2 shows time lapse sequences of two such photoactivation experiments. Phase images (figure 2*A* and 2*C*) and the corresponding fluorescence images (figure 2*B* and 2*D*) are shown. In figure 2*A*, we followed an axon that grew out of an explanted neural tube; in figure 2*C* we examined an isolated neuron dissociated from the neural tube. Before activation, as shown in the first frames (figure 2*B* and 2*D*), there was a small amount of fluorescent background in the neurons. This background was most likely due to inadvertent photoactivation during incubation or preparation of the culture. In the second frames, a photoactivation mark was made by exposing the cell through a slit projected onto the axon. The next three frames show the outgrowth of the axons and the relative positions of the activated marks collected as alternating shuttered phase and epifluorescent images. As the axons elongated, the activated marks translocated distally down the axon. On average, the axon shown in figure 2*A-B* elongated at 94 μm/hr and the mark moved at 71 μm/hr, or 75% the rate of growth cone advance. In contrast, the axon in figure 2*C-D* moved at 120 μm/hr while the mark moved considerably slower than the growth cone at 68 μm/hr or 56% the rate of growth cone advance. In both cases the photoactivated mark was made 20 μm from the growth cone.

Two characteristics of the position and intensity of the activation marks deserve mention. These characteristics were found in all cells examined in this report. (1) No detectable activated signal remained at the site of activation. (2) While the intensity of the signal in the mark decreased over time (see a more

quantitative treatment for the axon in figure 2*A/B* in figure 4*D*), there was no rapid decrease in the intensity of the mark. A rapid decrease would be expected if a significant portion of the signal were in a freely diffusible form of tubulin. Thirty seconds after activation, 90-95% of the signal remained. By contrast, in the mitotic spindle, 50% of the photoactivated signal is lost in 30 seconds (Mitchison, 1989).

There are inherent limits in the accuracy by which we could estimate the change in the intensity of the fluorescent marks. These limitations come from many sources, such as the nonlinearity of the ISIT camera, fluctuations in the light source, and the nonuniformity of the microscopic field. Nevertheless we have made an effort to estimate the causes of the loss of intensity with time. In the 21 minutes between the initial activation and the last frame shown in figure 2*A/B,* the decrease in the integrated intensity of the mark is about 50 percent (see intensity scan figure 4*D*). We estimate that 35% of the signal loss in this sequence is attributable to bleaching. In separate experiments, we found that 5 to 10% of the signal was lost in ten second unshuttered exposures of neurons labeled with photoactivatable tubulin. Since each image in this series represents 32 summed frames for a total of 1 second exposure, and images were collected every 30 seconds for 21 minutes, the total exposure is 42 seconds, and the overall intensity loss due to bleaching in this sequence should be ~35%. A second contributing factor was the non-uniformity of the camera field, which is readily visible in figure 2*A*, where the center of the field was brighter than the periphery. Correcting for a uniform background, we can estimate that this contributes about 20% of the gross intensity difference seen in Figure 2*B*. Within the accuracy of the measurements, these two contributing factors, bleaching and camera non-uniformity, accounted for most of the decrease in signal.

Figure 2. Distal translocation of microtubule polymer in elongating *Xenopus* axons. Phase images (*A, C*) and corresponding fluorescein signal (*B, D*) before UV photoactivation (pre) and at times indicated (minutes) following photoactivation. In *A*, the axon exits the explant at the top and growth cone grows down and to the right. In *C*, the cells were dissociated before plating and the cell body is out of the frame of the picture. The thin line indicates position of photoactivation mark at t=0. Note that in both sequences, the photoactivated mark translocates distally as the axon elongates behind the growth cone. Bar: 10 μm.

Figure 2

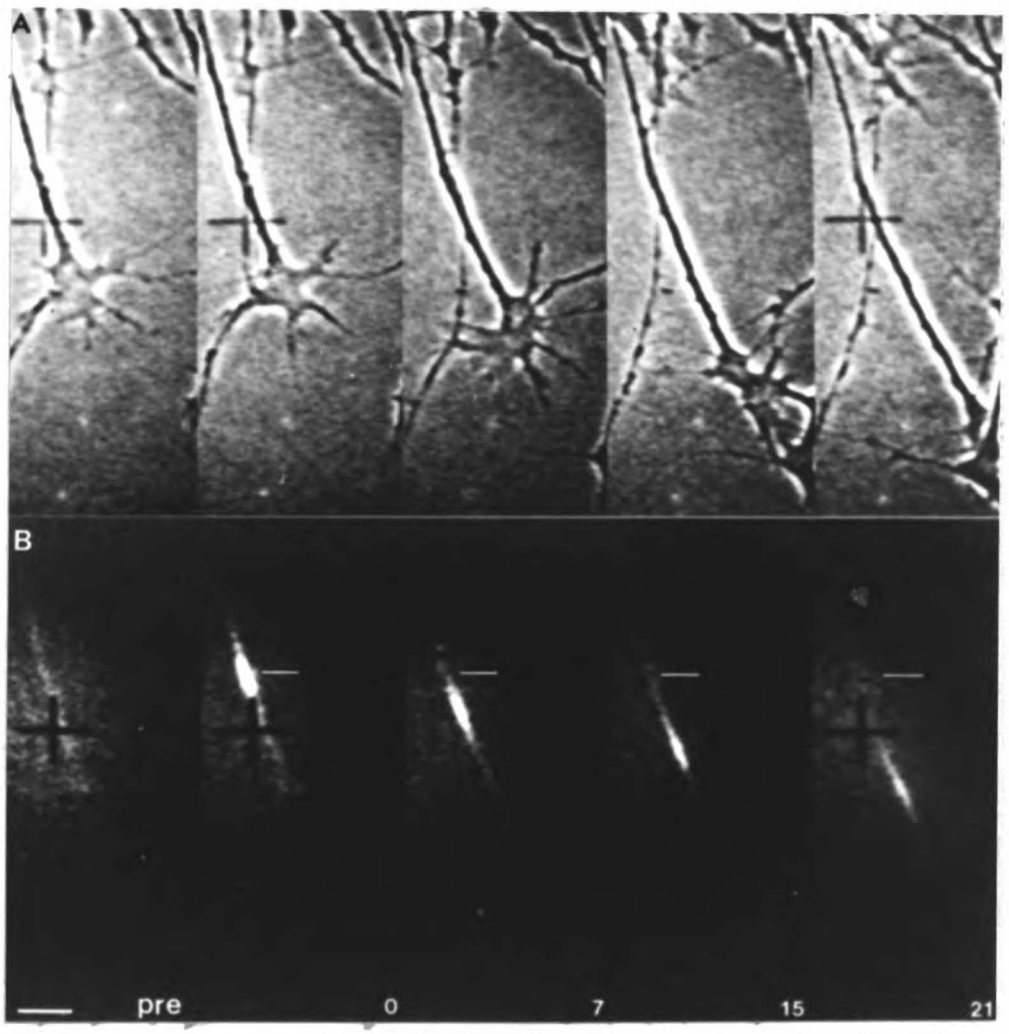

Figure 2

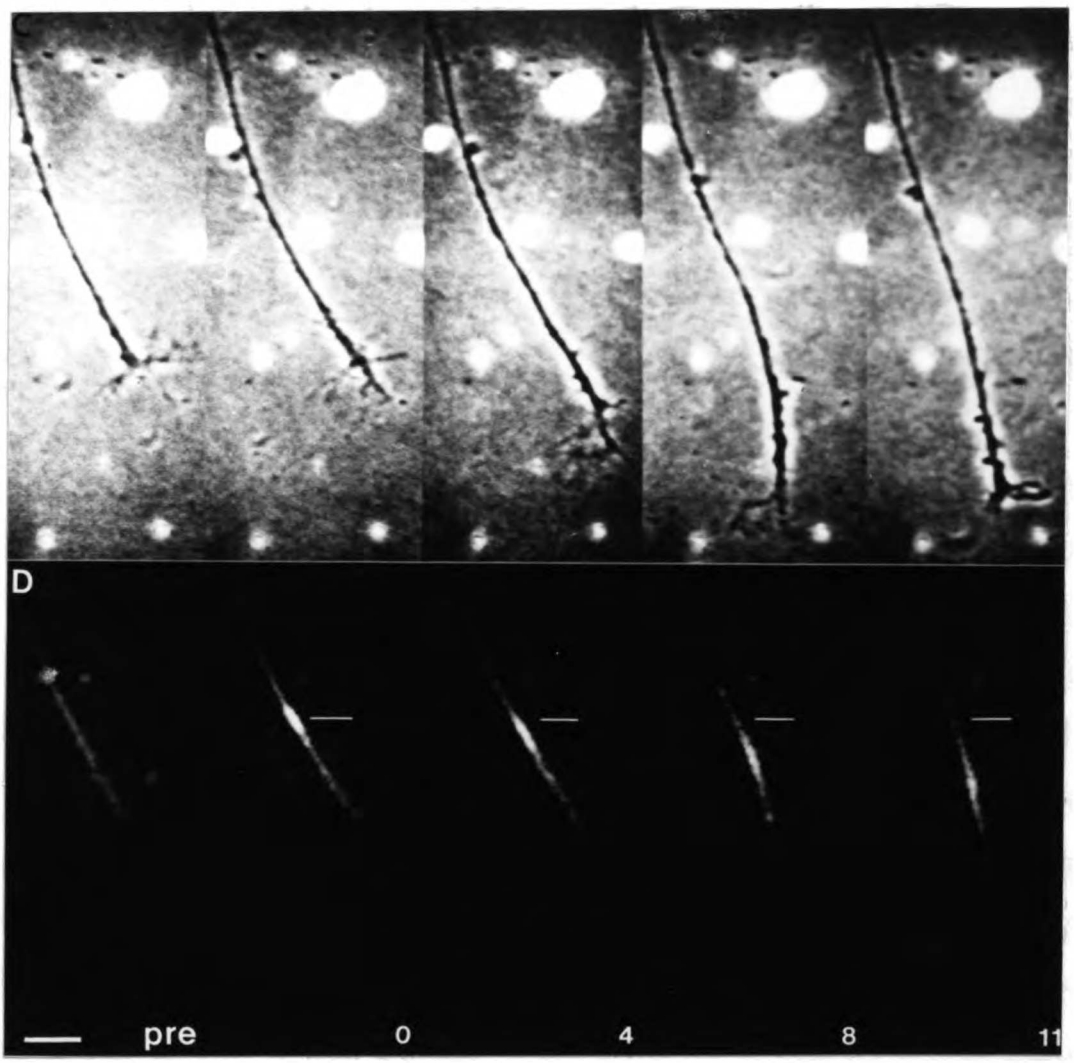

Is the moving signal on microtubules?

High resolution CCD images of activated tubulin in growth cones indicated that the signal was present as linear elements characteristic of individual microtubules (Figure 1*B*). However, since individual microtubules cannot be resolved in axons, further experiments were necessary to demonstrate that the moving signal we observed was on microtubules rather than in non-polymeric forms of tubulin. We performed two types of experiments to characterize the nature of the signal. First, we tested the persistance of label in neurons that were extracted with a non-ionic detergent to remove lipid membranes and soluble molecules. Second, we compared the diffusibility of the photoactivated tubulin signal *in vivo* with that of a photoactivated soluble dextran.

Figure 3 shows phase and fluorescence images of a neuron with two activated marks made before (3*A* and *C*) and after (3*B* and *D*) extraction. Immediately after activation, the cell was permeablized in a microtubule stabilizing buffer containing taxol, thereby effectively removing all soluble tubulin and membranous organelles, and preserving microtubule polymer. The activated regions in 3*A* were still visible in the extracted cell shown in 3*B*, while the phase image demonstrates that the extraction markedly lowered the phase density of the image (compare 3*C* and 3*D*). Furthermore, the polymer that remained after permeablization was very stable under these conditions in the absence of fixation. It was difficult to compare the intensities of the signals before and after extraction since the pH and ionic conditions of the milieu directly affect the fluorescence intensity of the fluorophore, and the internal characteristics of the cytosol are unknown.

When we compared the dispersal of the photoactivatable zone in neurons injected with photoactivatable tubulin with those injected with

photoactivatable dextran of molecular weight 10000, we found that the former behaved like a large polymer, while the latter behaved like a soluble molecule. As shown in Figure 4*A* the dextran signal dispersed almost completely in 104 seconds. By comparison, in Figure 4*B* there was very little spreading or loss of the labeled tubulin in 464 seconds. Figures 4*C* and 4*D* are scans of the fluorescence intensity versus distance along the axon for the photoactivated dextran and tubulin, respectively, over time. Data from 10 cells confirmed the qualitative observations; the dextran signal dispersed rapidly (data not shown). By measuring the width at half maximum of the intensity profiles, we calculated the apparent diffusion coefficients for both the dextran and the tubulin, making the formal assumption that both were behaving as diffusible molecules. The calculated diffusion coefficient for the labeled dextran was 2×10^{-8} cm^2/s while that for tubulin was 4×10^{-10} cm^2/s. If we take the dextran behavior as indicative of soluble macromolecules in the axoplasm, then the small apparent diffusion coefficient of tubulin indicates that the tubulin signal must be in an insoluble, presumably polymeric form. Since large microtubule polymers enmeshed in other elements of the cytoskeleton would be expected to have a negligible diffusion coefficient, the slow rate of broadening of the photoactivated signal is most likely to have other causes, such as slow sliding of microtubules as discussed below.

Figure 3. Detergent extraction following UV photoactivation of *Xenopus* neuron labeled with photoactivatable tubulin. Fluorescein signal (*A, B*) and corresponding phase images (*C, D*) before detergent extraction (*A, C*) and after detergent extraction (*B, D*) of a neuron labeled with photoactivatable tubulin and photoactivated at two positions along the axon. The field was shifted slightly after detergent extraction so the dark and light intensities in the field of the ISIT camera are not in register between the two sets of images. This caused the photoactivation mark closer to the cell body to appear brighter and the distal mark to appear dimmer following detergent extraction. Bar: 10 μm.

Figure 3

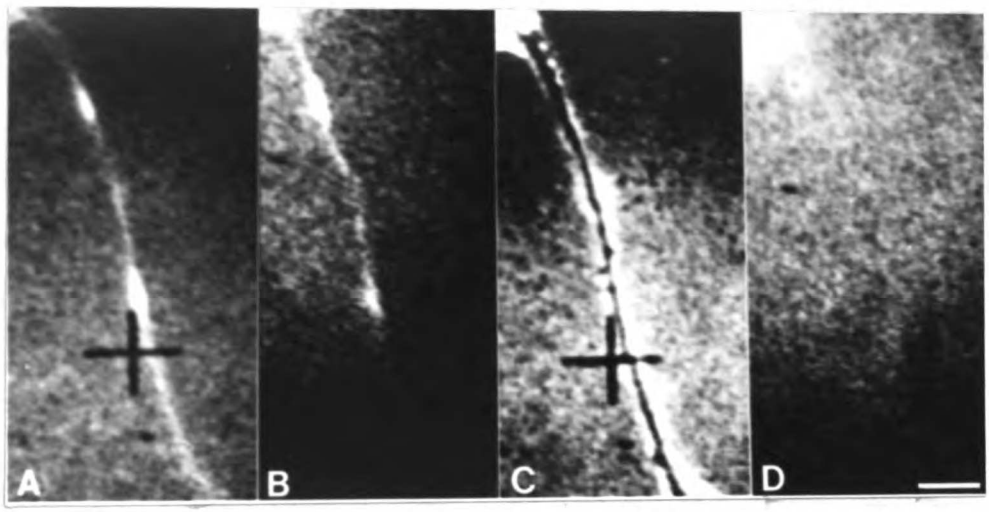

Figure 4. Comparison of the kinetics of diffusion of photoactivatable dextran with photoactivatable tubulin in *Xenopus* neurons. Fluorescein signal immediately following photoactivation and at times (in seconds) indicated for photoactivatable dextran (*A*) and photoactivatable tubulin (*B*). The dextran signal spread throughout the axon and almost returned to a pre-activation level after 105 seconds while the tubulin spread only minimally and decreased in intensity by 30% after 465 seconds. (*C* and *D*) Digitization of dextran and tubulin sequences over longer times matching frames in *A* and *B* respectively. The solid line is the fluorescein intensity at indicated times (in seconds) and is superimposed onto the fluorescence intensity immediately following photoactivation (dotted lines). Abscissa is distance from fiduciary mark on axon proximal to the photoactivated region, so movement of photoactivated tubulin signal is towards the growth cone. Bar: 10 μm.

Figure 4. Comparison of the kinetics of diffusion of photoactivatable dextran with photoactivatable tubulin in *Xenopus* neurons. Fluorescein signal immediately following photoactivation and at times (in seconds) indicated for photoactivatable dextran (*A*) and photoactivatable tubulin (*B*). The dextran signal spread throughout the axon and almost returned to a pre-activation level after 105 seconds while the tubulin spread only minimally and decreased in intensity by 30% after 465 seconds. (*C* and *D*) Digitization of dextran and tubulin sequences over longer times matching frames in *A* and *B* respectively. The solid line is the fluorescein intensity at indicated times (in seconds) and is superimposed onto the fluorescence intensity immediately following photoactivation (dotted lines). Abscissa is distance from fiduciary mark on axon proximal to the photoactivated region, so movement of photoactivated tubulin signal is towards the growth cone. Bar: 10 μm.

Figure 4

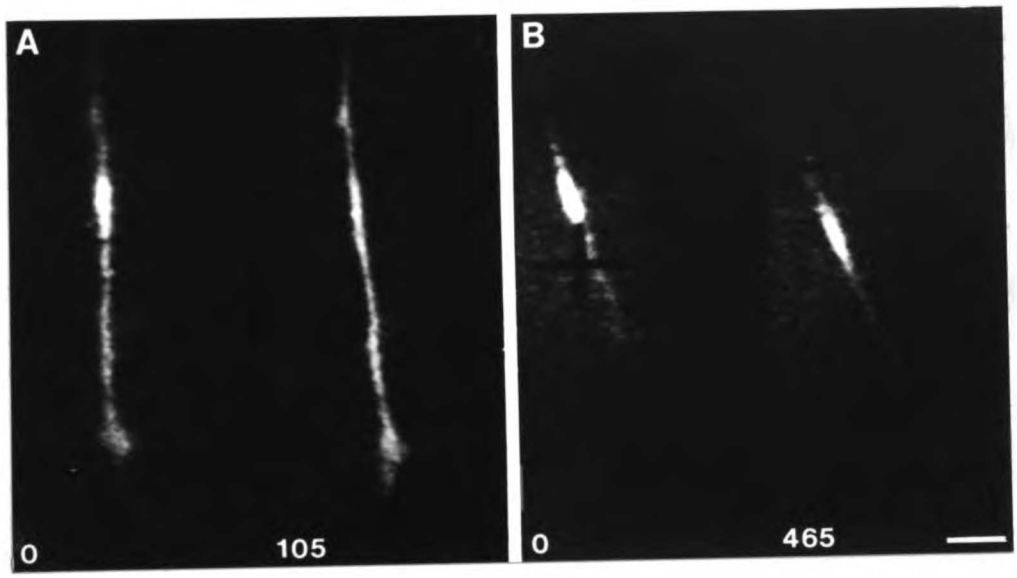

Figure 4

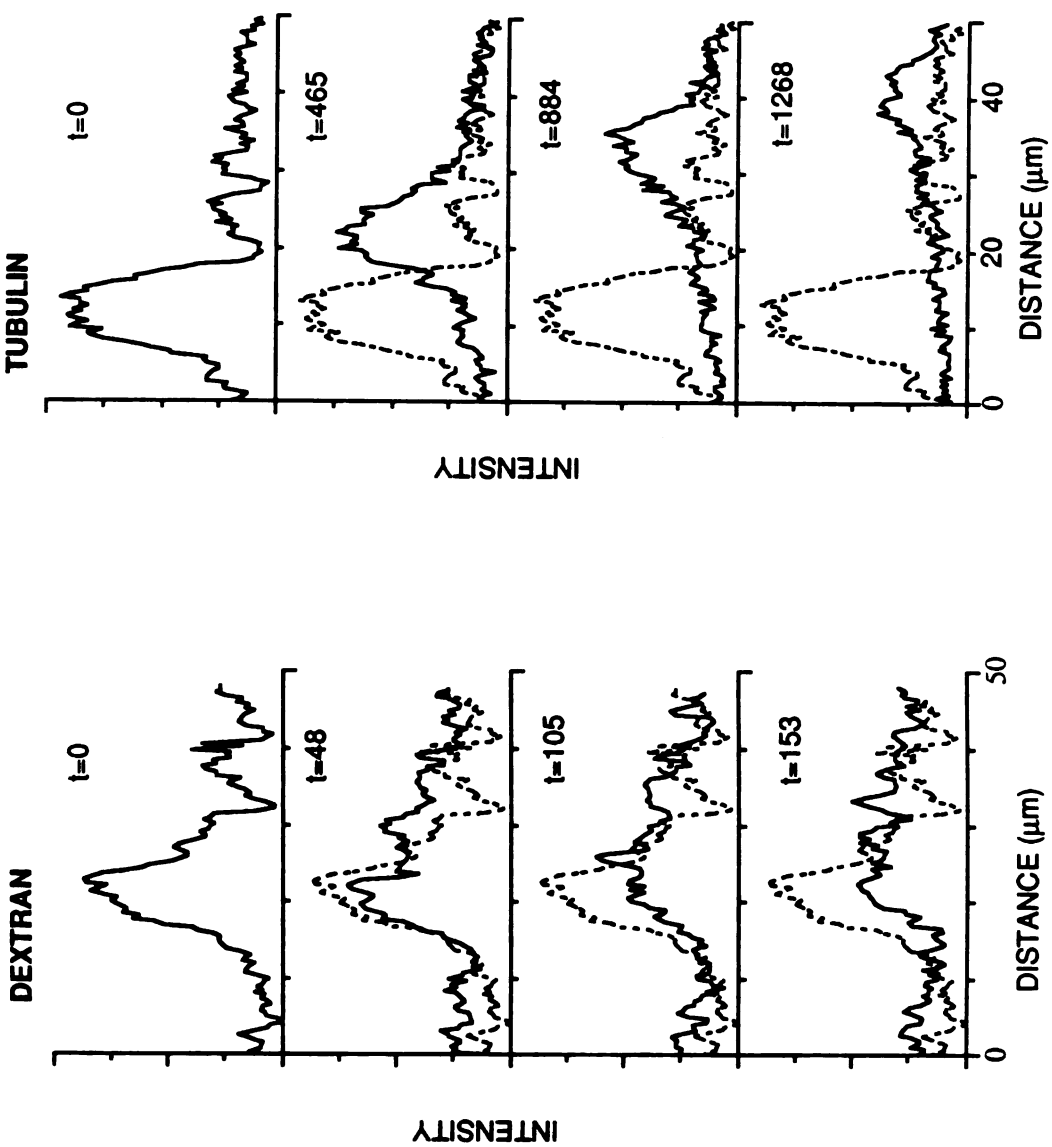
TUBULIN
t=0
t=465
t=884
t=1268
INTENSITY
0
20
40
DISTANCE (μm)
DEXTRAN
t=0
t=48
t=105
t=153
INTENSITY
0
50
DISTANCE (μm)

The rate of microtubule translocation varies with distance along the axon

Although the rates of microtubule translocation in the axon were often close to the rates of growth cone movement (see for example figure 2*A/B*), we observed many cases where the translocation rates were significantly slower than that of growth cone advance (figure 2 *C/D).* In 6 different experiments of 47 activation marks in 39 neurons, we found that in 46, the polymer advanced a measurable distance over the total observation period. In each experiment, our observation period lasted until the signal decayed to background levels (sometimes up to 45 minutes), or was obscured by objects in the field. The average rate of growth cone advance in the 39 neurons was 60 μm/hr ± 37 μm/hr (s.d.) with the fastest moving at 150 μm/hr. The tubulin polymer moved at 38.5 μm/hr ± 31.4 μm/hr (s.d.), with the fastest moving at 117 μm/hr. Therefore, on average, the growth cone advanced faster than the rate of microtubule translocation.

We suspected that there might be a relationship between the distance from the cell body and the relative rate of forward advance. Since many of our measurements were made on axons growing out of explants where the position of the cell body was difficult to identify, we correlated the rate of movement of the photoactivated mark with the distance from the growth cone. As shown in Figure 5, in neurons where the distance between the mark and the growth cone was less than 15 μm (solid bars), 43% of the marks moved at rates that were at least 80% of the rate of growth cone advance (pool 0.8-1.0 plus pool >1.0). In neurons where the activated mark was further than 15 μm from the growth cone (open bars), only 14% of the marks moved at rates that were 80% or greater than the rate of axon elongation; 50% of the marks moved at rates that were less than 40% of the rate of growth cone advance (pool 0-0.2 plus pool 0.2-0.4). It is important to note that microtubule translocation occurred at all positions

along the axon, even very close to the cell body, and that at all levels the polymer seemed to move as a coherent unit. Furthermore, microtubule polymer movement continued in the absence of axonal elongation in 3 out of 46 neurons (see figure 8).

Figure 5. Ratio of polymer translocation rates to corresponding growth cone advance rates as a function of the distance from the growth cone. The rate of polymer translocation was divided by the rate of advance of the neck of the growth cone (see Materials and Methods). Two pools were compared: neurons where photoactivations were made within 15 microns of the growth cone (filled bars; n=21) and neurons where photoactivations were made greater than 15 microns from the growth cone (open bars; n=22). Note that marks made closer to the growth cone moved faster than marks made greater than 20 μm from the growth cone.

Figure 5

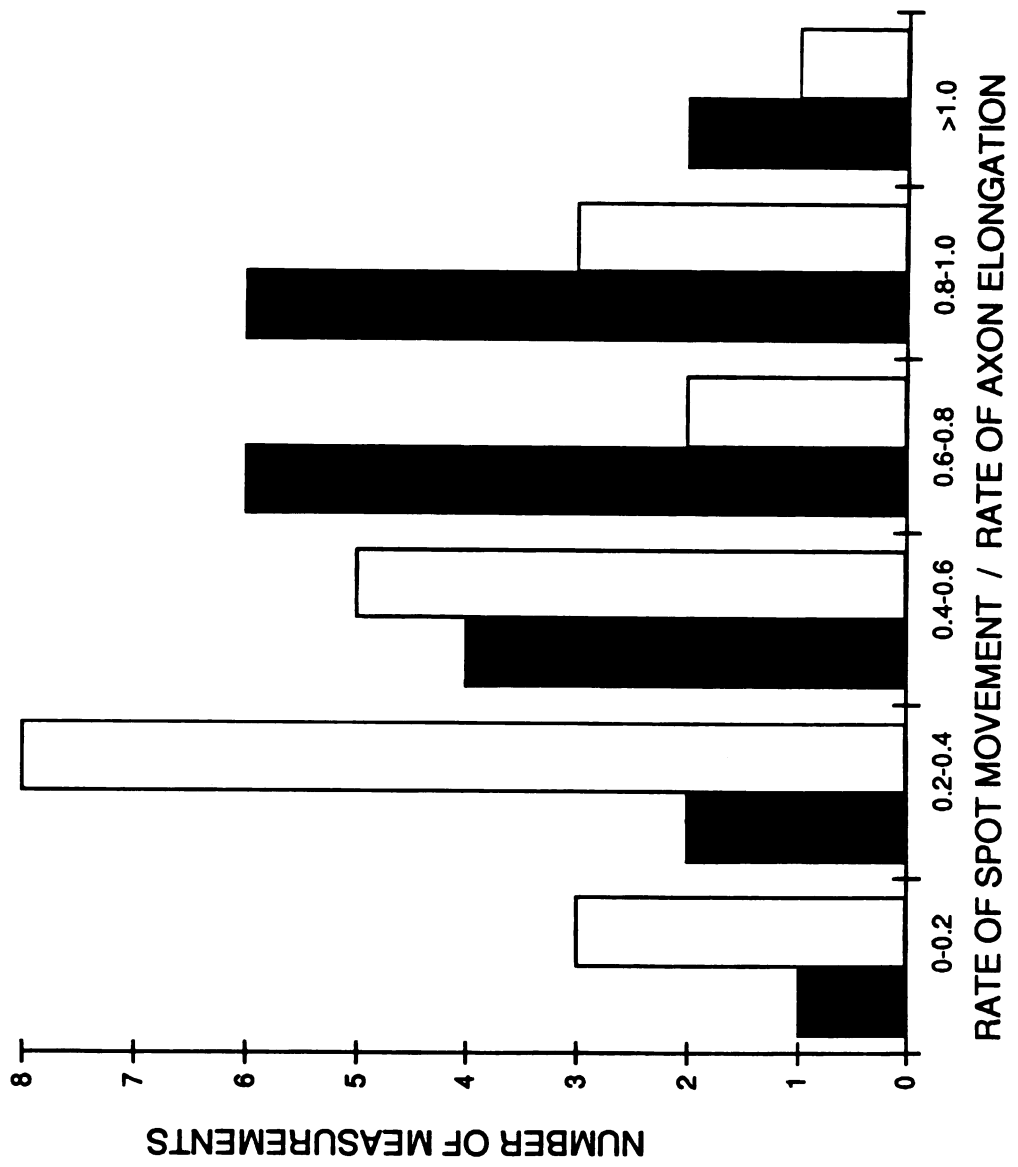
NUMBER OF MEASUREMENTS
0
1
2
3
4
5
6
7
8
0-0.2
0.2-0.4
0.4-0.6
0.6-0.8
0.8-1.0
>1.0
RATE OF SPOT MOVEMENT / RATE OF AXON ELONGATION

The rate of microtubule movement at different positions within single axons

Pooled data from many neurons indicated that the rate of polymer movement showed a tendency to vary with distance from the cell body. To follow the fate of microtubules at different positions along individual axons, we made multiple activation marks on dissociated neurons where both the cell body and the growth cone were visible. Figures 6*A* and 6*B* show frames of two of seven neurons that we studied with multiple activation marks. In Figures 6*C* and 6*D* we show plots of the positions of the growth cone and the individual marks as a function of time for each experiment. In the neuron in figure 6*A/C*, all three activated regions, at 0.48, 0.69, and 0.83 (distance from the cell body relative to the total axon length), moved out from the cell body at the same overall rate of 21 μm/hr. As the axon elongated, the growth cone (dotted line) advanced away from the distal-most mark, and continued to advance at an overall rate 2.6 times the rate of microtubule translocation. Neither the growth cone nor the polymer advanced in a smooth fashion, rather, both showed saltatory advance, which was especially notable in the growth cone.

The second neuron (figure 6*B/D*) displayed a rather different polymer behavior. In this case, while all three marks moved away from the cell body, the relative distances between the marks also increased, as did the distance from the distal-most mark to the growth cone. Therefore, the microtubule polymer moved at different rates at different positions in this axon. The spot closest to the cell body, at a relative position of 0.47, moved at the slowest rate (10.2 μm/hr), while the spot closest to the growth cone, at a relative position of 0.94, moved at the fastest rate (40.2 μm/hr). This fast rate was still slower than the overall rate of growth cone advance (66 μm/hr). While the two marks closest to the cell body advanced steadily, the mark closest to the growth cone seemed to reflect the saltatory growth cone behavior. Changes in the rate of polymer

movement in the distal-most mark sometimes preceded changes in the rate growth cone movement, while at other times changes in the rate of polymer movement lagged behind those of the growth cone. For example, in the first 2.5 minutes, the distal mark moved at a faster rate (72 μm/hr) than the growth cone (12 μm/hr). During the next 10 minutes, the distal mark slowed to 12 μm/hr, while the growth cone advance rate reached 156 μm/hr. At 13 minutes, the distal mark began to move at this faster rate and for the rest of the time course, followed the growth cone rate very closely.

Plots of life histories of all of these multiply marked neurons indicated that there were differences in polymer behavior along the proximo-distal axis. These differences were independent of axon length. In general, polymer close to the cell body moved slower and at a more consistent rate than polymer close to the growth cone. Yet as shown in figure 6*A/C*, in some cells marks made at different positions along the axon can move together. At all positions along the axon the polymer moved as the growth cone advanced.

Figure 6. Multiple photoactivations in two neurons. (*A* and *B*) Fluorescein signal (left panels) and corresponding phase images (right panels) immediately following photoactivation and at the indicated times (minutes) in *Xenopus* neurons labeled with photoactivatable tubulin. The thin lines indicate the positions of the marks immediately after photoactivation. (*C* and *D*) Life histories of the photoactivation marks and growth cone movements matching the neurons shown in *A* and *B*. The distances of the marks from the cell body immediately after photoactivation: (*A* and *C*) proximal mark (J) 37.3 μm; middle mark (H) 53.3 μm ; distal mark (♦) 63.7 μm; and the growth cone (dashed line) 77.0 μm. (*B* and *D*) proximal mark (J) 46.9 μm; middle mark (H) 69.1 μm; distal mark (♦) 93.5 μm; and the growth cone (dashed line) 99.2 μm. Note how the marks in *A/C* track together while those in *B/D* separate during axonal elongation. Bar: 10 μm.

Figure 6

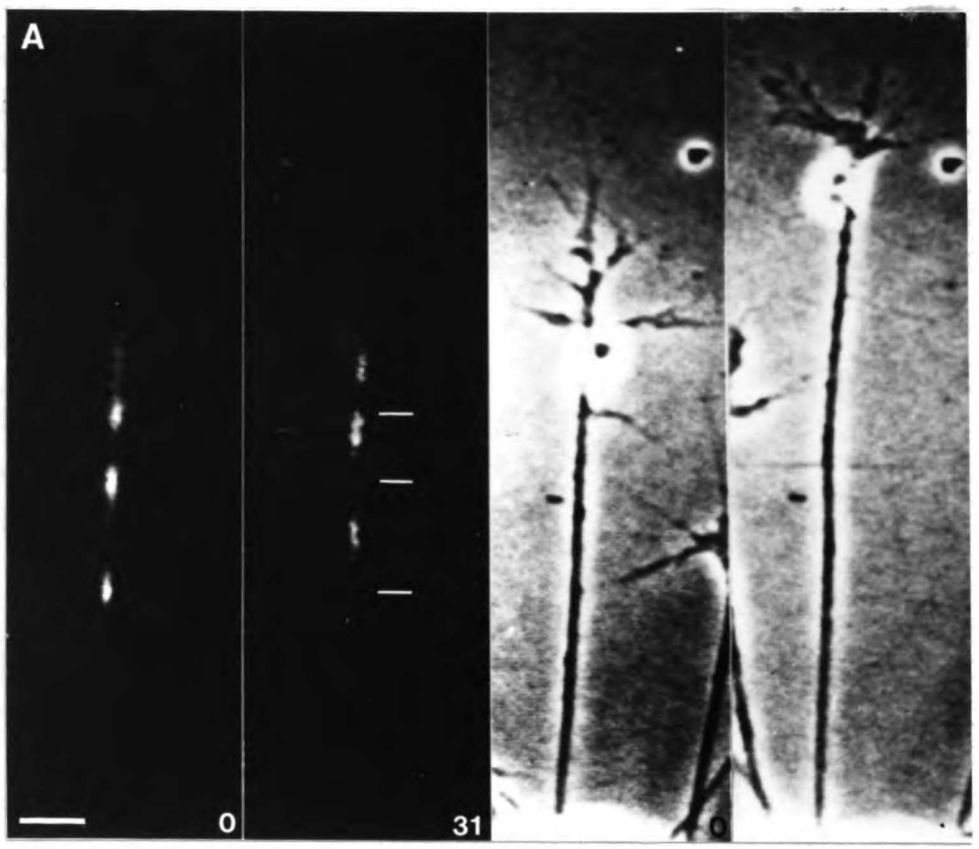

Figure 6

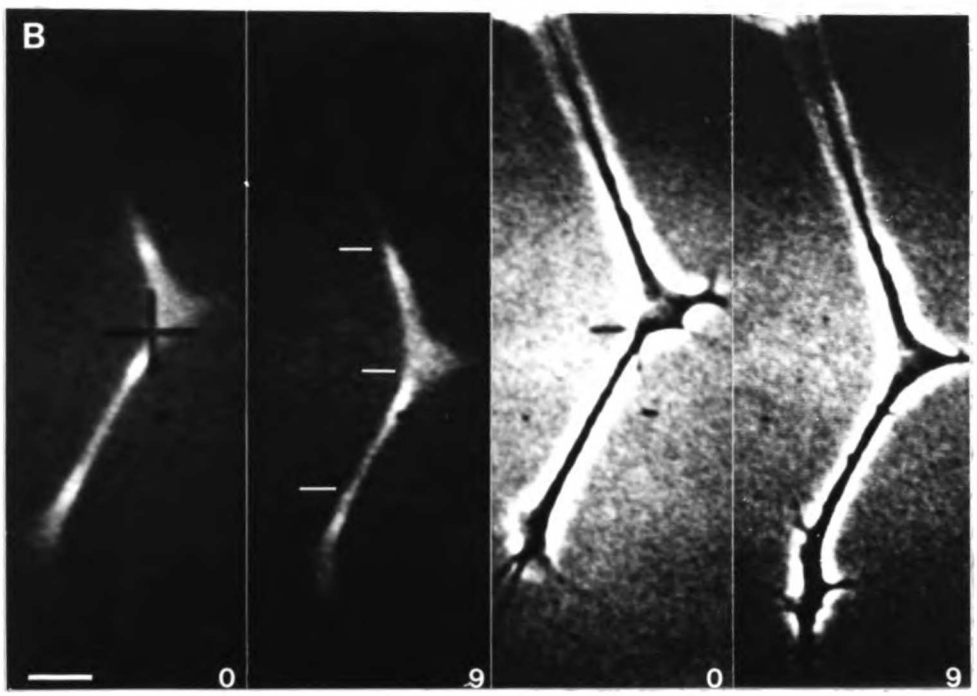

Figure 6

C.
DISTANCE MOVED (μm)
35
25
15
5
-5
0
20
40
TIME (min)
D.
DISTANCE MOVED (μm)
40
30
20
10
0
0
10
20
30
TIME (min)

Behavior of microtubule polymer near the growth cone

Over the long term, there must be a correlation between the advance of the growth cone and the growth of the cytoskeleton behind it. As discussed above, while the rate of microtubule advance along the axon is fairly uniform, near the growth cone the rate of polymer movement can display more rapid changes. We have examined, in greater detail, the relationship between microtubule advance near the growth cone, and the behavior of the growth cone for 21 neurons in which activation marks were made within 20 microns of the growth cone. We have found that this behavior falls into three categories, all of which a single neuron can possess at different times.

In the first category, shown in figure 7*A*, the growth cone advanced with a fairly uniform morphology (this is also true of the growth cone in figure 2A). As the growth cone advanced (figure 7*C*), both the neck (dotted line) and the distal tip of the growth cone also advanced; the microtubule polymer (figure 7*B*) moved at a rate similar to that of the growth cone. The distance between the photoactivated mark on the microtubule polymer (arrow, figure 7*C*) and the neck of the growth cone (dotted line, figure 7*C*) remained fairly constant. The rate of polymer advance (102 μm/hr) in this instance slightly exceeded the rate of growth cone advance (74 μm/hr). This coupling of microtubule polymer advance with growth cone advance was seen in 17 out of 21 neurons that moved at very different rates. We termed this behavior coupled elongation/translocation.

In the second category shown in figure 8, when the growth cone paused temporarily polymer movement continued. In figure 8*A/C*, the distal tip and the growth cone neck stalled, but microtubule advance continued (figure 8*B/C*). In this instance, the distance (double headed arrow, figure 8*C)* from the activated mark (arrow, figure 8*C*) to the neck of the growth cone (dotted line, figure 8*C*)

decreased as the microtubules advanced toward the growth cone. In this neuron and others, we noted an increase in the phase density within the growth cone. For example, in the last panel of figure 8*A* there is a prominent phase dense region that appears to hook to the left. We interpret this to be a bundle of microtubules and associated organelles that moved into and filled up the growth cone with microtubule polymer as the microtubule polymer advanced (see related descriptions in Tanaka and Kirschner, 1991). This sequence is a good example of continuous microtubule polymer movement into the growth cone in the complete absence of growth cone advance; a condition which we term extrusion.

In the third category, shown in figure 9, the proximal part of the growth cone membrane collapsed and that region of the growth cone was converted into new axon, a process we call conversion (Mitchison and Kirschner, 1988). During conversion (figure 9*A*), the distal tip of the growth cone paused while collapse of the membrane behind it had the effect of advancing the neck of the growth cone (dotted line, figure 9*C*), while a new segment of axon formed behind the neck. In this condition, the forward translocation of the microtubule polymer also paused (figure 9*B*) and, as a consequence there was a rapid increase (12 μm/133 sec = 324 μm/hr) in the distance from the mark to the growth cone. After conversion was complete, the growth cone and microtubules advanced together again, as shown in the last panel of figure 9*A/B*. We observed this process of growth cone conversion in 8 of 21 neurons.

Figure 7. Coordination of polymer movement with growth cone movement - coupled elongation/translocation. Phase images (*A*) and corresponding fluorescein images (*B*) at the times indicated (seconds) following photoactivation. (*C*) Tracing with superimposed fluorescein signal and phase outline of the growth cone from panels 1, 3 and 5. Note that distance (⟷) between photoactivation mark (arrow) and the neck of the growth cone (dashed line) remains fairly constant. Solid line shows starting position of photoactivation mark in B and C. Bar: 10 μm.

Figure 8. Coordination of polymer movement with growth cone movement - extrusion of polymer. Phase images (*A*) and corresponding fluorescein images (*B*) at the times indicated (seconds) following photoactivation. (*C*) Tracing with superimposed fluorescein signal and phase outline of the growth cone from panels 1, 3 and 5. Note that the growth cone advance stops and the distance (⟷) between the photoactivation mark (arrow) and the neck of the growth cone (dashed line) decreases indicating continued polymer movement in the absence of growth cone advance. Solid line indicates starting position of photoactivation mark. Bar: 10 μm.

Figure 9. Coordination of polymer movement with growth cone movement - growth cone conversion. Phase images (*A*) and corresponding fluorescein images (*B*) at the times indicated (seconds) following photoactivation. (*C*) Tracing with superimposed fluorescein signal and phase outline of the growth cone from panels 1, 3 and 5. Note the rapid increase in distance (⟷) between photoactivation mark (arrow) and the neck of the growth cone (dashed line) between the first and third panels as the growth cone membrane collapses proximally to form a new segment of axon. In the final panel of *A* and *B*, the

photoactivation mark once again starts to move out with the growth cone as conversion is complete. Solid line indicates starting position of photoactivation mark. Bar: 10 μm.

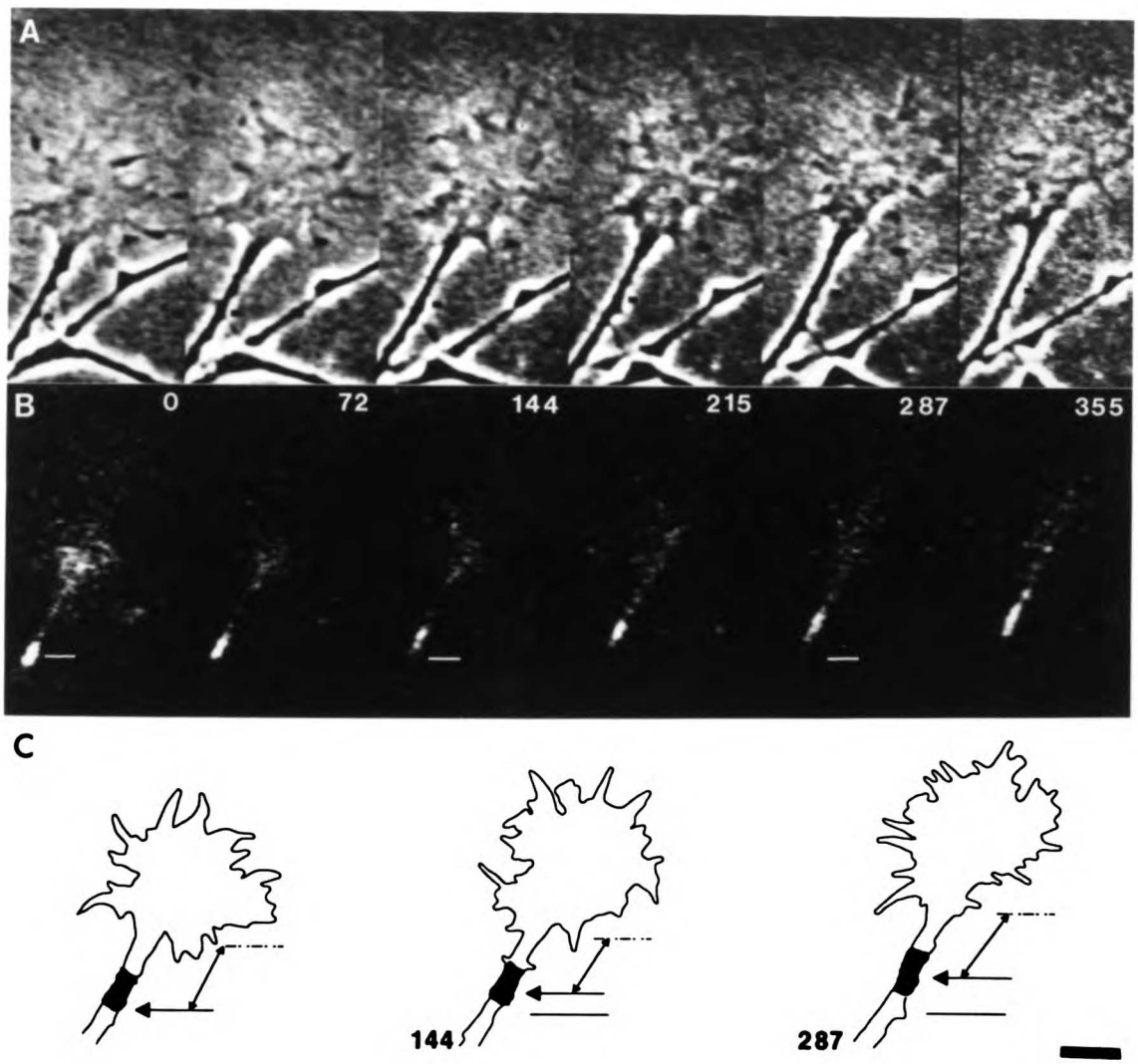
A
B
0
72
144
215
287
355
C
144
287

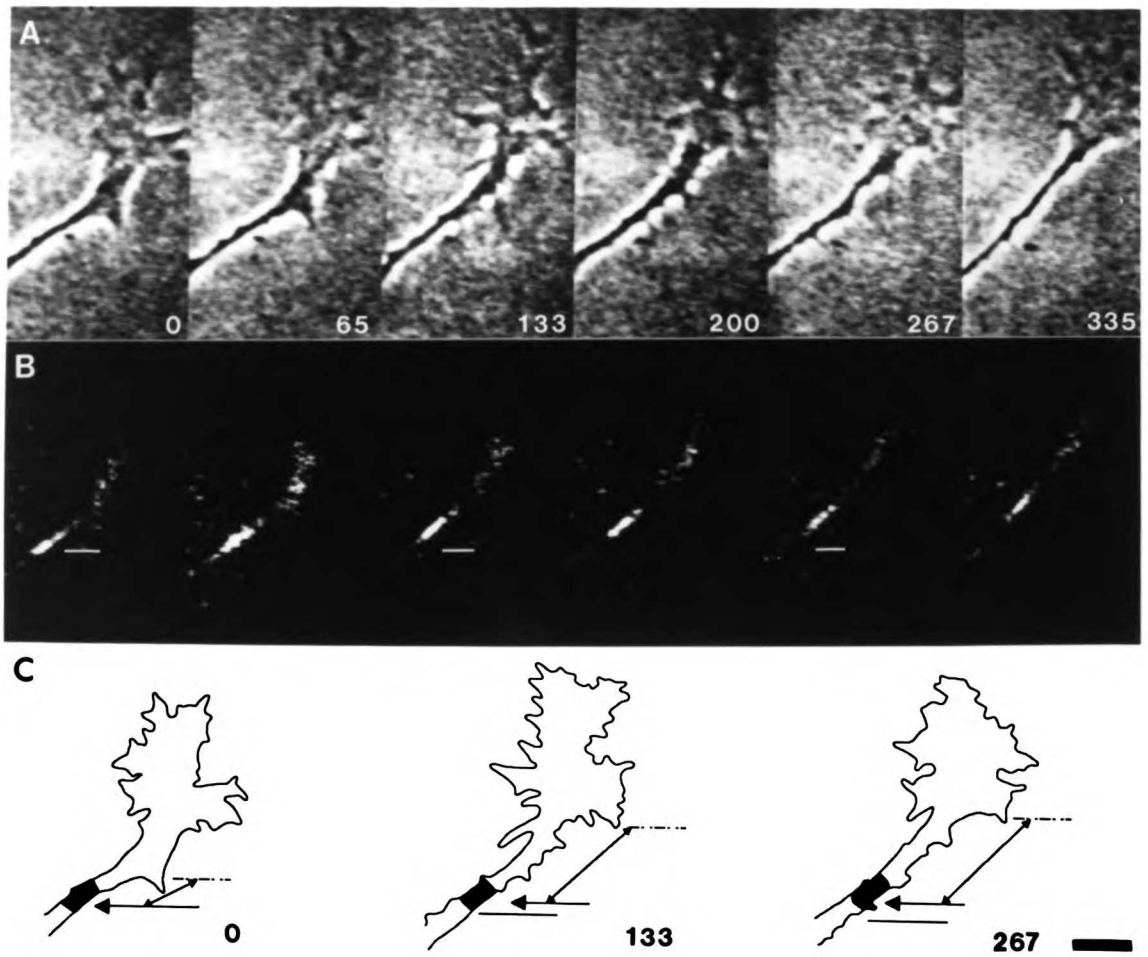
A
0
65
133
200
267
335
B
C
0
133
267

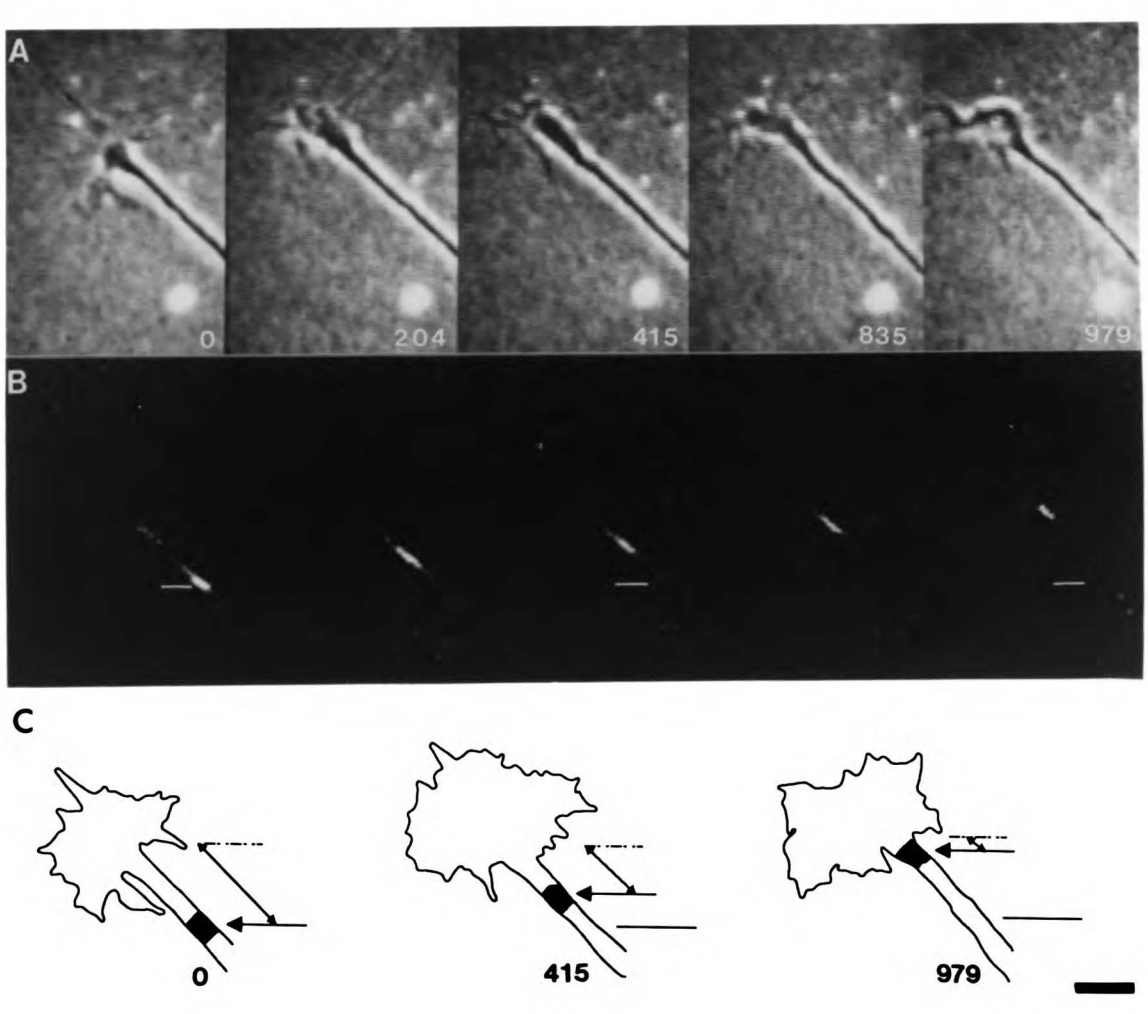
A
0
204
415
835
979
B
C
0
415
979

DISCUSSION

The properties of photoactivated microtubules in the axon

The interpretation of the photoactivation experiments depends on whether we can be certain that the photoactivatable probe remains on tubulin, whether that tubulin is functional, and whether we can assess if the tubulin is in a monomeric or polymeric form. Bulk chemical methods for characterizing the labeled tubulin in the embryo would be of little value because the derivatized tubulin may be handled differently in different cell types in different regions of the embryo. Instead, we have had to base our assessment of the photoactivatable probe on the physical and functional properties of tubulin in the specific cells that we are studying.

In growth cones, photoactivated tubulin was visible as linear polymers of uniform intensity and caliber (figure 1*B*). These images were similar to those seen with rhodamine labeled tubulin (figure 1*C*). It is likely that the photoactivatable signal in the axon is also present on polymer, some of which is presumably continuous with microtubules in the growth cone (see also Tanaka and Kirschner, 1991).

Several features of the photoactivatable signal in axons suggest that it is present primarily on polymer. First, at all points along the axon the fluorescent mark translocated coherently without leaving a significant trailing signal at the site of photoactivation (Figures 2*B*, 2*D*, 6*A*, 6*B*, 7*B*, 8*B*, 9*B*). Second, significant signal remained after detergent extraction which should solubilize all monomer (figure 3). Third, the slow spreading of the photoactivated mark was unlike that expected for soluble tubulin. These characteristics of the labelled tubulin will be discussed below.

The coherence of the activated signal on tubulin during extensive transport in the axon has several implications. If the axon contained a transport

form of tubulin that was separate from a stationary polymeric form (Weisenberg et al., 1988; Weisenberg et al., 1987), the signal would be expected to split into two phases, a stationary polymer phase and a moving transport phase. Since we could detect no separation of the signal into two phases, most of the signal must therefore be on one form of tubulin, or the transport form and the axonal polymer must be translocating together.

The diffusion of the photoactivatable tubulin is inconsistent with most of the signal being on monomer. If there were an appreciable monomer phase, the fluorescent signal again should have split into two components - a diffusible component representing the soluble tubulin that rapidly spread isotropically and a non-diffusible component representing the microtubule polymer that could have either been stationary or could have translocated. Our analysis of the intensity data at short time points following photoactivation rule out the existence of such a diffusible phase consisting of more than 10% of the total tubulin. As a model for the expected behavior of monomeric tubulin, we used photoactivatable dextran of slightly smaller Stokes radius than monomeric tubulin to measure diffusion in the axon (figure 4*A*/*C*). We calculated an apparent diffusion coefficient for this photoactivatable dextran; it behaved as a soluble component in a medium of about 10 times the viscosity of water, a value similar to that observed for the diffusion of dextran in other cells (Lang et al., 1986; Luby-Phelps et al., 1986). The photoactivated tubulin behaved very differently. If we estimate the apparent diffusion coefficient for tubulin based on the spreading of the photoactivatable zone, it was 50 times slower than the dextran, corresponding to the free diffusion in the cell environment of a molecule of 10^{10} Daltons, a particle larger than a centriole. Most likely the signal is not diffusing at all, and the slow spreading of the fluorescent mark is due to some other mechanism such as sliding of individual microtubules (see

below). These properties of the photoactivated tubulin in the axon: non-extractability, coherence through transport, and non-diffusibility are all characteristics of polymer and not monomer.

Microtubule assembly in axons

The vectorial movement of tubulin polymer from the cell body towards the growth cone is the predominant feature of microtubule behavior in the axons that we have studied. Overall microtubules translocated throughout the axon at a slower rate (38.5 ± 31.4 μm/hr) than that of growth cone advance (60 ± 37 μm/hr). Furthermore, polymer nearer the cell body moved slower than polymer near the growth cone (Figure 5, Figure 6*C/D*). These three observations, vectorial transport of polymeric tubulin, a gradient in the rate of polymer movement as a function of distance from the cell body, and rate of growth cone advance which exceeds the rate of polymer movement, must be explained in terms of the sites of microtubule assembly, the number of microtubules in the axon, and the mechanisms and rates of microtubule translocation.

Microtubule assembly in or near the cell body is strongly supported by these photoactivation experiments. The coherent vectorial movement of polymeric tubulin as close as 15 μm to the cell body requires that tubulin polymer must be generated already at this level. The movement of the microtubule polymer cannot be due to a general elastic expansion of the axon, since translocation can occur in the absence of axon growth (figure 8). The movement in multiply marked axons is also incompatible with elastic expansion; in some cases all of the marks moved as a coherent unit (figure 6*A/C*). Assembly of microtubules in or near the cell body and vectorial transport of tubulin polymer down the axon is supported by metabolic pulse-labeling experiments in many neuronal cell types *in vivo* (Hoffman and Lasek, 1975;

Lasek et al., 1984) and *in vitro* (Black et al., 1986). The rates of movement that we have observed are in the range of those for tubulin transport determined by metabolic labeling in nerves *in vivo*. In *Xenopus* embryonic neurons in culture, we found that microtubule polymer moved an average of 38.5 μm/hr (0.9 mm/day) with the fastest movement at 117 μm/hr (2.8 mm/day) near the growth cone. Kinetic differences in tubulin transport as determined by metabolic labeling *in vivo* vary with cell type (Oblinger et al., 1987) and state of the neuron (Hoffman and Lasek, 1980; McKerracher et al., 1990) but vary from 1 to 5 mm/day. While tubulin *in vivo* is sometimes found to be transported at two different velocities in the same neuron (Hoffman and Lasek, 1980), we have only observed a single polymeric transport phase whose velocity increases from the cell body to the growth cone.

The separation of the photoactivated marks in some of the multiply marked neurons could have two explanations. Microtubules could be telescoping out in the neuron, causing the microtubule density to decrease with the distance from the cell body. There is some evidence that microtubule number is in fact greater in the proximal axon than in the distal axon (Bray and Bunge, 1981; Letourneau, 1982). Alternatively, the microtubules could telescope out, but the density could be held constant by intercalary assembly along the axon from a pool of monomer. We imagine that this assembly would be at the ends of overlapping microtubules. Assembly along the axon has support from experiments using microinjection (Keith and Blane, 1990; Okabe and Hirokawa, 1988), photobleaching (Lim et al., 1990; Okabe and Hirokawa, 1990) and immunohistochemistry (Baas and Black, 1990; Lim et al., 1989). However, the monomeric subunits driving this assembly would ultimately have to come from the cell body, and would have to move down the axon by diffusion, as discussed below. We cannot distinguish between these two mechanisms of

extension of the axonal microtubule cytoskeleton. However, a slow telescoping of the microtubules, with or without intercalary assembly, is the most likely explanation for the broadening of the photoactivatable zones. For example in figure 6*B*, the distal mark moved 30 µm while the proximal mark moved 25 µm, producing a 20% increase in extension of the intervening microtubules in the axon. During this time, the individual zones broadened about 30%. Thus both the length of the zones and the distance between them increased in similar proportions, suggesting that the same process, telescoping, with or without intercalary assembly, was responsible.

Near the growth cone, photoactivatable marks often moved at rates comparable to that of the growth cone. However, in most cases the growth cone moved faster than the movement of the mark, suggesting either a drastic thinning of microtubules near the growth cone, or new assembly with subunits presumably provided either by diffusion or by depolymerization of microtubules in the axon. Tanaka and Kirschner (1991) have observed apparent elongation of microtubules in the growth cone. However, it is difficult to resolve the relative contributions of forward translocation and assembly to microtubule elongation. Assembly at the growth cone is supported by immunohistochemical (Baas and Black, 1990; Lim et al., 1989) drug inhibition (Bamburg et al., 1986) and photobleaching studies (Lim et al., 1990; Okabe and Hirokawa, 1990). For the relatively short neurons studied here, there would be no difficulty for subunits to be provided to the growth cone by diffusion. Microinjection experiments of derivatized tubulin in cultured pheochromocytoma cells and dorsal root ganglion cells *in vitro* have suggested that diffusion is sufficient to bring subunits to all regions of the cell body and axon (Keith, 1987; Keith and Blane, 1990; Lim et al., 1989; Okabe and Hirokawa, 1988), where they can be incorporated into microtubules. These cells have short processes, where

diffusion of subunits throughout the cell can occur in seconds or minutes. However in axons longer than 1mm, diffusion would not accomplish appreciable transport of tubulin within a day. Therefore, the physical limitations of diffusion argue strongly for some mechanism of tubulin transport in long axons. The pulse-labeling experiments and our direct visualization of vectorial transport of microtubules argue that such a mechanism exists and that it comprises polymer assembly in the cell body or in the proximal axon and its subsequent movement down the axon. For long axons, translocation would be the only practical known means of axonal growth.

Microtubule translocation and growth cone behavior

Using photoactivation, we have correlated the translocation of microtubules in the axon just proximal to the growth cone with the movements of the growth cone and noted three general patterns of behavior: (1) coupled elongation/translocation, during which the polymer moves at virtually the same rate as growth cone; (2) extrusion, during which the growth cone slows, pauses or stops altogether and the polymer continues to move forward; and (3) conversion, during which the polymer pauses as the proximal region of the growth cone collapses to form a new segment of axon. We believe that these three polymer behaviors that we observed near the growth cone are related to the three different microtubule distributions that are generated in the growth cone (Tanaka and Kirschner, 1991). During coupled elongation/translocation (figure 7), the rate of microtubule polymer translocation equals that of growth cone advance. In this situation, microtubules may advance as a splayed array. During extrusion (Tanaka and Kirschner: figure 6 and figure 8; this manuscript: figure 8), the rate of polymer translocation exceeds that of growth cone

advance. As a result, axonal microtubules may move into the growth cone. When this mass of extruded microtubules collides with the growth cone margin, we imagine that looped arrays would be formed. During conversion (figure 9), the growth cone may contain a dense array of looped microtubules which compresses into a bundle proximally and straightens distally. The corresponding event is seen in detail by Tanaka and Kirschner (1991). Though there is a complementarity between the direct visualization of microtubules and photoactivation of tubulin, neither method allows us yet to estimate accurately the relative contribution of microtubule polymerization and forward translocation to the formation of new microtubules in the growth cone. Furthermore, while we can classify microtubule polymer movement near the growth cone into three general behaviors, our data highlight the fact that there may only be a loose coupling between polymer movement and growth cone advance.

The interpretation of photobleaching and other experiments

Three previous experiments using photobleaching of rhodamine-labeled microtubules in pheochromocytoma cells (Lim et al., 1989) and dorsal root ganglion cells (Lim et al., 1990; Okabe and Hirokawa, 1990) failed to find any evidence for vectorial flow, and concluded that axons assemble by adding subunits at the growth cone. (However, see also Keith, 1987, who found support for axonal transport of tubulin in photobleached axons). The simplest explanations for the failure of the photobleaching experiments to find vectorial transport is that the cells used in those experiments had much different behavior from the *Xenopus* neurons or that the experimental methodologies of photobleaching experiments emphasized features different from the photoactivation experiments. We will briefly discuss the possible sources of

discrepancy between the photobleaching experiments and our photoactivation experiments.

The primary cultured neurons from *Xenopus* neural tube explant cultures grew 5 to 30 times more rapidly than the cell types used in the photobleaching experiments; if translocation was correspondingly slower in these cells, the precision of measuring movement would be much less than in the photoactivation experiments. There are also inherent differences in sensitivity between photobleaching and photoactivation experiments. Photoactivation is most sensitive to the slowest exchanging component of a complex system. This property has allowed the successful demonstion of the poleward flux of kinetochore microtubules during metaphase in the presence of other rapid kinetic behaviors of microtubules (Mitchison, 1989; Sawin and Mitchison, 1991). Interestingly, while photoactivation experiments easily detected this poleward movement, photobleaching experiments could not (Gorbsky and Borisy, 1989; Gorbsky et al., 1987).

A serious problem that has plagued all fluorescence experiments is photodamage. In general, photoactivation has advantages over photobleaching since the light energy (number of photons) required to photoactivate a caged fluorophore molecule is several orders of magnitude less than that required to photobleach a fluorophore. During photobleaching, oxygen radicals are produced that can damage cells. The total amount of light energy absorbed by the cell during the observation period is much less with photoactivation since only the photoactivated, rather than the total, labeled tubulin is fluorescent. Other potential targets for photodamage are putative microtubule motors which have been shown to be very sensitive to photodamage (Marya et al., 1990). For example, purified kinesin and dynein are irreversibly inactivated when subjected to light in the presence of

fluorescently labeled microtubules *in vitro* (R. Vale, personal communication). Therefore, if microtubule motors are required for microtubule translocation in the axon, local photobleaching might damage such a motor without causing any detectable ultrastructural changes. The simplest way to resolve the discrepancies between the results obtained here and the photobleaching experiments would be to use the photoactivatable probe in the cell types used in the photobleaching experiments and vice versa.

The mechanism of microtubule translocation

The coherence of the photoactivatable spots on microtubules suggests that the microtubules are linked together. Cross-bridges that may be involved in microtubule bundling have been detected between components of the cytoskeleton in axons (Hirokawa, 1982; Hirokawa et al., 1988; Hirokawa and Yorifuji, 1986). Though bundling seems to be an early event in the conversion of the microtubule array in growth cones to that of the axon in these neurons (Tanaka and Kirschner, 1991), it is not clear whether the microtubules are strongly cross-linked. The spreading of the photoactivatable marks in multiply activated axons and the broadening of each photoactivatable zone suggests that microtubules may move relative to one another. An activity which may cause microtubule sliding *in vitro* has been purified from brain (Shpetner and Vallee, 1989) and microtubule sliding is implicated in Teleost cone elongation (Gilson et al., 1986; Warren and Burnside, 1978). The present data supports evidence for sliding of microtubules in the axon that was originally conjectural (Lasek, 1986).

What powers the vectorial transport of microtubules in the axon? Since microtubule transport continues in the absence of axonal growth, membrane expansion at the growth cone cannot be responsible for pulling microtubules

towards the growth cone. It also seems unlikely to us that neurons can act like toothpaste tubes, where a process restricted to the cell body could exert a force that would drive microtubule movement at long distances. A microtubule-based mechanochemical motor working along the sides of microtubules, such as dynein, plausibly could generate movement of the proper polarity (Paschal et al., 1987). While the observed rates of polymer movement in these cells are slower than the rates of dynein-generated movement observed *in vitro* (Paschal and Vallee, 1987), the physical load on such a motor might account for the slower rate of transport. However, if translocation is powered by a microtubule motor, against what stationary phase is this motor moving? Microtubules could move relative to other microtubules, as they do in cilia and flagella. If this is the case, we would have expected to see a stationary phase of photoactivated microtubules, which we did not observe. It is possible that the stationary phase is exceedingly small, and detection would require an imaging system with greater sensitivity than that used in these experiments. Other cytoskeletal components, such as cortical actin are candidates for a stationary phase relative to which the microtubules might move (Fath and Lasek, 1988; Hirokawa, 1982; Schnapp and Reese, 1982) . However, all these components must be themselves transported (Black and Lasek, 1980) so that it seems that no components would be truly stationary and that some would equilibrate between stationary and moving phases.

REFERENCES

Baas, P. W., and M. M. Black. 1990. Individual microtubules in the axon consist of domains that differ in both composition and stability. *J. Cell Biol.* 111: 495-509.

Bamburg, J. R. 1988. The axonal cytoskeleton: stationary or moving matrix? *TINS.* 11: 248-249.

Bamburg, J. R., D. Bray, and K. Chapman. 1986. Assembly of microtubules at the tip of growing axons. *Nature.* 321: 778-790.

Black, M. M., P. Keyser, and E. Sobel. 1986. Interval between the synthesis and assembly of cytoskeletal proteins in cultured neurons. *J Neurosci.* 6: 1004-1012.

Black, M. M., and R. J. Lasek. 1980. Slow components of axonal transport: two cytoskeletal networks. *J Cell Biol.* 86: 616-623.

Brady, S. T., R. J. Lasek, and R. D. Allen. 1982. Fast axonal transport in extruded axoplasm from squid giant axon. *Science.* 218: 1129-1131.

Brady, S. T., R. J. Lasek, and R. D. Allen. 1985. Video microscopy of fast axonal transport in extruded axoplasm: a new model for study of molecular mechanisms. *Cell Motility.* 5: 81-102.

Bray, D., and M. B. Bunge. 1981. Serial analysis of microtubules of cultured rat sensory neurons. *J. Neurocytol.* 10: 589-605.

Burdwood, W. O. 1965. Rapid bidirectional particle movement in neurons. *J Cell Biol.* 27: 115A.

Fath, K. R., and R. J. Lasek. 1988. Two classes of actin microfilaments are associated with the inner cytoskeleton of axons. *J Cell Biol.* 107: 613-621.

Gilson, C. A., N. Ackland, and B. Burnside. 1986. Regulation of reactivated elongation in lysed cell models of teleost retinal cones by cAMP and calcium. *J Cell Biol.* 102: 1047-1059.

Gorbsky, G. J., and G. G. Borisy. 1989. Microtubules of the kinetochore fiber turn over in metaphase but not in anaphase. *J. Cell Biol.* 109: 653-662.

Gorbsky, G. J., P. J. Sammak, and G. G. Borisy. 1987. Chromosomes move poleward in anaphase along stationary microtubules that coordinately disassemble from their kinetochore ends. *J. Cell Biol.* 104: 9-18.

Harris, W. A., C. E. Holt, T. A. Smith, and N. Gallenson. 1985. Growth cones of developing retinal cells *in vivo,* on culture surfaces, and in collagen matrices. *J. Neurosci.* 13: 101-122.

Hirokawa, N. 1982. Cross-linker system between neurofilaments, microtubules, and membranous organelles in frog axons revealed by the quick-freeze, deep-etching method. *J Cell Biol.* 94: 129-142.

Hirokawa, N., S. Hisanaga, and Y. Shiomura. 1988. MAP2 is a component of crossbridges between microtubules and neurofilaments in the neuronal cytoskeleton: quick-freeze, deep-etch immunoelectron microscopy and reconstitution studies. *J Neurosci.* 8: 2769-2779.

Hirokawa, N., and H. Yorifuji. 1986. Cytoskeletal architecture of reactivated crayfish axons, with special reference to crossbridges among microtubules and between microtubules and membrane organelles. *Cell Mot Cytoskel.* 6: 458-468.

Hoffman, P. N., and R. J. Lasek. 1975. The slow component of axonal transport. Identification of major structural polypeptides of the axon and their generality among mammalian neurons. *J Cell Biol.* 66: 351-366.

Hoffman, P. N., and R. J. Lasek. 1980. Axonal transport of the cytoskeleton in regenerating motor neurons: constancy and change. *Brain Res.* 202: 317-333.

Hollenbeck, P. J. 1989. The transport and assembly of the axonal cytoskeleton. *J Cell Biol.* 108: 223-227.

Hyman, A., D. Drechsel, D. Kellog, S. Salser, K. Sawin, P. Steffen, L. Wordeman, and T. J. Mitchison. 1990. Preparation of modified tubulins. *Methods Enzymol.* 196: 478-485.

Keith, C. H. 1987. Slow transport of tubulin in the neurites of differentiated PC12 cells. *Science.* 235: 337-339.

Keith, C. H., and K. Blane. 1990. Sites of tubulin polymerization in PC12 cells. *J Neurochem.* 54: 1258-1268.

Krafft, G. A., R. T. Cummings, J. P. Dizig, L. J. Brvenik, W. R. Sutton, and B. R. Wars. (1986). Fluorescence activation and photodissipation (FDP). In Nucleocytoplasmic Transport, R. Peters, and M. Trendelenberg, ed., (New York: Springer-Verlag), pp. 35-52.

Lang, I., M. Scholz, and R. Peters. 1986. Molecular mobility and nucleocytoplasmic flux in hepatoma cells. *J Cell Biol.* 102: 1183-1190.

Lasek, R. J. 1986. Polymer sliding in axons. *J. Cell Sci [Suppl].* 5: 161-179.

Lasek, R. J., J. A. Garner, and S. T. Brady. 1984. Axonal transport of the cytoplasmic matrix. *J Cell Biol.* 99: 212s-221s.

Letourneau, P. C. 1982. Analysis of microtubule number and length in cytoskeletons of cultured chick sensory neurons. *J Neurosci.* 2: 806-814.

Lim, S. S., K. J. Edson, P. C. Letourneau, and G. G. Borisy. 1990. A test of microtubule translocation during neurite elongation. *J Cell Biol.* 111: 123-130.

Lim, S. S., P. J. Sammak, and G. G. Borisy. 1989. Progressive and spatially differentiated stability of microtubules in developing neuronal cells. *J Cell Biol.* 109: 253-263.

Luby-Phelps, K., D. L. Taylor, and F. Lanni. 1986. Probing the structure of cytoplasm. *J Cell Biol.* 102: 2015-2022.

Marya, P. K., P. E. Fraylich, and P. A. Eagles. 1990. Characterization of an active, fluorescein-labelled kinesin. *Eur. J. of Biochem.*

Matsumoto, T. 1920. The granules, vacuoles, and mitochondria in the sympathetic nerve-fibers cultivated *in vitro. John Hopkins Hosp Bull.* 31: 91-93.

McKerracher, L., M. Vidal-Sanz, and A. J. Aguayo. 1990. Slow transport rates of cytoskeletal proteins change during regeneration of axotomized retinal neurons in adult rats. *J. Neurosci.* 10: 631-648.

Mitchison, T., and M. Kirschner. 1988. Cytoskeletal dynamics and nerve growth. *Neuron.* 1: 761-772.

Mitchison, T. J. 1989. Polewards microtubule flux in the mitotic spindle: evidence from photoactivation of fluorescence. *J. Cell Biol.* 109: 637-652.

Nakai, J. (1964). The movement of neurons in tissue culture. In Primitive Motile Systems in Cell Biology., R. Allen, and N. Kamiya, ed., (London New York: Academic Press), pp. 377-385.

Oblinger, M. M., S. T. Brady, I. G. McQuarrie, and R. J. Lasek. 1987. Cytotypic differences in the protein composition of the axonally transported cytoskeleton in mammalian neurons. *J. Neurosci.* 7: 453-462.

Okabe, S., and N. Hirokawa. 1988. Microtubule dynamics in nerve cells: analysis using microinjection of biotinylated tubulin into PC12 cells. *J. Cell Biol.* 107: 651-664.

Okabe, S., and N. Hirokawa. 1990. Turnover of fluorescently labeled tubulin and actin in the axon. *Nature.* 343: 479-482.

Paschal, B. M., H. S. Shpetner, and R. B. Vallee. 1987. MAP 1C is a microtubule-activated ATPase which translocates microtubules *in vitro* and has dynein-like properties. *J. Cell Biol.* 105: 1273-1282.

Paschal, B. M., and R. B. Vallee. 1987. Retrograde transport by the microtubule-associated protein MAP 1C. *Nature.* 330: 181-183.

Sawin, K. E., and T. J. Mitchison. 1991. Poleward microtubule flux mitotic spindles assembled *in vitro*. *J Cell Biol.* 112: 941-954.

Schnapp, B. J., and T. S. Reese. 1982. Cytoplasmic structure in rapid-frozen axons. *J Cell Biol.* 94: 667-679.

Schroer, T. A., and M. P. Sheetz. 1991. Functions of microtubule-based motors. *Ann Rev of Phys.* 53: 629-652.

Schulze, E., and M. Kirschner. 1986. Microtubule dynamics in interphase cells. 102: 1020-1031.

Shpetner, H. S., and R. B. Vallee. 1989. Identification of dynamin, a novel mechanochemical enzyme that mediates interactions between microtubules. *Cell.* 59: 421-432.

Tanaka, E., and M. Kirschner. 1991. Microtubule behavior in the growth cones of living neurons during axon elongation. *J Cell Biol submitted.*

Vale, R. D. 1987. Intracellular transport using microtubule-based motors. *Ann Rev Cell Biol.* 3: 347-378.

Vallee, R. B., and G. S. Bloom. 1991. Mechanisms of fast and slow axonal transport. *Annu Rev Neurosci.* 14: 53-92.

Warren, R. H., and B. Burnside. 1978. Microtubules in cone myoid elongation in the teleost retina. *J Cell Biol.* 78: 247-259.

Weisenberg, R. C., J. Flynn, B. C. Gao, and S. Awodi. 1988. Microtubule gelation-contraction in vitro and its relationship to component a of slow axonal transport . *Cell Motil Cytoskeleton.* 10: 331-340.

Weisenberg, R. C., J. Flynn, B. C. Gao, S. Awodi, F. Skee, S. R. Goodman, and B. M. Riederer. 1987. Microtubule gelation-contraction: essential components and relation to slow axonal transport. *Science.* 238: 1119-1122.

Weiss, P., and H. B. Hiscoe. 1948. Experiments on the mechanism of nerve growth. *J Exp Zool.* 107: 315-396.

CHAPTER 4

Conclusions and Perspectives

CONCLUSIONS AND PERSPECTIVES

While several major questions have been addressed in this thesis - how the stability of individual microtubules in cultured fibroblasts may be regulated, and where assembly of microtubule polymer occurs in elongating axons - many more questions were generated than answered. In this section, I will present the major questions that have been generated by the experiments presented here and some experimental approaches that would be necessary to address these questions. In the process of addressing these questions, I will reflect on our current thinking on how the microtubule cytoskeleton is generated and maintained during axonal elongation. In presenting these questions, I will concentrate on experiments in *Xenopus* primary neural tube cultures with broad use of knowledge gained from other systems, detailing explicitly where our knowledge of the *Xenopus* system falls short.

What are the microtubule dynamics in Xenopus axons? What is the monomer/polymer ratio, and what is the turnover time for transported axonal polymer - does this differ in different regions of the neuron or under different experimental conditions?

The results presented in this thesis demonstrate that microtubule polymer is the transport form for tubulin within elongating *Xenopus* axons. There is significant assembly of new microtubules at the cell body, and these microtubules are transported distally within the axon. However, our experiments also demonstrate that this transported polymer turns over; that is, the signal that we detect decays over time. Presumably the monomer which is generated from the transported polymer is free to diffuse and assemble within the elongating axon. Our experiments were not performed in a manner which

could reliably quantitate the microtubule turnover in these axon. Using the technique of photoactivation of fluorescence to study the monomer/polymer dynamics within these axons, we can gain a lot of information about how the axonal microtubule cytoskeleton is generated, transported and maintained over time. These sorts of experiments can yield some information about the actual behavior of the axonal microtubules as well as some information about the structure of the axonal cytoskeleton. Combined with the knowledge of how purified tubulin behaves *in vitro,* we can determine the nature of the factors which influence the axonal microtubules. However, an understanding of these dynamics must be coupled with an in depth investigation of the morphology of the axonal cytoskeleton in these axons. In this section, I will describe experiments to investigate quantitatively the microtubule dynamics within these axons. Some questions that these techniques can address: whether all the polymer can turnover in the axon, or whether only a portion of the polymer turns over? Is there a population of stable microtubules, and if so, are these distributed along the axon or concentrated in certain regions of the axon? How far can polymer which is generated within the cell body be transported distally in the axon before it turns over? One major site of assembly distally in the axon is the growth cone. Can we determine where the subunits that are required for this distal assembly are generated? Before addressing the mechanisms of polymer transport within the axon, I'd like to state the case for making more quantitative studies of microtubule dynamics in neurons since these approaches are used in the following sections, and can tell us a lot about the structure and dynamics of the axonal microtubules. First, more quantitative studies would be important to examine axonal microtubule dynamics more carefully than those presented in this study. Due to the non-linearity of the ISIT camera, it was not possible for me make anything but gross quantitative

measurements based on fluorescence intensity. The ISIT camera was useful for measuring the actual movement of the polymer, but fell short for quantitative measurements of polymer turnover or for measuring the monomer/polymer ratio in these neurons. This would ideally be done on a system with linear response characteristics such as the cooled CCD. Several different quantitative measurements would be useful.

Monomer/polymer ratio

It would be interesting to know the monomer:polymer ratio in axons. The monomer: polymer ratio combined with the total tubulin concentration gives an indication of the critical concentration for tubulin assembly in these axons. Assembly of purified tubulin *in vitro* occurs at concentrations above about 10μM. If tubulin assembly occurs at lower or higher concentrations in axons, then there must be factors (such as MAPs) which affect the critical concentration. From inspection of published electron micrographs of cross-sections of axons in culture and *in situ*, we have estimated the tubulin concentration in axons due to polymer to range around 600μM*. At this high tubulin concentration less than 1% of the tubulin should be in monomeric form. Higher concentrations of monomer might indicate that neurons regulate the polymer level using active mechanisms to increase the monomer concentration, such as monomer sequestering proteins. Alternatively, physical effects such as high hydrostatic pressure can affect microtubule polymerization. To measure the

* These concentrations were calculated based on counting the number of microtubules in published electron micrograph cross-sections of axons, assuming that each microtubule contains 1600 subunits per 1μm length, measuring the neurite cross-sectional diameter, and calculating the volume of a 1μm length of the neurite The calculation of concentration is therefore the number of subunits/volume converted into moles/liter: hippocampal neuron (1) in culture: 620μM (Baas, 1988); chick embryo dorsal root ganglia in culture (1) 520μM (Bray, 1984); frog olfactory neurons *in situ* (average of 25) 590μM (Burton, 1984); rat retinal ganglion cells in culture (3) 722μM, 600μM and 598μM (Kleitmen, 1988).

monomer/polymer ratio, fluorescence intensity measurements of photoactivated regions are compared immediately following photoactivation and at short time points thereafter. The rapid decrease in intensity immediately following photoactivation is due to the monomer content which is free to diffuse from the site of photoactivation. Using the ISIT camera, I estimated the monomer content to be about 5-10% of the total tubulin. Similar figures were found by Okabe and Hirokawa (1990) in adult rat DRGs using FRAP. It is possible that such high measurements for monomer concentration could be due to the several experimental artifacts. The presence of free dye not bound to tubulin would behave similarly to monomer. It would probably be difficult to measure the amount of free dye in the these *Xenopus* neurons, but one approach would be to make extracts from neural tubes from injected embryos, photoactivate the caged fluorescein, and then measure the amount of bound vs free dye with an antibody to fluorescein. The low amount of labeling in these embryos might be below the level of detection. An easier approach would be to treat these axons with taxol and then measure the monomer/polymer ratio. Taxol should cause all the monomer to be assembled into polymer and there should be no detectable monomer; all rapidly diffusible signal would be due to free dye. Another factor which would generate artificially high measurements, would be differential incorporation of labeled vs unlabeled tubulin. We don't feel that this is such a great possibility in the *Xenopus* system. It has been shown in other systems that tubulin which is not incorporated into polymer is more rapidly degraded than tubulin which is functional and can assemble into polymer (Caron, 1985). In these embryos, the labeled tubulin has gone through 10 to 15 cycles of assembly and disassembly. If the injected derivatized tubulin were not competent for assembly, this tubulin would remain as monomer and would presumably be degraded.. Labeled tubulin which was able to undergo cycles

of assembly and disassembly would preferentially be retained within the embryo. In fact, we don't know how tubulin degradation is regulated in the early *Xenopus* embryo and whether this regulation is similar to that found in other systems. Finally, our estimates of the polymer concentration estimated from electron micrographs of other neuronal types may not apply to *Xenopus* embryonic axons. If the tubulin concentration in these axons were much lower than the concentrations that we've calculated from published electron micrographs, then we would expect a correspondingly higher proportion of the total tubulin to be present as monomer. For example, if the tubulin concentration in *Xenopus* embryonic neurons were 50 μM rather than 600 μM as we determined from electron micrographs (detailed above), with a critical concentration for tubulin assembly of 10 μM, then we would expect the *Xenopus* neurons to contain 20% of the tubulin concentration as monomer. We have not analyzed cross-sections of axons in culture at the EM level and have little knowledge of the microtubule polymer concentration within these *Xenopus* neurons. Therefore, it would be good to make our own estimates of the tubulin concentration due to polymer in these *Xenopus* neurons by looking at cross-sections of axons at the EM level.

Polymer turnover time

Since these studies presented here indicate that microtubule polymer is the transport form of tubulin, it would be important to know the polymer turnover time. Since we don't know the mechanism of microtubule polymer movement in these axons, the polymer turnover time might give us some clue to the nature of this mechanism and the structure of the axonal cytoskeleton. For example, since the microtubule bundle appears to be transported as a coherent unit, are individual microtubules within the bundle turned over during transport or does

turnover occur only in specific regions of the axon such as branch points. The polymer turnover time is measured by the time that it takes for the stable fluorescence to decay to background levels and is an indication of the stability of microtubules. In many cells, the more recently assembled, labile microtubules are rich in the unmodified tyrosinated form of a-tubulin, whereas older, more stable microtubules contain the post-translationally modified detyrosinated and/or acetylated form (Gundersen et al., 1987; Schulze et al., 1987; Webster et al., 1987). Post-translationally modifed microtubules tend to have a slower turnover time in fibroblasts (Schulze et al., 1987), and stable microtubules in axons of cultured rat sympathetic neurons are detyrosinated and acetylated (Baas and Black, 1989). Axonal microtubules have recently been shown to consist of two domains. The plus ends of the microtubules are composed of unmodified α-tubulin which is labile to nocodozole, while the minus ends are post-translationally modified and stable to nocodozole treatment (Baas and Black, 1990). Baas and Black postulated that the minus end segments of the microtubules serve as stable transportable nucleating sites in the axon, while the plus ends are dynamic and can grow and shrink. Microtubule assembly does occur in the cell body (Okabe and Hirokawa, 1988), on the plus ends of microtubules along the axon tube (Baas and Black, 1990; Okabe and Hirokawa, 1988), and in the growth cone (Baas and Black, 1990; Bamburg et al., 1986; Black et al., 1989; Tanaka and Kirschner, 1991). By quantitatively measuring the polymer turnover time via the decay of fluorescence in photoactivated marks over time, we might gain evidence of this predicted behavior and morphology in *vivo* in *Xenopus* neurons. We have not yet done morphological studies at the EM level on *Xenopus* neurons, and hence, several fundamental parameters of the microtubule cytoskeleton such as microtubule number, length or polarity are not known. Furthermore we don't

know whether the microtubules contain two domains with different stabilities as in the sympathetic neurons studied by Baas and Black. Such ultra-structural studies are essential for a more complete understanding of the microtubule dynamics during axonal elongation in *Xenopus* neurons. I have personally done immunofluorescence on the microtubules in these *Xenopus* neuronal cultures which were not presented in this thesis. I found that the microtubules in the growth cone were stained for tyrosinated tubulin and did not contain acetylated or detyrosinated tubulin. The axonal microtubules stained for both unmodified and post-translationally modified forms of tubulin.

If the axonal bundle of microtubules in *Xenopus* embryonic axons were composed of polymers of different lengths, with stable and labile domains staggered along the axon, then we could make some predictions for how the fluorescence might decay over time. Figure 1 illustrates graphically how different arrays would give different fluorescence decay measurements over time. A staggered array with microtubules composed of both labile and stable domains as shown in figure 1a might give decay kinetics shown in figure 1b: there would be a rapid decay due to monomer (segment *m*), followed by a slower decay due to the labile plus ends turning over (segment *l*), and finally a much slower decay due to label in the stable domains (segment *s*) which turn over very slowly.

If the microtubules do not contain segmented domains with different turnover times, and are instead uniform (figure 1*c)* we would expect microtubule turnover also to be more uniform as shown in figure 1*d*. Here we would still have the rapid decay due to monomer (segment *m*) and then a slower monophasic decay due to polymer (segment *p*). Since there are indications that axons do not contain the capacity to nucleate new microtubules (Baas and Heidemann, 1986), and that new nucleation sites are only generated in the cell

body, such a mechanism of polymer turnover would lead to a gradual decrease in polymer number over time and presumably to a decrease in polymer number in a proximal-distal gradient. Such proximal-distal gradients in microtubule number have been documented in several neuron cell types in culture (Bray and Bunge, 1981; Letourneau, 1982).

A third possible scenario is that the microtubules might display different stabilities dependent on their position within the axon. One possible arrangement is shown in figure 1e with fluorescence decay kinetics shown in figure 1f. In this hypothetical example, the stable microtubules (*s*) are predominant near the cell body, the labile microtubules (*l*) are near the growth cone and microtubules of intermediate stability (*i*) lie between. We might similarly imagine changes in stability depending on the length of the neurite or on culture conditions such as plating substrate. While this third model is extreme and meant for illustration of kinetic possibilities, there are reasons to believe that microtubules may show different stabilities/turnover times based on location in the axon. For instance, microtubules in and near the growth cone would be expected to turn over more rapidly, since the growth cone contains a cluster of microtubule ends which have been shown to be dynamic (Tanaka and Kirschner, 1991) and stain exclusively for unmodified tubulin. In addition, other studies have shown that that axonal growth is more sensitive to microtubule depolymerizing drugs applied locally at the growth cone than applied either to the axon or the cell body (Bamburg et al., 1986). Bamburg et al argued that the differential sensitivity of axonal growth to locally applied drugs implies that microtubules in the growth cone are dynamic and that microtubules in the axon and cell body are non-dynamic. However, as discussed above axonal microtubules in *Xenopus* may contain two domains with different dynamics and post-translational modifications. Baas has shown that axonal unmodified

microtubule domains display the same drug sensitivity as unmodified microtubules in the growth cone. Depolymerizing drugs might only affect axonal growth when all the microtubules in a region are depolymerized. To depolymerize both labile and stable domains on axonal microtubules requires much higher drug concentrations and longer incubation times (Baas and Black, 1990; Baas and Heidemann, 1986). Therefore, the differential susceptibility of axonal growth to depolymerizing drugs applied to the growth cone may be due to the fact that the growth cone contains only labile plus ends of microtubules, while in axons, the labile plus ends of microtubules are staggered and lie adjacent to stable microtubules.

Figure 1

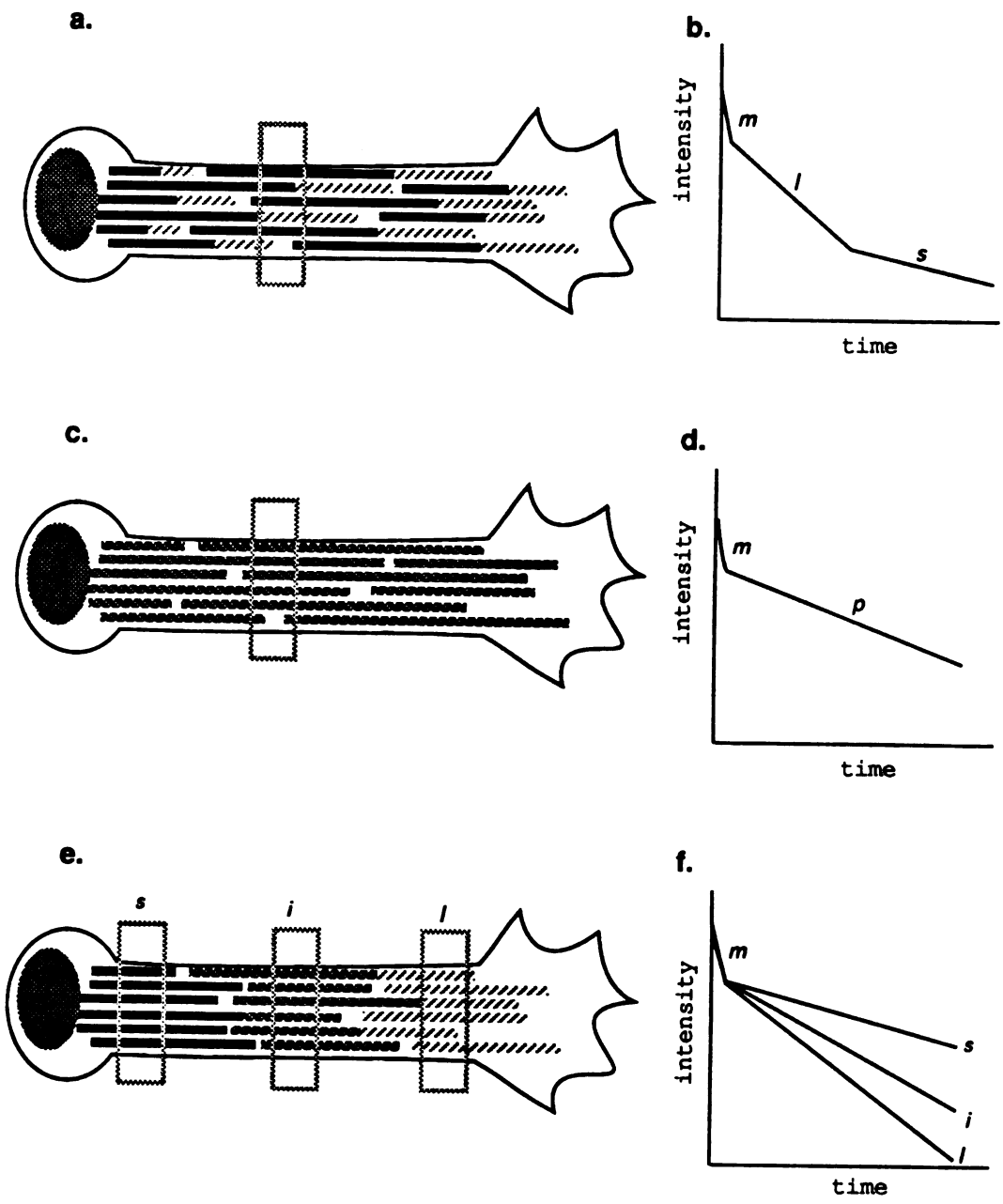
a.
b.
intensity
m
l
s
time
c.
d.
intensity
m
p
time
e.
s
i
l
f.
intensity
m
s
i
l
time

Polymer sliding

Finally, the amount of microtubule sliding within the axon could be measured. The slow but measurable spreading of the photoactivated spot over time that we observed in our experiments is possibly due to sliding of microtubules relative to one-another. This spreading could be more accurately measured using a quantitative system. In addition, the use of a cooled CCD system might be able to detect a small stationary phase of polymer, if such a phase exists.

In our experiments we compared the spreading of the photoactivated label on tubulin to the spreading of photoactivated label on dextran. We assumed that the dextran would behave as monomer. Dextran could actually be used to probe the mesh size of the axonal cytoplasm to diffusion of inert molecules and in so doing to get an idea for how monomer should behave within the axon. In my observations of the movement of dextran within the axon, I had the distinct impression that there was a bias of movement of the dextran towards the growth cone. This was difficult to quantitate due to the small number of axons which I observed. However, it might be interesting to follow up. Since dextrans are available in different sizes, and they label well with caged-fluorescein, it would be fairly simple to get an idea whether "soluble" molecules are free to diffuse within the axon.

The mechanism of microtubule polymer transport in Xenopus neurons: 1. Does microtubule sliding (relative to other microtubules) occur in Xenopus neurons?

In our experiments we saw significant evidence of bulk polymer movement in *Xenopus* neurons. It appears that in these neurons, the entire microtubule bundle moves distally in the axon as a single entity, and we could detect no stationary phase of microtubule polymer. It is possible that there are

links between the microtubules which allow this coherent movement of microtubules through transport against some as-yet-unknown stationary phase. However, we saw some evidence that there may be sliding of microtubules relative to one-another within the microtubule bundle. As mentioned in the conclusion of chapter 2, there are several systems in which sliding of microtubules relative to one another is implicated in the elongation of cellular structures (ie dark adaptation in teleost retina (Burnside, 1976), or light stimulation in *Blepharisma japonicum* (Matsuoka and Shigenaka, 1985)). If it could be demonstrated that microtubules are indeed sliding relative to one another in these *Xenopus* neurons, this might imply that some portion of the axonal cytoskeleton consists of stable stationary microtubules against which the microtubule bundle is tranlocated. As mentioned above, there is really very little that we know about the morphology of the cytoskeleton in these embryonic *Xenopus* neuronal cultures. From immunofluorescent studies and from imaging of rhodamine labeled microtubules *in vivo* (Tanaka and Kirschner, 1991) it appears as though the microtubules may lie bundled together in the axon, or that several bundles may intertwine throughout the axonal length. This impression is strengthened by observing the microtubules in neurons where growth cone collapse and axonal retraction occurs. During axonal retraction, it appears as though the microtubules "corkscrew" back into the axon, and the impression of several intertwined bundles of microtubules is very strong. We also know next to nothing about microtubule associated proteins in these *Xenopus* neurons. Both Elly and I have tried valiantly to find immunofluorescent staining for tau protein in these neuronal cultures with no success. However, western blotting of neural tube cultures indicates that tau immunoreactivity does not appear until later, around stage 30-32 (Elly Tanaka, David Drechsel, personal communication).

Several approaches should be used to look for evidence of sliding microtubules. First, quantitative measurements of the slow spreading of photoactivated zones should be made to determine the possible rates of polymer sliding. These are mentioned above and in the conclusion to chapter 2.

Second, the conditions under which the spreading occurs should be further investigated. For example, in combination with studies of membrane movements (see below) it might be determined that slow spreading of the photoactivated zones (evidence for sliding) occurs under conditions when membrane insertion occurs. Membrane insertion along a length of axon would be detected by monitoring the separation of beads or other particles attached to the membrane (see below). Other evidence for sliding is a separation between photoactivated marks as shown in chapter 2.

A direct demonstration of microtubule sliding would require an immunohistochemical study at the EM level. Using an antibody which reacts with fluorescein but not with caged-fluorescein , it would be possible to detect sliding of microtubules. A photoactivated mark would be made on the axon. If the neuron were fixed immediately, the staining on the microtubules for photoactivated (fluorescein) tubulin should lie in register (see figure 2a) adjacent to unstained (caged) microtubule segments. To look for evidence of sliding of microtubules neurons are fixed at later times following photoactivation. If sliding of microtubules occurred in neurons, staining on microtubules should lie out of register. This would be most likely to occur In neurons where evidence of sliding is good as evidenced by the slow spreading of a single photoactivated zone (figure 2b), or the separation of multiple photoactivated marks (figure 2c). As indicated in figure 2c, it would be advantageous to use multiply marked neurons and follow the photoactivated

regions for a while with video before fixation so that the history of the photoactivated region could be known (ie. rate of axonal elongation, rate of spread of photoactivated zone etc.).

I tried to do some staining with antibodies to fluorescein in these neurons. However, though photoactivated caged-fluorescein fluoresces as fluorescein, antigenically it is different. Using dot blots it is possible to screen antibodies for the ability to bind to photoactivated caged-fluorescein and not to caged-fluorescein. These antibodies should first be used to stain microtubules in fibroblasts injected with caged fluorescein tubulin to determine whether the fixation affects their usefulness for immunofluorescence. In addition, candidate antibodies should be adsorbed against *Xenopus* neuronal cultures to reduce non-specific staining.

In chapter 2, we proposed that sliding could be one mechanism by which the separation of photoactivated marks occurs in neurons. If sliding does occur, we might expect to see a decrease in polymer number per cross-section in long axons relative to short axons, or along the proximal-distal axis of the axon upon examining microtubules at the EM level. Such proximal-distal gradients in microtubule number have been seen in neurons (Bray and Bunge, 1981; Letourneau, 1982). However, there are several other possible mechanisms by which changes in microtubule density might occur. Polymer annealing has been demonstrated *in vitro* but has not been shown *in vivo*. In addition, dynamic instability of microtubules within the axon could result in a loss of some microtubules and increase in length of others as mentioned above.

Figure 2

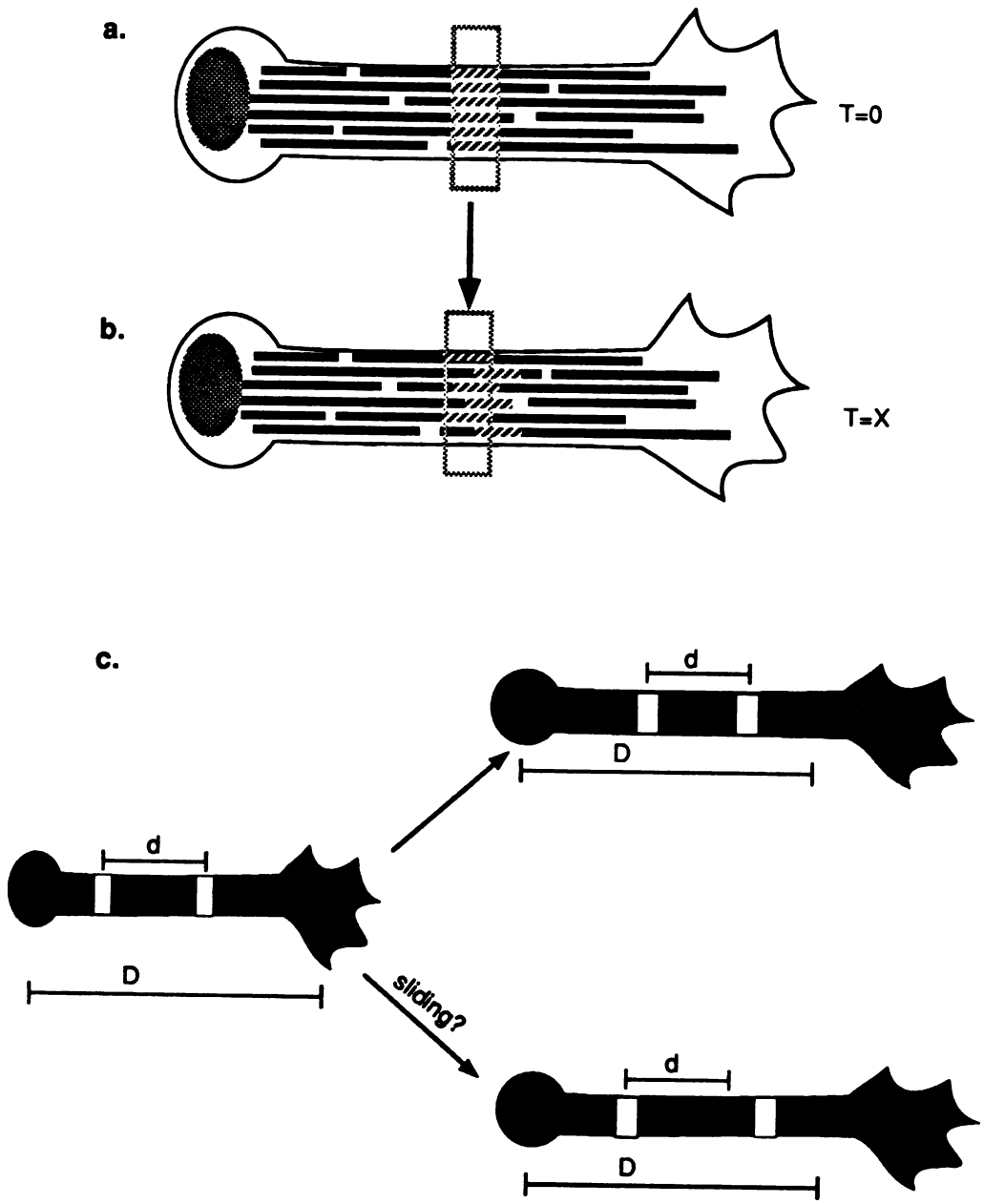

The mechanism of microtubule polymer transport in Xenopus neurons: 2. Are membrane movements correlated with movement of microtubule polymer in Xenopus neurons?

Okabe and Hirokawa reported preliminary experiments comparing photoactivation of fluorescence of caged-fluorescein tubulin in *Xenopus* neurons and in mouse dorsal root ganglion neurons (Okabe and Hirokawa, 1991). In mouse DRGs photobleaching of fluorescence studies had previously indicated that the microtubule polymer was stationary and that assembly of the cytoskeleton occurred at the growth cone (Okabe and Hirokawa, 1990). These preliminary experiments confirmed that the photoactivated spot moves in the *Xenopus* neurons but found that the photoactivated regions are stationary in mouse DRGs. They further report that small beads attached to the surface of the neurons also move in the *Xenopus* neurons but not in the mouse DRGs . The implication of the bead experiment is that microtubule movement is directly coupled to membrane movement. An interpretation of the bead experiment is that in mouse DRGs plasma membrane expansion occurs at the growth cone, likewise microtubule assembly, so beads attached to the axonal membrane do not move and neither does microtubule polymer,. In *Xenopus* neurons, bead movement distally along the axon indicates that plasma membrane expansion occurs proximally and/or along the length of the axon as does microtubule movement and assembly detected by photoactivation of fluorescence. There is wide support for the idea that expansion of the neuronal plasma membrane occurs primarily at the growth cone rather than along the length of the axon as indicated for *Xenopus* neurons in the Okabe and Hirokawa experiment. This support comes from labeling studies with fluorescent lectins or carmine particles (Bray, 1970), (Feldman et al., 1981), pulse-chase experiments with ferritin-labeled lectins and with phospholipid precursors (Pfenninger and Johnson,

1983; Pfenninger and Maylie-Pfenninger, 1981)), and autoradiography of radiolabeled membrane proteins (Griffin et al., 1981; Tessler et al., 1980). However, there are several reports that under situations where neurons undergo "towed" growth (Weiss, 1941) during which the neurons elongate in response to applied tension, membrane insertions occurs along the length of the axon as well (Campenot, 1985; Zheng et al., 1991). There are several precedents for cytoplasmic membrane movement coupled to microtubules (endoplasmic reticulum, vesicles etc.), and at least one report of plasma membrane movement coupled with microtubules as in the cortical rotation of early *Xenopus* embryos (Houliston and Elinson, 1991). It would be important to carefully examine the relationship between membrane movement and polymer movement in the *Xenopus* neurons. One way is to use the approach of Okabe and Hirokawa using beads that adhere to the surface. Several different kinds of beads or particles could be used such as carboxylate or polystyrene or small glass particles which stick non-specifically to the surface, beads with lectins bound to the surface, and beads with antibodies against different surface antigens. Since different membrane components may have different mobility within the axon, different types of beads or small glass particles would help determine if there are membrane components which are transported along with the microtubules vs those which are stationary.

Is bulk microtubule polymer transported from the cell body distally in neurons other than early embryonic Xenopus neurons?

Previous studies, using the technique of fluorescence recovery after photobleaching (FRAP), indicated that the microtubules in several types of neuronal cells were not transported distally in the axon. These studies indicated that all polymer assembly which contributed to axonal growth

occurred at the growth cone and implied that the transport form for tubulin in neurons was monomer rather than polymer. These photobleaching studies were done following direct microinjection of labeled tubulin into fused PC12 cells (Lim et al., 1989), adult rat DRG neurons (Okabe and Hirokawa, 1990) and embryonic chick DRG neurons (Lim et al., 1990). One way to address the discrepancy in these results is to label the microtubules in these other neuronal cell types with caged-fluorescein tubulin and determine whether marks made by photoactivation of fluorescence move in these (or other) neuronal cell types as they do in embryonic *Xenopus* neurons. Unlike the labeling in the *Xenopus* neurons, labeling of these cell types requires direct microinjection of labelled tubulin. One of the greatest hurdles to overcome in these experiments is to achieve a uniform labeling following microinjection of the labeled tubulin so that the labeled tubulin faithfully represents microtubule dynamics in these neurons. The best way to achieve uniform labeling, is to depolymerize all the microtubules in the neurons following microinjection either with nocodozole or with incubation at cold temperatures and then to allow neuronal regrowth to occur.

Since neuronal cells often lift off the substrate following such treatments, it might be necessary to coinject rhodamine labelled tubulin or rhodamine labelled dextran so that successfully injected cells can be relocated. In the following paragraphs, I will briefly and casually describe the attempts that I have made to microinject various neuronal cell types, the obstacles that I found, and some tricks that may be helpful.

Microinjection of chick dorsal root ganglion cells.

Since these are primary neuronal cultures, they involve a lot of preparation time for dissecting, plating, outgrowth and microinjection. The major problems with using this system are that the microinjection process is

very difficult and that the cells do very poorly under illumination, even though they grow quite well in culture.

Microinjection is difficult since the DRG cell body seems to act like a slightly underinflated balloon; that is, the membrane indents a lot before the needle actually pierces the membrane. Usually, the nucleus gets speared in the process and one is left studying microtubule dynamics in enucleated neurons. The biggest trick that I can offer is to place the (very sharp) needle right up against the cell body, then tap gently on the microscope until the needle enters the cell body. Biggest problems - 1) keeping the needle from clogging without having such a huge needle that the DRG gets blown away 2) Keeping the DRGs happy and healthy on the microscope stage during the long process of microinjecting, allowing the tubulin to become incorporated, relocating microinjected cells, photoactivation and observation. Temperature seems to be a major factor. Larger coverslips (40mm) are nice because there is a greater opportunity to choose the cells to microinject, however there is a steep heat gradient from the heat source at the edge of the coverslip, to the center of the coverslip (4-5^{o}C). Smaller coverslips seem to help overcome this problem but there are fewer cells to choose from. Other approaches which various people suggested (but were never tested) to help get the needle into the cell body: varying the pH of the injection medium transiently; or "ringing" the cells with electrical current. (From talking to several electrophysiologists, it seemed to me that were this approach successful, it would be due to the needle vibrating - the same effect is accomplished by tapping on the microscope - and doesn't require an electrophysiology setup).

I have found that it is possible to freeze the dissected DRGs before plating so that preparation time for individual experiments is decreased. However, there is significant cell death so larger numbers of cells have to be

plated to compensate. I found that freezing after the collagenase step but before pre-plating was the most successful routine. The cells freeze well in "MEM-CPM", obtained from the cell culture facility. I simply resuspend the cells after the collagenase step in MEM-CPM, triturate briefly and then placed the vials at -70°C. I have found that frozen cells are only good for 3 to 4 days, even when stored in liquid nitrogen. After thawing, I pre-plated the DRG's for longer periods (2-2.5 hours) than with fresh preparations.

Microinjection of PC12 neurons

PC12 cells are relatively "easy" to culture. The axons elongate fairly rapidly after priming (20-50 microns/hour). There are several distinct advantages to using PC12 cells: 1) they have been fairly well characterized in culture, 2) they can be transfected, so that in later studies it might be interesting to follow microtubule dynamics in PC12 neurons that have been transfected with altered MAPS, signalling proteins, or membrane receptors. I have only tried a little to microinject these neurons. I think the best way would be to prime for a week or so with NGF, triturate the neurons and then replate onto new substrates. If you don't add NGF immediately, the axons don't elongate right away but the cell bodies are fairly adherent. Adherent cell bodies allows for easier microinjection and for the tubulin pool to equilibrate. Then NGF can be added to induce elongation. There are several other tricks that I have never tried with PC12 cells - 1) fusing PC12 cells with PEG to generate giant cells: this was used in experiments where biotin tubulin was microinjected for EM level studies (Okabe and Hirokawa, 1988) 2) using other agents in the presence of NGF to block outgrowth during injection. Sphingosine will inhibit axon elongation in PC12 cells. Apparently, when the cells are released from sphingosine block, they elongate more rapidly than untreated cultures. This

may indicate that sphingosine blocks the actual elongation without hindering the accumulation of the components necessary for neuronal outgrowth.

Other approaches

Trituration of chick dorsal root ganglion neurons in the presence of isosmotic sucrose and labeled proteins has been reported to be useful for introducing labeled proteins into neurons. J. Bamburg reported at a meeting that he had used this approach to introduce fluorescent actin into embryonic chick DRGs. Elly and I (independently) tried to label using this approach. We both obtained the same result - labelled neurons, but label only in large "vesicles." Bamburg told me that he does the labeling in the presence of actin depolymerizing factor (ADF) a small protein which complexes with actin and keeps it in monomeric form. He said that when he tried to label the neurons with actin alone, he was unsuccessful, presumably because the actin aggregated and the larger aggregates could not get into the cells. I tried once to label DRGs with tubulin plus nocodozole hoping that the tubulin would remain dimeric, but was unsuccessful. The advantages of this approach, if successful, are that 1) since it is a bulk labeling method, numerous neurons are labeled in the culture, and 2) since the labeling is done prior to outgrowth, incorporation of label into polymer would be uniform and not require treatments to depolymerize microtubules.

Microinjection into *Xenopus* retinal ganglion cell neurons

The growth of individual retinal ganglion cell fibers have recently been observed *in vivo* with time-lapse video (Harris et al., 1987). The fibers were stained with the lipophilic fluorescent dye, DiI, inserted into the retina. By removing the eye on the other side of the *Xenopus* embryo, the path and behavior of the growth cones could be observed in the optic tract and tectum. This system might be an ideal one for determining whether transport of

polymeric tubulin occurs in axons within the embryo. This experiment should be done in collaboration with Bill Harris and Christine Holt at San Diego who have indicated that they might consider such a collaboration. There are several difficulties in to using this experimental system to examine polymer transport *in vivo*. Although these neurons are *Xenopus* embryonic neurons, they are not labeled by injection into the two-celled stage embryo. Therefore, they require direct microinjection. In addition to all the problems with microinjecting individual cells detailed above, it is not possible to do these experiments using a conventional microinjection set-up; rather an electrophysiology set-up must be used since the injections are done into the retinal ganglion cells within the eye. In addition, it would be hard to determine the age of the neurons which are being injected, or how long the processes are at the time of injection. The advantages of this system are that 1) our direct experience indicates that *Xenopus* neurons are much less susceptible to photodamage, and 2) the caged-fluorescein signal might be higher than that observed by after passage through the embryo.

How much does polymer assembly at the growth cone actually contribute to axonal elongation in Xenopus neurons?

There is a discrepancy between the data that Elly Tanaka obtained for microtubule assembly in the growth cone using rhodamine tubulin, and that I measured following photoactivatable tubulin marks made near the growth cone neck. Using photoactivation of fluorescence, we determined that there was a significant contribution to axonal elongation from assembly at the growth cone, since in almost every instance of axon elongation, microtubule polymer movement was slower than growth cone advance. Elly was able to make some measurements on growth rates of individual microtubules, however she

estimated that extrusion of microtubule polymer from the axon into the growth cone made a significant contribution to the growth cone polymer content and therefore to total axonal elongation. While I did find significant evidence of microtubule polymer movement into the growth cone, this was not a prominent feature, but rather usually occurred transiently during pausing of the growth cone. After a lot of video-gazing, one possibility that occurs to me is that while the growth and shrinkage rates that Elly measured are valid, the amount of microtubule rescue in the growth cone was underestimated, and that microtubules only shrink back to the central bundle. The central bundle may function in microtubule rescue possibly via stabilization through lateral microtubule-microtubule contacts. Also, the amount of polymer assembly might have been underestimated in Elly's experiments, since individual microtubule elongation rate measurements could only be made in the periphery of the growth cone where single microtubles are visible. If significant microtubule polymer assembly actually occurs on microtubules that form the central bundle, this growth would not have been measured. Significant microtubule polymer assembly in the central bundle of the growth cone coupled with a rescue function by the central bundle would allow the central bundle to serve as a sort of moving nucleation site for microtubule assembly within the growth cone. In order to make better measurements on the rate of microtubule growth in the growth cone and to estimate the contribution of growth cone polymer which is converted to axonal polymer, it would be important to be able to do double labeling studies using rhodamine tubulin for looking at individual microtubule dynamics in the growth cone (measurements of individual growth and shrinkage rates) and caged-fluorescein tubulin to look at bulk microtubules (to determine when axonal polymer is being extruded into the growth cone versus growth cone polymer being converted to axonal polymer). The amount of

labeling that I was able to achieve in *Xenopus* neurons by microinjecting at the two cell stage was not sufficient for a double labeling study - too much signal is decayed by the neurula stage. However, one possible way to increase labeling in the *Xenopus* neurons would be to inject multiple smaller blastomeres later on in development, ie in 128-256-512 stage embryos. However, the 512-stage embryo occurs at 5 hours post-fertilization whereas the neurons are cultured approximately 36 to 48 hours post-fertilization. Therefore microinjection at this stage might not help much. We don't really know how fast the injected tubulin turns over and when the bulk of the turnover occurs in the embryo- ie whether the largest amount of turnover occurs in the early blastomeres or whether the tubulin is turned over at the same rate all along. However it can't hurt to try to increase the labeling by injecting later. Initially it would be important to test marking of prospective dorsal blastomeres by injecting a fixable dye such as dextran or colloidal gold (Niehrs and De Robertis, 1991) using the pico spritzer. Then after successful neuronal labeling has been achieved using colloidal gold, to attempt to use labeled tubulin. The other possibility is to try to microinject these neurons directly with tubulin to increase the labeling. The problems with direct microinjection have been discussed in detail above.

What factors influence the rate and characteristics of polymer transport in Xenopus axons? What are the effects of drugs such as nocodozole and cytochalasin? What is the role of tension?

The coherence of the photoactivatable spots on microtubules through transport reported in chapter 2, suggests that the microtubules might be linked together. The data presented in Figure 6 of chapter 2 indicate that long segments of the axon (~25μm) can transport as a single unit. However, the slow-spreading of the photoactivated regions in many of the observed cases

indicates that these links, if present, would allow some microtubule movement relative to one another as discussed above in the section above on sliding. If such links between microtubules were present, we might be able to disrupt some of the links locally in the axon and see how such a treatment might affect bulk microtubule transport within the axon. As mentioned above, Baas and Black determined that the plus end segments of axonal microtubules consist of unmodified α-tubulin, which are labile to treatment with nocodozole. Low doses of nocodozole have been shown to cause neurite retraction if applied at the growth cone, while the same concentration does not cause retraction if applied locally to the axon or cell body. As mentioned above, this difference in susceptibility might be due to the presence of overlapping stable domains which link the microtubules in the axonal bundle. Therefore, it may be possible to apply nocodozole locally to the axon at a dose which does not cause retraction, but causes an effect on transport of polymer due to depolymerization of the labile segments of the microtubules. The effect of nocodozole might be manifest as a change in the rate of transport of a photoactivated mark, or a change in the spreading of the photoactivated region at the site of nocodozole application.

Similarly, the effect on microtubule transport of local or bath applied cytochalasin treatment could be determined. Cytochalasin treatment affects the pathfinding ability of neurons and affects growth cone morphology and motility, however neurons continue to elongate in the presence of cytochalasin. There is support in the literature for interactions between the actin cytoskeleton and the axonal microtubule network. For instance, neurons treated with cytochalasin, are not susceptible to retraction induced by microtubule depolymerizing drugs (Solomon and Magendantz, 1981). Heidemann and Buxbaum (Heidemann and Busbaum, 1990) propose that there is a

complementarity between tension and compression forces due to different cytoskeleton elements and this interaction acts to integrate and regulate axonal growth. Measurements of tension and compression in neurites treated with nocodozole or cytochalasin indicate that the actin network is under tension and supported by the microtubule cytoskeleton which itself is under compressive forces (Dennerll et al., 1988)

Neurons undergo "towed growth" *in situ* after establishing synaptic contacts (Weiss, 1941). Bray (Bray, 1984) showed that this process could be mimicked *in vitro* by attaching the growth cone to a needle and applying a force to the needle to move the growth cone away from the cell body thereby causing much more rapid than normal elongation of the axon behind the towed growth cone. The process of towed growth was further characterized in a series of experiments in Steve Heidemann's lab, examining the role of mechanical tension in neurite elongation and characterizing the components of the towed growth process. They found that the initial component of the elongation is due to elasticity in the neuron while the later phase of elongation involves actual "growth" of the neuron (Dennerll et al., 1988; Dennerll et al., 1989; Zheng et al., 1991). They have determined that neurons will undergo undergo an elastic increase in length (that is an immediate and reversible increase in length) at tensions below a threshold amount (100 μdynes) and then growth (that is, a sustained increase in length) proportional to the applied tension above the threshold amount (Zheng et al., 1991). They have further found that while taxol does not inhibit the increase during the elastic phase of elongation, taxol application does inhibit the increase in axonal length due to growth.

In reflecting on these results there are several experiments which come to mind. Since the microtubule polymer bundle is continuous from the cell body to the growth cone (though individual microtubules are not), an increase in

length of the axon must result in an overall increase in length of the microtubule bundle. We might imagine that since taxol does not affect the initial rapid elastic phase, that this phase of elongation might result in microtubules sliding relative to one another without an increase in individual polymer length. However, the later phase which they term "growth" is sensitive to taxol, and therefore may require polymer assembly. Using photoactivation it would be very interesting to follow these two phases. This might be done in collaboration with Steve Heidemann since his lab is set up for pulling neurons with calibrated forces. The beauty of these experiments is that they can be relatively well controlled. Rather than waiting for a neuron to do a certain behavior, such as grow at a certain rate, these parameters can be controlled in the experiment making it much easier to obtain the desired data. One experiment would be to make two photoactivation marks on the neuron and then deflect the neuron in between to cause an increase in axonal length as shown in figure 3. Using calibrated needles, the amount of tension in the axon could be measured as a function of the increase in length of the axonal segment, and the amount of sliding which occurs could be measured by the increase in length of the photoactivated zone. The second experiment would be to make several photoactivations on a neuron, attach the growth cone to a needle and pull the neurite from the growth cone, to see where the growth in the microtubule polymer occurs. In this experiment, either the rate of growth or the amount of tension used to pull the neurite could be held constant or varied to determine how these parameters influence microtubule polymer movement and assembly. An additional possibility would be to use quantitative fluorescence measurements here as detailed above to determine how the polymer turnover time or monomer:polymer ratio are affected by growth rate and tension.

Figure 3

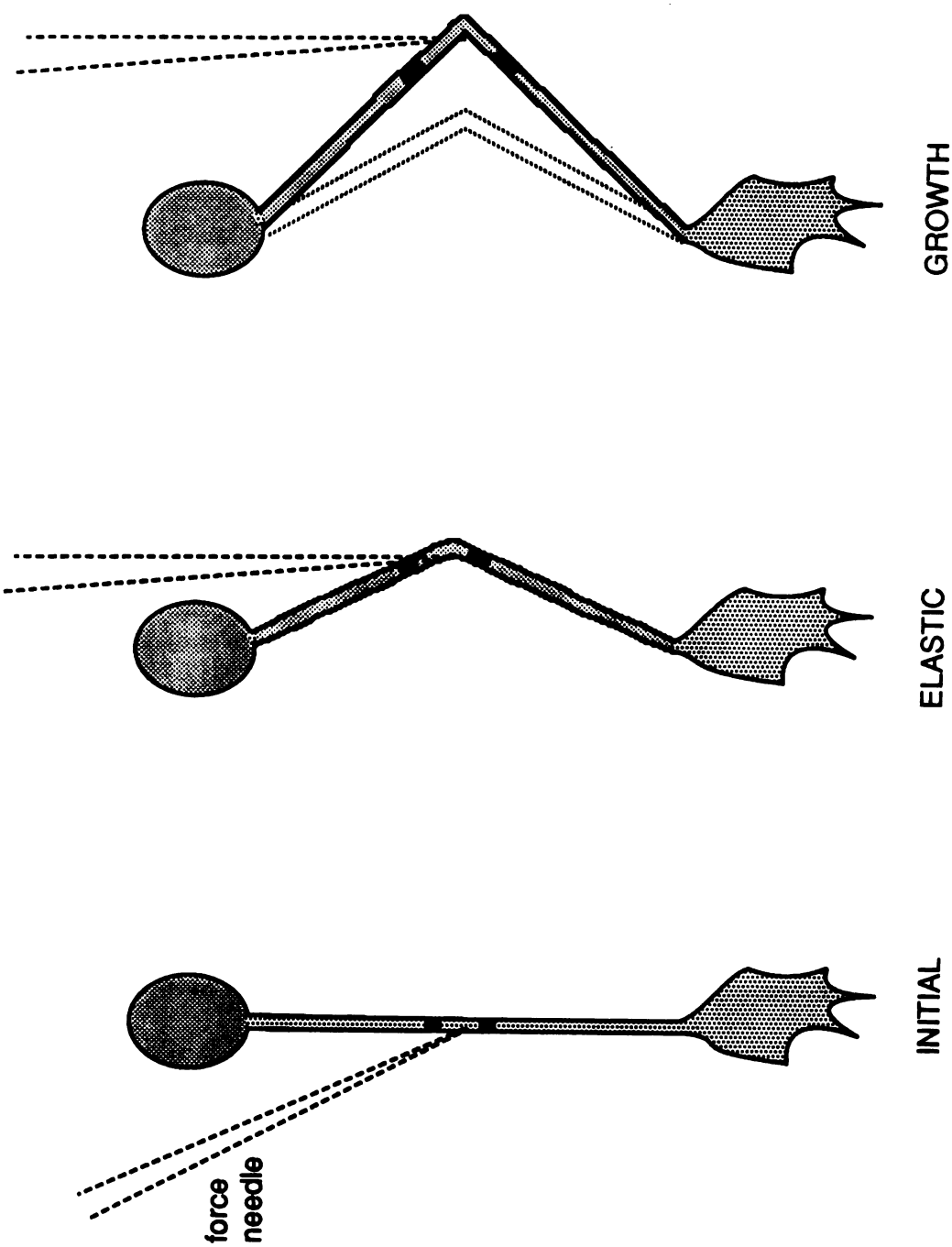

Xenopus neural tube cultures as a model system for axonal elongation, what are the advantages and limitations?

As a final conclusion I would like to evaluate the *Xenopus* neural tube cultures as a model system for studying axonal elongation. There are several advantages and unfortunate drawbacks to our choice of the *Xenopus* neural tube cultures for these experiments. In this section I will analyze the potential for this system as well as its limitations.

There are several major advantages to the *Xenopus* culture system presented in this thesis. First, these neurons grow rapidly and are relatively insensitive to photodamage compared to other neurons that we have tried. Second, as shown in this thesis, it is possible to bulk label the neurons in the culture via cytoplasmic inheritance after injection into the early blastomeres. It is also possible to introduce the RNA for interesting proteins or modifed proteins and determine the effects on axonal growth processes. James Sabry has already succeeded in expressing the serotonin receptor in these neurons using this approach.

The major drawbacks to this system is that it is not very well characterized, either at the level of individual neuronal morphology (EM level) or in terms of neuronal subtypes, and there are very few *Xenopus* reagents (ie. antibodies or cloned genes) that can be used to probe.this system. Since it is a mixed population of neurons, it is not unreasonable to expect inconsistent results due to unavoidably collecting data on several different neuronal subtypes. It has been widely documented in the literature that different neuronal populations behave differently under similar experimental conditions, as in the differences in axonal transport rates measured using metabolic labeling from different populations of neurons, or from the same neuronal type under different physiological conditions (ie regeneration vs homeostasis). This

system would benefit greatly from an in depth characterization of the neurons in these cultures and the development of some *Xenopus* reagents. Several other problems are that while the bulk labeling approach has distinct advantages, the major drawback is the low level of labeling which makes imaging and immunological approaches very difficult. The last problem is the variability in these cultures due both to seasonal variation and to infections within the cultures. In light of all these drawbacks, I think the benefits of this system already outweigh the disadvantages; it would be well worth the time and effort to continue the development and use of *Xenopus* embryonic neurons as a model system for studying axonal elongation and development.

Finally, a quote:

> ".... it has been shown that the first manifestations of activity observable in the differentiating nerve cell are of the same fundamental nature as those found not only in other embryonic cells but also in the protoplasm of the widest variety of organisms. The movement which results in the drawing out of a compact cell into a long filament, the primitive nerve fiber, it is but a specific form of that general type of movement common to all primitive protoplasm. In studying the secondary factors which influence the laying down of the specific nerve paths of any organism, we are concerned, therefore, primarily with the laws which govern the direction and intensity of protoplasmic movement, and it is the analysis of these phenomena to which students of the ontogenetic and regenerative development of the nervous system must now direct their attention....."
>
> R.G. Harrison, 1910

REFERENCES

Baas, P. W. , J. S. Deitch, M. M. Black, G. A. Banker. 1988. Polarity orientation of microtubules in hippocampal neurons: uniformity in the axon and nonuniformity in the dendrite. *Proc. Natl. Acad. Sci. USA* 85:8335-8339

Baas, P. W., and M. M. Black. 1989. Compartmentation of alpha-tubulin in neurons: identification of a somatodendritic-specific variant of alpha-tubulin . *Neuroscience.* 30: 795-803.

Baas, P. W., and M. M. Black. 1990. Individual microtubules in the axon consist of domains that differ in both composition and stability. *J. Cell Biol.* 111: 495-509.

Baas, P. W., and S. R. Heidemann. 1986. Microtubule reassembly from nucleating fragments during the regrowth of amputated neurites. *J. Cell Biol.* 103: 917-927.

Bamburg, J. R., D. Bray, and K. Chapman. 1986. Assembly of microtubules at the tip of growing axons. *Nature.* 321: 778-790.

Black, M. M., P. W. Baas, and S. Humphries. 1989. Dynamics of alpha-tubulin deacetylation in intact neurons. *J Neurosci.* 9: 358-368.

Bray, D. 1970. Surface movements during the growth of single explanted neurons. *Proc. Natl. Acad. Sci. USA.* 65: 905-910.

Bray, D. 1984. Axonal growth in response to experimentally applied mechanical tension. *Dev. Biol.* 102: 379-389.

Bray, D., and M. B. Bunge. 1981. Serial analysis of microtubules of cultured rat sensory neurons. *J. Neurocytol.* 10: 589-605.

Burnside, B. 1976. Microtubules and actin filaments in teleost visual cone elongation and contraction. *J Supramol Struct.* 5: 257-275.

Burton, P. R. 1984. Luminal material in microtubules of frog olfactory axons: structure and distribution. *J. Cell Biol.* 99:520-528

Campenot, R. B. 1985. The regulation of nerve fiber length by intercalated elongation and retraction. *Dev. Brain Res.* 20: 149-154.

Caron, J. M., A. L. Jones, and M. W. Kirschner. 1985. Autoregulation of tubulin synthesis in hepatocytes and fibroblasts. *J. Cell Biol.* 101: 1763-1772.

Dennerll, T. J., H. C. Joshi, V. L. Steel, R. E. Buxbaum, and S. R. Heidemann. 1988. Tension and Compression in the cytoskeleton of PC-12 neurites II: Quantitative measurements. *J. Cell Biol.* 107: 665-674.

Dennerll, T. J., P. Lamoureux, R. E. Buxbaum, and S. R. Heidemann. 1989. The Cytomechanics of axonal elongation and retraction. *J. Cell Biol.* 109: 3073-3083.

Feldman, E. L., D. Axelrod, M. Schwartz, A. M. Heacock, and B. W. Agranoff. 1981. Studies on the localization of newly added membranes in growing neurites. *J. Neurobiol.* 12: 591-598.

Griffin, J. W., D. L. Price, D. B. Drachman, and J. Morris. 1981. Incorporation of axonally transported glycoproteins into axolemma during nerve regeneration. *J. Cell Biol.* 88: 205-214.

Gundersen, G. G., S. Khawaja, and J. C. Bulinski. 1987. Postpolymerization detyrosination of α-tubulin: a mechanism for subcellular differentiation of microtubules. *J. Cell Biol.* 105: 251-264.

Harris, W. A., C. E. Holt, and F. Bonhoeffer. 1987. Retinal axons with and without their somata, growing to and arborizing in the tectum of *Xenopus* embryos: a time-lapse video study of single fibres *in vivo* . *Development.* 101: 123-33.

Harrison, R. G. 1910. The outgrowh of the nerve fiber as a mode of protoplasmic movement. *J. Exp. Zool.* 17: 521-544

Heidemann, S. R., and R. E. Busbaum. 1990. Tension as a regulator and integrator of axonal growth. *Cell Motil. Cytoskeleton.* 17: 6-10.

Houliston, E., and R. P. Elinson. 1991. Evidence for the involvement of microtubules, ER, and kinesin in the cortical rotation of fertilized frog eggs. *J Cell Biol.* 114: 1017-1028.

Kleitmen, N., P. Wood, M. I. Johnson, R. P. Bunge. 1988. Schwann cell surfaces but not extracellular matrix organized by Schwann cells support neurite outgrowth from embryonic rat retina. *J. Neuroscience* 8:653-663.

Letourneau, P. C. 1982. Analysis of microtubule number and length in cytoskeletons of cultured chick sensory neurons. *J Neurosci.* 2: 806-814.

Lim, S. S., K. J. Edson, P. C. Letourneau, and G. G. Borisy. 1990. A test of microtubule translocation during neurite elongation. *J Cell Biol.* 111: 123-130.

Lim, S. S., P. J. Sammak, and G. G. Borisy. 1989. Progressive and spatially differentiated stability of microtubules in developing neuronal cells. *J Cell Biol.* 109: 253-263.

Matsuoka, T., and Y. Shigenaka. 1985. Mechanism of cell elongation in *Blepharisma japonicum,* with special reference to the role of cytoplasmic microtubules. *Cytobios.* 42: 215-226.

Niehrs, C., and E. M. De Robertis. 1991. Ectopic expression of a homeobox gene changes cell fate in *Xenopus* embryos in a position-specific manner. *EMBO J.* 10: 3621-3629.

Okabe, S., and N. Hirokawa. 1988. Microtubule dynamics in nerve cells: analysis using microinjection of biotinylated tubulin into PC12 cells. *J. Cell Biol.* 107: 651-664.

Okabe, S., and N. Hirokawa. 1990. Turnover of fluorescently labeled tubulin and actin in the axon. *Nature.* 343: 479-482.

Okabe, S., and N. Hirokawa. 1991. Differential behavior of photoactivated microtubules in growing axons of mouse and *Xenopus* neurons: Analysis using caged-fluorescein labeled tubulin. *J. Cell Biol.* 115: 173a.

Pfenninger, K. H., and M. P. Johnson. 1983. Membrane biogenesis in the sprouting neuron. I. Selective transfer of newly synthesized phospholipid into the growing neurite. *J. Cell Biol.* 97: 1038-1042.

Pfenninger, K. H., and M.-F. Maylie-Pfenninger. 1981. Lectin labeling of sprouting neurons. II. Relative movement and appearance of glycoconjugates during plasmalemmal expansion. *J. Cell Biol.* 89: 547-559.

Schulze, E., D. J. Asai, J. C. Bulinski, and M. Kirschner. 1987. Posttranslational modification and microtubule stability. *J. Cell Biol.* 105: 2167-2177.

Solomon, F., and M. Magendantz. 1981. Cytochalasin separates microtubule disassembly from loss of asymmetrical morphology. *J. Cell Biol.* 89: 157-161.

Tanaka, E., and M. Kirschner. 1991. Microtubule behavior in the growth cones of living neurons during axon elongation. *J Cell Biol.* 115: 345-63.

Tessler, A. L., L. Autillo-Gambetti, and P. Gambetti. 1980. Axonal growth during regeneration: a quantitative autoradiographic study. *J. Cell Biol.* 87: 197-203.

Webster, D. R., G. G. Gundersen, J. C. Bulinski, and G. G. Borisy. 1987. Assembly and turnover of detyrosinated tubulin in vivo. *J. Cell Biol.* 105: 265-276.

Weiss, P. 1941. Nerve Pattern: The mechanics of nerve growth. *Growth.* 5: 163-203.

Zheng, J., P. Lamoureus, V. Santiago, T. Dennerll, R. E. Buxbaum, and S. R. Heidemann. 1991. Tensile regulation of axonal elongation and initiation. *J. Neurosci.* 11: 1117-1125.